

Page	SCIENTIFIC RESEARCH
323	Isolation, Structural Determination of Flavone Glycosides from the Leaves of <i>Syzygium cumini</i> and their Cytotoxic Evaluation - Nguyen Thi Van, Nguyen Thi Hue, Vu Van Nam, Trinh Thi Thanh Van, Nguyen Thuy Linh, Tran Thu Huong, Cao Duc Tuan, Pham Van Cuong, Doan Thi Mai Huong
329	Chemical Constituents of the Dichloromethane Extract of <i>Ganoderma cochlear</i> - Vu Thi Hanh Yen, Nguyen Van Vinh Ha, Tran Viet Hung, Bui Hong Cuong, Pham Thi Huong, Nguyen Thi Duyen
334	Steroid and Triterpenoid Compounds Isolated from <i>Amanita pantherina</i> and their Anti-Inflammatory Activity - To Dao Cuong, Hoang Le Minh, Nguyen Phuong Dai Nguyen, Nguyen Huu Kien, Nguyen Thi Hoa, Truong Thi Viet Hoa, Truong Thi Thuy Nhung
340	Determination of Strychnine and Brucine by HPLC for Better Quality Control of <i>Strychni semen</i> - Vu Ngan Binh, Pham Thi Thanh Ha, Dang Thi Ngoc Lan, Do Thi Bich Diep, Nguyen Quynh Chi, Do Quyen, Huynh Truc Thanh Ngoc, Nguyen Thi Ngoc Dung, Sysay Palamy, Chiobouaphony Phakeovilay
347	Quality Evaluation of <i>Phellodendron amurense</i> Collected in Vietnam Using HPLC-DAD and QAMS Methods - Nguyen Thi Ha Ly, Do Thi Hang, Nguyen Minh Khoi
354	Development and Validation of Quantitative Analysis of L-Dopa from <i>Mucuna pruriens</i> - Le Thi Loan, Dang Minh Tu, Dang Viet Hau, Nguyen Thi Thu Trang, Luong Thi Lan, Ha Van Oanh, Nguyen Van Tai
361	Anti-Aggregatory and Anti-Coagulant Activities of <i>Polygonum cuspidatum</i> Extracts - Le Hong Luyen, Nguyen Thi Van Anh
366	Potential Activities of <i>Artemisia vulgaris</i> Methanol Extract Against NTERA-2 Cancer Stem Cells - Trieu Ha Phuong, Tran Le Nam Khanh, Nguyen Thi Cuc, Nguyen Thi Nga, Do Thi Phuong, Le Hoang Ngan Ha, Nguyen Thi Giang An, Nguyen Trung Nam, Do Thi Thao
371	Acute Oral Toxicity and Anti-Inflammatory Effect of the Standardized Extract from <i>Vitex trifolia</i> L. Fruits - Do Thi Hong Khanh, Bui Thanh Tung, Pham Thi Nguyet Hang, William R. Folk
377	Binary Ethosomes for Enhancing Skin Delivery of Rutin by Solvent Injection - Nguyen Hong Van, Phan Huu Phuoc, Nguyen Xuan Tung

JOURNAL OF MEDICINAL MATERIALS

License N^o 313/GP-Ministry of Information & Communication of the Socialist Republic of Vietnam
dated 23/7/2002. ISSN 1859-4735

EDITOR IN CHIEF

Assoc. Prof. Dr. Sci. Nguyen Minh Khoi

SECRETARIAL BOARD

Assoc. Prof. PhD. Do Thi Ha

MEMBER OF EDITORIAL BOARD

Assoc. Prof. PhD. Bui Thi Bang

Prof. PhD. Nguyen Gia Chan

Assoc. Prof. PhD. Le Tung Chau

Assoc. Prof. PhD. Nguyen Thuong Dong

Assoc. Prof. PhD. Le Viet Dung

Assoc. Prof. PhD. Nguyen Tien Dat

Assoc. Prof. Dr. Sci. Do Trung Dam

Prof. PhD. Nguyen Minh Duc

Assoc. Prof. PhD. Pham Thi Nguyet Hang

PhD. Phan Thuy Hien

PhD. Nguyen Ba Hoat

Assoc. Prof. PhD. Pham Thanh Huyen

Assoc. Prof. PhD. Nguyen Thi Thu Huong

Assoc. Prof. PhD. Tran Hung

Assoc. Prof. Dr. Sci. Nguyen Minh Khoi

Prof. PhD. Pham Thanh Ky

Assoc. Prof. PhD. Tran Cong Luan

Prof. PhD. Nguyen Hai Nam

Prof. Doan Thi Nhu

Prof. Dr. Sci. Tran Van Sung

Assoc. Prof. PhD. Nguyen Van Tap

Assoc. Prof. PhD. Nguyen Thi Bich Thu

Assoc. Prof. PhD. Phuong Thien Thuong

Prof. PhD. Na Minkyun

INSTRUCTION

Journal of Medicinal Materials which belongs to Ministry of Health publishes original articles and reviews on medicinal plants and animals, remedies, the work for cultivating, processing and storing medicinal plants, conservation and development of Vietnam Natural Resources of Medicinal Materials, biodiversity conservation in order to create raw material sources for traditional medicine and pharmaceutical industry.

Requirements for submitting the articles:

1. The manuscripts have not been published or submitted to any scientific journals.
2. Professional terms have to be applied to international law namely IUPAC, DICP latin and Vietnam Pharmacopeia.
3. Submitting all articles in 1,5 spaced 12 point Times New Roman (Unicode) in Microsoft Office word or compatible file in English. Each article must not exceed 6 pages, A4 including tables/graphs/diagrams/illustrations and references. Abbreviations must be annotated.

Article submission to the Editor at the address: Journal of Medicinal Materials -Vietnam National Institute of Medicinal Materials, Ministry of Health, No 3B Quang Trung Street, Hoan Kiem District, Hanoi, Vietnam and submit Microsoft Office word file of the article through the E-mail: tapchiduoclieu@nimm.org.vn or tapchiduoclieu@gmail.com.

4. Process and presentation of the items in the article:

- a. Title: The title should be short and informative, no point at the end of the title and 14 point Times New Roman Font.
 - b. Surname and name of all authors and the address of the institution are not included: Academic title, Degree.
 - c. English summary: Title of article, objective, object, and method, result and conclusion are presented in an abstract of ≤ 200 words. Keywords show the main meanings of the research, a maximum of 6 words or phrases.
 - d. The contents of all parts are marked from **1 to 5**: **1.** Background including the aim of the research. **2.** Object and research method. **3.** Results. **4.** Discussion. **5.** Conclusion.
 - e. References: Each article does not exceed 10 references. A reference should be presented as follows: name, family name and middle name of authors are written in full name by Vietnamese without marks. The family name is written in full, middle name and name are written in abbreviation (with foreign name). All the authors' surnames and initial(s) should appear in the full reference for the source (separated by commas).
5. The article is not given back to the author if it is not published.
 6. Reviews: The reviews should have full references and data sources. They are presented in A4 size, less than 10 pages including tables, graphs, and references.

Author of the article must be responsible to the Editorial Board, the public opinions and the rules relating to the Press Law, copyright and intellectual property rights.

ISOLATION, STRUCTURAL DETERMINATION OF FLAVONE GLYCOSIDES FROM THE LEAVES OF *SYZYGIUM CUMINI* AND THEIR CYTOTOXIC EVALUATION

Nguyen Thi Van,^{1,2} Nguyen Thi Hue¹, Vu Van Nam¹, Trinh Thi Thanh Van¹, Nguyen Thuy Linh¹, Tran Thu Huong², Cao Duc Tuan³, Pham Van Cuong¹*, Doan Thi Mai Huong¹*

¹Institute of Marine Biochemistry, Vietnam Academy of Science and Technology (VAST), Hanoi, Vietnam;

²Hanoi University of Science and Technology, Hanoi, Vietnam;

³Hai Phong University of Medicine and Pharmacy, Hai Phong, Vietnam

*Corresponding author: phamvc@imbc.vast.vn; huongdm@imbc.vast.vn

(Received August 14th, 2024)

Summary

Isolation, Structural Determination of Flavone Glycosides from the Leaves of *Syzygium cumini* and their Cytotoxic Evaluation

Five flavone glycosides were isolated from the EtOAc and aqueous extracts of *Syzygium cumini* (L.) Skeels leaves. Their chemical structures were elucidated as quercetin 3-*O*-neohesperidoside (**1**), rutin (**2**), quercetin 3-*O*- α -L-rhamnopyranoside (**3**), kaempferol 3-*O*-neohesperidoside (**4**), and afzelin (**5**) on the basis of detailed analyses of the 1D and 2D NMR spectroscopic data and in comparison with the literature data. All isolated compounds (**1-5**) were estimated for their cytotoxicity against KB, MCF-7, HepG2, and A549 human cancer cell lines. Unfortunately, these compounds were inactive against all four tested human cancer cell lines at the concentration of 128 μ g/mL. To the best of our knowledge, compounds **1** and **4** were first reported from the *Syzygium* genus, while compounds **3** and **5** were isolated from the leaves of *Syzygium cumini* for the first time.

Keywords: *Syzygium cumini*, Myrtaceae, Flavone glycosides, Quercetin, Kaempferol, Cytotoxicity.

1. Introduction

The genus *Syzygium* is one of the genera of the family Myrtaceae comprising 1200-1800 species, which spread out over the world [1, 2] and have been commonly found in Southeast Asia. Many species of the genus *Syzygium* are known for their traditional use in various diseases, such as burns and wounds (*S. aromaticum*), tooth infections and toothache [3]; abdominal pain, indigestion, and diarrhea (*S. cordatum* and *S. guineese*) [4]; dysentery, menorrhagia, asthma, and ulcers (*S. cumini*) [5]; hemorrhages, syphilis, leprosy, ulcers, and lung diseases (*S. jambos*) [6]; mouth ulcers and irregular menstruation (*S. malaccense*); coughs and colds (*S. suboriculare*) [7]; diabetes mellitus (*S. caryophyllatum*, *S. cumini*, *S. malaccense*, and *S. samarangens*) [8]; etc. A few *Syzygium* species have been extensively studied for their phytochemical as well as their biological activities. Of those, *S. cumini*, *S. samarangense*, and *S. jambos* were the most investigated species with the reported pharmacological activities, including antioxidant, antiviral, anti-diabetic, and hepatoprotective properties [9],[10]. Accordingly,

flavonoids, terpenoids, alkaloids, and their glycosides were mainly found in the *Syzygium* genus [11],[12]. Recently, there have been few publications relating to the chemical constituents and biological activities of the *Syzygium* genus in Vietnam, for example: *S. myrsinifolium* [13], *S. attopeuense* [14], *S. cerasiforme* [15], etc.

In the course of a screening program of the flora in Vietnam, the ethyl acetate extract of *S. cumini* leaves showed significant cytotoxicity against the KB cell line (40.9% inhibition at the concentration of 1 μ g/mL). Thus, herein we report the isolation and structural elucidation of five known compounds, including quercetin 3-*O*-neohesperidoside (**1**), rutin (**2**), quercetin 3-*O*- α -L-rhamnopyranoside (**3**), kaempferol 3-*O*-neohesperidoside (**4**), and afzelin (**5**) (Fig. 1). Also, they were evaluated for their cytotoxicity against four human cancer cell lines (KB, HepG2, A549, and MCF-7).

2. Materials and methods

2.1. Plant materials

The leaves of *Syzygium cumini* were collected in Vinh Linh, Quang Tri, Vietnam, in April 2022

and identified by Dr. Nguyen The Cuong of the Institute of Ecology and Biological Resources, Vietnam Academy of Science and Technology (VAST). A voucher specimen (VN-1236F) was deposited at the Institute of Marine Biochemistry, VAST.

2.2. General experiment procedures

NMR spectra were recorded on a Bruker 600 MHz spectrometer operating at 150 MHz for ^{13}C -NMR and at 600 MHz for ^1H -NMR. The ^1H chemical shift was referenced to CD_3OD at δ_{H} 3.31 ppm, respectively, while the ^{13}C chemical shift was referenced to the solvent peak at δ_{C} 49.0 (CD_3OD). TLC *silica gel* Merck 60 F₂₅₄ was used as thin layer chromatography. Column chromatography (CC) was carried out using *silica gel* 40 - 63 μm , YMC RP-18 (30 - 50 μm), Sephadex LH-20, and Dianion HP-20. Medium pressure liquid chromatography (MPLC) was performed on a Biotage-Isolera One system (Sweden).

2.3. Extraction and isolation

Dried and ground leaves of *S. cumini* (1.0 kg) were extracted with MeOH (5 times \times 4 L, 24 h) at room temperature. The MeOH solutions were combined and concentrated under reduced pressure to obtain 75 g of the MeOH residue. The MeOH residue was suspended in H_2O (1 L) and then partitioned successively with *n*-hexane (5 times \times 1 L), CH_2Cl_2 (5 times \times 1 L), and EtOAc (5 times \times 1 L). The extracts were concentrated under reduced pressure to give *n*-hexane (H, 10 g), CH_2Cl_2 (D, 30 g), EtOAc (E, 15 g), and aqueous extracts (W, 15 g), respectively.

The ethyl acetate extract (E, 15 g) was subjected to MPLC over *silica gel* using mixtures of CH_2Cl_2 and MeOH (0% to 100% MeOH in CH_2Cl_2) to give 7 fractions E1-E7. Fraction E2 (2.2 g) was separated on a Sephadex LH-20 column (MeOH/ CH_2Cl_2 8/2, *v/v*), giving 6 subfractions E2.1-E2.6. Subfraction E2.5 (0.31 g) was purified by C_{18} -reversed phase *silica gel* CC, eluting with $\text{H}_2\text{O}/\text{MeOH}$ (from 0% to 100% MeOH in H_2O) and followed by CC (*n*-hexane/acetone 1/1, *v/v*) to provide **5** (2.0 mg). Fraction E4 (4.5 g) was subjected to CC on Sephadex LH-20 (100% MeOH), giving 8 subfractions E4.1-E4.8. Subfraction E4.7 (1.72 g) was separated by CC on *silica gel* using a mixture of $\text{CH}_2\text{Cl}_2/\text{MeOH}$ (0% to 100% MeOH in CH_2Cl_2) and followed by CC on RP C_{18} eluting with

$\text{H}_2\text{O}/\text{MeOH}$ (from 0% to 100% MeOH in H_2O) to give **3** (4.2 mg). The aqueous extract (W, 15 g) was chromatographed on a Diaion HP-20 column, eluting with $\text{H}_2\text{O}/\text{MeOH}$ (from 0% to 100% MeOH in H_2O) to give 4 fractions W1-W4. Fraction W4 (8.0 g) was separated on a Sephadex LH-20 column (MeOH), giving 6 subfractions W4.1-W4.6. Subfraction W4.2 (1.4 g) was subjected to RP C_{18} CC, eluting with $\text{H}_2\text{O}/\text{MeOH}$ (from 0% to 100% MeOH in H_2O) to give 5 subfractions W4.2.1-W4.2.5. Subfraction W4.2.3 (0.18 g) was purified by CC on Sephadex LH-20 (MeOH), followed by CC on *silica gel* using a mixture of $\text{CH}_2\text{Cl}_2/\text{MeOH}/\text{HCOOH}$ (9/1/0.1, *v/v/v*) to give **1** (2.0 mg). Subfraction W4.2.4 (0.19 g) was subjected to CC on Sephadex LH-20 column (MeOH) to give **2** (2.5 mg) and **4** (2.8 mg).

Quercetin 3-O-neohesperidoside (1): Yellow powder, α_{D}^{25} -213.63 (*c* 0.208, MeOH), ^1H -NMR (600 MHz, CD_3OD , (see Table 2), ^{13}C -NMR (150 MHz, CD_3OD) (see Table 1).

Rutin (2): Yellow powder, α_{D}^{25} +1.64 (*c* 0.60, MeOH) [16], ^1H -NMR (600 MHz, CD_3OD) (see Table 2), ^{13}C -NMR (150 MHz, CD_3OD) (see Table 1).

Quercetin 3-O- α -L-rhamnopyranoside (3): Yellow powder, α_{D}^{25} -145.13 (*c* 0.28, MeOH) [17], ^1H -NMR (600 MHz, CD_3OD) (see Table 2), ^{13}C -NMR (150 MHz, CD_3OD) (see Table 1).

Kaempferol 3-O-neohesperidoside (4): Yellow powder, α_{D}^{25} -128.95 (*c* 0.208, MeOH) [18], ^1H -NMR (600 MHz, CD_3OD) (see Table 2), ^{13}C -NMR (150 MHz, CD_3OD) (see Table 1).

Afzelin (5): Yellow powder, α_{D}^{25} -183.10 (*c* 0.168, MeOH) [19], ^1H -NMR (600 MHz, CD_3OD) (see Table 2), ^{13}C -NMR (150 MHz, CD_3OD) (see Table 1).

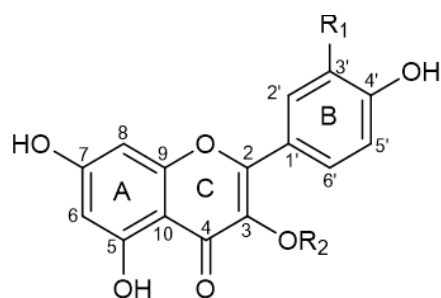
2.4. Cytotoxic assay

The cytotoxic activities of compounds **1-5** were evaluated against KB, HepG2, A549, and MCF-7 human cancer cell lines. The cells were cultured at 37°C in DMEM medium supplemented with 10% fetal bovine serum (FBS), 100 U/mL penicillin, and 100 $\mu\text{g}/\text{mL}$ streptomycin in a 5% CO_2 incubator. Cells between 5 and 20 passages were used for the assays. The cytotoxic activity was measured by using a modified MTT assay [20]. Viable cells were seeded in 96-well plates at a density of 3×10^4 cells/mL. Cells were treated with four concentrations of test compounds (2, 8, 32, and 128 $\mu\text{g}/\text{mL}$) and then incubated at 37°C

for 72 h in fresh DMEM medium. Cells were subsequently incubated at 37°C with MTT (0.5 mg/mL) for 4 h. After removal of the supernatant, formazan crystals were dissolved in DMSO, and the optical density was measured at 540 nm.

Ellipticine was used as a positive control. All cytotoxicity assays were performed in triplicate in three independent experiments.

3. Results and discussion



Compound	Aglycone	R ₁	R ₂
1	Quercetin	OH	Rha-(1→2)-Glc
2	Quercetin	OH	Rha-(1→6)-Glc
3	Quercetin	OH	Rha
4	Kaempferol	H	Rha-(1→2)-Glc
5	Kaempferol	H	Rha

Fig. 1. Structures of the isolated compounds 1-5

Compound **1** was isolated as a yellow solid. The ¹H NMR spectrum of **1** revealed the proton signals of an ABX aromatic ring system at δ_H 7.63 (1H, dd, $J = 2.4, 8.4$ Hz, H-6'), 6.89 (1H, d, $J = 8.4$ Hz, H-5'), 7.64 (1H, d, $J = 2.4$ Hz, H-2') and two *meta*-coupled aromatic protons at δ_H 6.19 (1H, d, $J = 2.4$ Hz, H-6), 6.38 (1H, d, $J = 2.4$ Hz, H-8). Additionally, the ¹H-NMR spectrum of compound **1** exhibited the signals of two sugar moieties, including two anomeric protons at δ_H 5.76 (1H, d, $J = 7.2$ Hz, H-1'') and 5.25 (1H, br s, H-1'''), eight oxymethines at δ_H 3.25-4.07, one oxymethylene at δ_H 3.75 (1H, dd, $J = 2.4, 12.0$ Hz, Ha-6''), 3.56 (1H, dd, $J = 4.2, 12.0$ Hz, Hb-6''), one doublet methyl at δ_H 1.00 (3H, d, $J = 6.0$ Hz, CH₃-6'''), which were characteristic of a β -D-glucopyranosyl and an α -L-rhamnopyranosyl moiety. The ¹³C-NMR spectrum of compound **1** showed the presence of twenty-seven carbon signals, including twelve carbons at δ_C 62.3 (C-6''), 71.7 (C-4''), 78.3 (C-5''), 78.9 (C-3''), 80.1 (C-2''), and 100.4 (C-1'') and 17.6 (C-6'''), 70.0 (C-

5'''), 72.3 (C-3'''), 72.4 (C-2'''), 73.2 (C-4'''), and 102.6 (C-1''') of the glucopyranosyl and rhamnopyranosyl moieties, respectively; fourteen aromatic carbons, and one ketone carbon at δ_C 179.3 (C-4) which were assigned for a flavonoid aglycone. This assignment was supported by the COSY spectrum of **1** which showed three spin-spin interaction systems of protons: H-5'/H-6', H-1''/H-2''/H-3''/H-4''/H-5''/H-6'', and H-1'''/H-2'''/H-3'''/H-4'''/H-5'''/H-6'''. In the HMBC spectrum of **1**, the correlation of H-2'' (δ_H 3.68) with C-1''' (δ_C 102.6), H-1'' (δ_H 5.25) with C-2'' (δ_C 80.1) revealed that the rhamnopyranosyl moiety was connected to the glucopyranosyl moiety at C-2''. Next, the HMBC correlation of the proton H-1'' (δ_H 5.76) with C-3 (δ_C 134.6) determined that the glucopyranosyl moiety was connected to the flavonoid unit at C-3. Thus, the detailed analysis of the 1D and 2D-NMR spectra of **1** and comparison with the literature led to the assignment of **1** as quercetin 3-*O*-neohesperidoside [21].

Table 1. ¹³C-NMR data of compounds 1-5

Carbon	δ_C^a				
	1	2	3	4	5
2	158.4	159.4	158.2	161.3	158.6
3	134.6	135.6	136.2	134.4	136.2
4	179.3	179.5	179.4	179.4	179.7
5	163.2	163.5	166.0	161.3	161.6
6	99.9	100.0	99.9	100.3	99.9
7	166.0	166.1	166.1	166.0	165.9
8	94.6	95.0	94.8	94.7	94.8
9	158.4	158.6	159.3	158.5	159.3
10	105.9	105.7	106.0	105.9	106.0

Carbon	δ_C^a				
	1	2	3	4	5
1'	123.2	123.2	123.0	123.1	122.7
2'	117.2	117.7	117.0	132.1	131.9
3'	146.0	145.9	146.4	116.1	116.5
4'	149.6	149.8	149.8	158.5	163.2
5'	116.0	116.1	116.4	116.1	116.5
6'	123.5	123.6	122.8	132.1	131.9
1''	100.4	104.7	103.6	100.3	103.5
2''	80.1	75.7	72.0	80.1	72.0
3''	78.9	78.2	72.2	78.9	72.2
4''	71.7	71.4	73.2	71.9	73.2
5''	78.3	77.3	71.9	78.4	71.9
6''	62.3	68.6	17.7	62.3	17.7
1'''	102.6	102.4		102.6	
2'''	72.4	72.3		72.4	
3'''	72.3	72.1		72.3	
4'''	74.6	74.0		74.1	
5'''	70.0	69.7		69.9	
6'''	17.6	17.9		17.5	

^a: recorded in methanol-*d*₄ at 150 MHz.

Compound **2** was isolated as a yellow powder. The ¹H-NMR spectrum of **2** was similar to those of **1**, including the characteristic signals of a quercetin aglycone at δ_H 6.21 (1H, d, *J* = 2.4 Hz, H-6), 6.40 (1H, d, *J* = 2.4 Hz, H-8), 7.62 (1H, dd, *J* = 2.4, 8.4 Hz, H-6'), 6.87 (1H, d, *J* = 8.4 Hz, H-5'), and 7.76 (1H, d, *J* = 2.4 Hz, H-2'). Besides, the ¹H-NMR spectrum of **2** also showed the proton signals of a β -D-glucopyranosyl moiety at δ_H 3.47 (1H, m, H-2''), 3.41 (1H, m, H-3''), 3.26 (1H, m, H-4''), 3.33 (1H, m, H-5''), 3.80 (1H, dd, *J* = 1.8, 11.4 Hz, H-6''a), 3.38 (1H, m, H-6'' b), 5.10 (1H, d, *J* = 7.8 Hz, H-1'') and an α -L-rhamnopyranosyl moiety at δ_H 3.62 (1H, dd, *J* = 1.8, 3.6 Hz, H-2'''), 3.52 (1H, dd, *J* = 3.6, 9.6 Hz, H-3'''), 3.28 (1H, m, H-4'''), 3.45 (1H, m, H-5'''), 1.11 (1H, d, *J* = 6.6 Hz, CH₃-6'''), and 4.52 (1H, d, *J* = 1.8 Hz, H-1'''). Analysis of the

¹³C-NMR spectrum with the aid of the HSQC experiment revealed the resonances of twenty-seven carbons, including one carbonyl carbon at δ_C 179.5 (C-4), fourteen aromatic carbon signals, and twelve carbon signals of a rhamnopyranosyl and a glucopyranosyl moieties. In the HMBC spectrum of **2**, the correlation of H-1'' (δ_H 5.10) with C-3 (δ_C 135.6) determined that the glucopyranosyl moiety was connected to the flavonoid unit at C-3. Next, the correlation of H-1''' (δ_H 4.52) with C-6'' (δ_C 68.6) revealed that the rhamnopyranosyl moiety was connected to the glucopyranosyl moiety at C-6'' instead of the C-2'' position in compound **1**. Complete analysis of the 1D, 2D-NMR of **2**, and comparison with the reported values indicated that compound **2** was quercetin-3-*O*-rutinoside or rutin [12],[16],[22].

Table 2. ¹H-NMR data of compounds **1-5**

Proton	δ_H^b mult. (<i>J</i> in Hz)				
	1	2	3	4	5
6	6.19 d (2.4)	6.21 d (2.4)	6.22 d (1.8)	6.20 d (2.4)	6.22 d (1.8)
8	6.38 d (2.4)	6.40 d (2.4)	6.39 d (1.8)	6.40 d (2.4)	6.40 d (1.8)
2'	7.64 d (2.4)	7.76 d (2.4)	7.36 d (2.4)	8.06 d (9.0)	7.78 dd (2.4, 7.2)
3'	-	-	-	6.91 d (9.0)	6.96 dd (2.4, 7.2)
5'	6.89 d (8.4)	6.87 d (8.4)	6.93 d (8.4)	6.91 d (9.0)	6.96 dd (2.4, 7.2)
6'	7.63 dd (2.4, 8.4)	7.62 dd (2.4, 8.4)	7.32 dd (2.4, 8.4)	8.06 d (9.0)	7.78 dd (2.4, 7.2)
1''	5.76 d (7.2)	5.10 d (7.8)	5.37 d (1.8)	5.74 d (7.8)	5.40 d (1.8)
2''	3.68 dd (7.2, 9.0)	3.47 m	4.23 dd (3.0, 1.8)	3.63 t (7.8)	4.24 dd (1.8, 3.0)
3''	3.58 d (9.0)	3.41 m	3.76 dd (3.0, 9.6)	3.57 t (7.8)	3.72 dd (1.8, 3.0)
4''	3.45 dd (2.4, 9.0)	3.26 m	3.36 m	3.32 m	3.35 m
5''	3.25 m	3.33 m	3.44 dd (6.0, 9.6)	3.25 m	3.33 m

Proton	δ_H^b mult. (J in Hz)				
	1	2	3	4	5
6''	3.75 dd (2.4, 12.0) 3.56 dd (4.2, 12.0)	3.80 dd (1.8, 11.4) 3.38 m	0.96 d (6.0)	3.52 dd (5.4, 12.0) 3.74 dd (2.4, 12.0)	0.94 d (6.0)
1'''	5.25 br s	4.52 d (1.8)	-	5.25 br s	-
2'''	4.02 dd (1.8, 3.6)	3.62 dd (1.8, 3.6)	-	4.02 dd (1.8, 3.0)	-
3'''	3.80 dd (3.0, 9.6)	3.52 dd (3.6, 9.6)	-	3.80 dd (3.0, 9.6)	-
4'''	3.38 m	3.28 m	-	3.35 m	-
5'''	4.07 dd (6.0, 9.6)	3.45 m	-	4.05 dd (6.6, 9.6)	-
6'''	1.00 d (6.0)	1.11 d (6.6)	-	0.98 d (6.6)	-

^b recorded in methanol-*d*₄ at 600 MHz

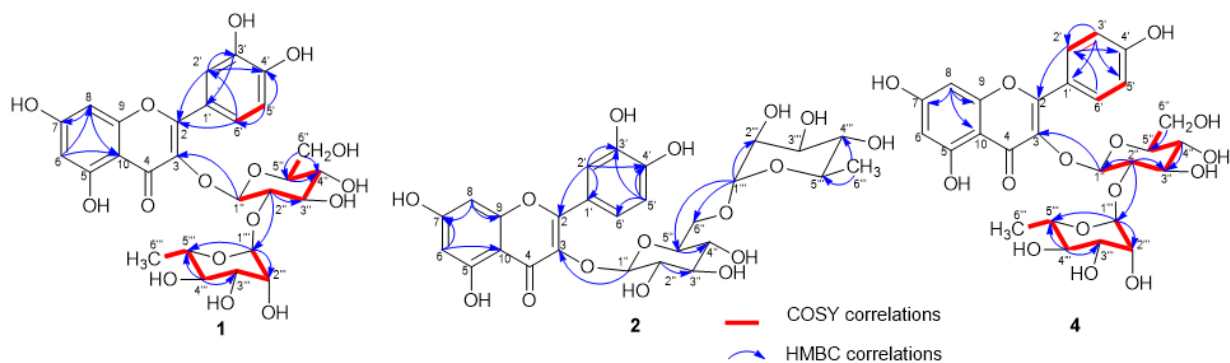


Fig. 2. HMBC and COSY interactions of compounds **1**, **2**, and **4**

Compound **3** was isolated as a yellow powder. The ¹H-NMR spectrum of **3** exhibited the presence of an ABX aromatic ring system at δ_H 7.32 (1H, dd, $J = 2.4, 8.4$ Hz, H-6'), 6.93 (1H, d, $J = 8.4$ Hz, H-5'), 7.36 (1H, d, $J = 2.4$ Hz, H-2'); two *meta*-coupled aromatic protons at δ_H 6.19 (1H, d, $J = 1.8$ Hz, H-6), 6.39 (1H, d, $J = 2.4$ Hz, H-8) and one α -L-rhamnopyranosyl moiety at δ_H 5.37 (1H, d, $J = 1.8$ Hz, H-1'''), 4.23 (1H, dd, $J = 1.8, 3.0$ Hz, H-2'''), 3.76 (1H, dd, $J = 3.0, 9.6$ Hz, H-3'''), 3.36 (1H, m, H-4'''), 3.44 (1H, dd, $J = 6.0, 9.6$ Hz, H-5'''), 0.96 (1H, d, $J = 6.0$ Hz, CH₃-6''). Analysis of the ¹H-NMR and ¹³C-NMR spectra of compound **3** showed similarities with those of compound **1**, except for the disappearance of one glucopyranosyl moiety in compound **3**. On the basis of these data and in comparison with the literature, compound **3** was determined as quercetin-3-*O*- α -L-rhamnopyranoside [23].

Compound **4** was isolated as a yellow powder. The ¹H-NMR spectrum of **4** was similar to those of **1** including two anomeric protons at δ_H 5.74 (1H, d, $J = 7.8$ Hz, H-1'') and 5.25 (1H, br s, H-1'''), eight oxymethines at δ_H 3.25-4.05, one methylene at δ_H 3.52 (1H, dd, $J = 5.4, 12.0$ Hz, Ha-6''), 3.74 (1H, dd, $J = 2.4, 12.0$ Hz, Hb-6''), one

doublet methyl at δ_H 0.98 (3H, d, $J = 6.6$ Hz, CH₃-6'''), which were characteristic of a β -D-glucopyranosyl and an α -L-rhamnopyranosyl moieties, respectively. Additionally, the ¹H-NMR spectrum with the support of the HSQC spectrum of **4** showed the signals of a kaempferol aglycone at δ_H 6.20 (1H, d, $J = 2.4$ Hz, H-6), 6.40 (1H, d, $J = 2.4$ Hz, H-8), 6.91 (2H, d, $J = 9.0$ Hz, H-3', H-5') and 8.10 (2H, d, $J = 9.0$ Hz, H-2', H-6'). The ¹H-¹H COSY spectrum of **4** revealed four spin-spin interaction systems for the following protons: H-2'/H-3', H-5'/H-6', and H-1''/H-2''/H-3''/H-4''/H-5''/H-6'', and H-1'''/H-2'''/H-3'''/H-4'''/H-5'''/H-6''', as shown in Fig. 2. In the HMBC spectrum of **4**, the correlation of H-2'' (δ_H 3.63) with C-1''' (δ_C 102.6), H-1''' (δ_H 5.25) with C-2'' (δ_C 80.1) revealed that the rhamnopyranosyl moiety was connected to the glucopyranosyl moiety at C-2''. Next, the correlation of H-1'' (δ_H 5.74) with C-3 (δ_C 134.4) determined that the glucopyranosyl moiety was connected to the kaempferol unit at C-3. Complete analysis of the 1D, 2D-NMR of **4**, and comparison with the reported values indicated that compound **4** was kaempferol 3-*O*-neohesperidoside [21].

Compound **5** was isolated as a yellow powder.

The ¹H-NMR and ¹³C-NMR spectra of compound **5** showed similarities with those of compound **4**, except for the disappearance of one glucopyranosyl moiety in compound **5**. Thus, on the basis of analysis of the NMR data of **5**, and comparison with the literature, compound **5** was structurally elucidated as kaempferol 3-*O*- α -L-rhamnoside or afzelin [19].

The cytotoxic activities of compounds **1-5** were evaluated *in vitro* against KB, HepG2, A549, and MCF-7 cell lines. Unfortunately, all the compounds were inactive against all tested cell lines at a 128 μ g/mL concentration. These results were consistent with those of compounds **3** and **5**, which were previously reported [24],[25].

4. Conclusion

Investigation of the chemical constituents of the EtOAc and water extracts from the leaves of *Syzygium cumini* resulted in the isolation and

structural elucidation of five flavone glycosides: quercetin 3-*O*-neohesperidoside (**1**), rutin (**2**), quercetin 3-*O*- α -L-rhamnopyranoside (**3**), kaempferol 3-*O*-neohesperidoside (**4**), and afzelin (**5**) on the basis of detailed analyses of their 1D and 2D NMR spectroscopic data and in comparison with the literature values. All isolated compounds (**1-5**) were estimated for their cytotoxicity against KB, MCF-7, HepG2, and A549 human cancer cell lines. However, they were inactive against four tested human cancer cell lines at 128 μ g/mL concentration. To the best of our knowledge, compounds **1** and **4** were first reported from the *Syzygium* genus, while compounds **3** and **5** were isolated from the leaves of *S. cumini* for the first time.

Acknowledgments: This research was financially supported by the Vietnam Academy of Science and Technology (VAST) (Grant No. KHCBS.03/22-24).

References

1. Ahmad B., Baider C., Bernardini B., Biffin E., Brambach F., Burslem D., Byng J. W., Christenhusz M., Florens F., Lucas E. (2016), *Syzygium* (Myrtaceae): Monographing a taxonomic giant via 22 coordinated regional revisions. *PeerJ Preprints*. 4: e1930v1. **2.** Reza A. A., Haque M. A., Sarker J., Nasrin M. S., Rahman M. M., Tareq A. M., Khan Z., Rashid M., Sadik M. G., Tsukahara T. (2021), Antiproliferative and antioxidant potentials of bioactive edible vegetable fraction of *Achyranthes ferruginea* Roxb. in cancer cell line. *Food Science Nutrition*. 9(7), 3777-3805. **3.** Batiha G. E.-S., Alkazmi L. M., Wasef L. G., Beshbishy A. M., Nadwa E. H., Rashwan E. K. (2020), *Syzygium aromaticum* L.(Myrtaceae): Traditional uses, bioactive chemical constituents, pharmacological and toxicological activities. *Biomolecules*. 10(2), 352. **4.** Dharani N. (2016), A review of traditional uses and phytochemical constituents of indigenous *Syzygium* species in East Africa. *Pharmaceutical Journal of Kenya*. 22(4), 123-127. **5.** Jadhav V., Kamble S., Kadam V. (2009), Herbal medicine: *Syzygium cumini*: A review. *Journal of Pharmacy Research*. 2(8), 1212-1219. **6.** Reis A. S., De Sousa Silva L., Martins C. F., De Paula J. R. (2021), Analysis of the volatile oils from three species of the genus *Syzygium*. *Research, Society Development*. 10(7), e13510716375. **7.** Cock I. E., Cheesman M. (2018), Plants of the genus *Syzygium* (Myrtaceae): A review on ethnobotany, medicinal properties and phytochemistry. *Bioactive Compounds of Medicinal Plants: Properties Potential for Human Health*, 35-84. **8.** Ediriweera E., Ratnasooriya W. (2009), A review on herbs used in treatment of diabetes mellitus by Sri Lankan ayurvedic and traditional physicians. *Ayurveda*. 30(4), 373-391. **9.** Sobeh M., Mahmoud M. F., Petruk G., Rezaq S., Ashour M. L., Youssef F. S., El-Shazly A. M., Monti D. M., Abdel-Naim A. B., Wink M. (2018), *Syzygium aqueum*: A polyphenol-rich leaf extract exhibits antioxidant, hepatoprotective, pain-killing and anti-inflammatory activities in animal models. *Frontiers in Pharmacology*. 9, 566. **10.** Sobeh M., Youssef F. S., Esmat A., Petruk G., El-Khatib A. H., Monti D. M., Ashour M. L., Wink M. (2018), High resolution UPLC-MS/MS profiling of polyphenolics in the methanol extract of *Syzygium samarangense* leaves and its hepatoprotective activity in rats with CCl₄-induced hepatic damage. *Food Chemical Toxicology*. 113, 145-153. **11.** Famuyide I. M., Fasina F. O., Eloff J. N., McGaw L. J. (2020), The ultrastructural damage caused by *Eugenia zeyheri* and *Syzygium legatii* acetone leaf extracts on pathogenic *Escherichia coli*. *BMC Veterinary Research*. 16(1), 326. **12.** Rahim E. N. A., Ismail A., Omar M. N., Rahmat U. N., Ahmad W. A. N. W. (2018), GC-MS analysis of phytochemical compounds in *Syzygium polyanthum* leaves extracted using ultrasound-assisted method. *Pharmacognosy Journal*. 10(1), 110-119. **13.** Trang D. T., Tai B. H., Hoang N. H., Cuc N. T., Bang N. A., Dung D. T., Yen D. T. H., Huong P. T. T., Dung N. V., Hang D. T. T., (2024), Undescribed triterpenes from the leaves of *Syzygium myrsinifolium* with their α -glucosidase and α -amylase inhibition activity. *Chemistry & Biodiversity*. 21(3), e202400124. **14.** Van K. P., Hai N. B., Huu T. B., Xuan N. N., Hai Y. P., Huy H. N., Thi T. D., Thi D. D., Van T. N., Tuan A. L., (2023), Undescribed phenolic glycosides from *Syzygium atopeuense* and their inhibition of nitric oxide production. *Chemistry & Biodiversity*. 20(9), e202301037. **15.** Hai N. B., Thi D. D., Huu T. B., Hai Y. P., Xuan N. N., Thi T. H. T., Thi T. D., Van T. N., Tuan A. L., Thi H. N., (2023), New isopropyl chromone and flavanone glucoside compounds from the leaves of *Syzygium cerasiforme* (Blume) Merr. & LM Perry and their inhibition of nitric oxide production. *Chemistry & Biodiversity*. 20(3), e202201048. **16.** Ganbaatar C., Gruner M., Mishig D., Duger G., Schmidt A. W., Knölker H. J. (2015), Flavonoid glycosides from the aerial parts of *Polygonatum odoratum* (Mill.) Druce growing in Mongolia. *The Open Natural Products Journal*. 8(1), 1-7. **17.** Kiem P. V., Minh C. V., Dat N. T., Cai X. F., Lee J. J., Kim Y. H. (2003). Two new phenylpropanoid glycosides from the stem bark of *Acanthopanax trifoliatus*. *Archives of Pharmacal Research*, 26(12), 1014-1017. **18.** Gamez E. J., Luyengi L., Lee S. K., Zhu L. F., Zhou B. N., Fong H. H., Pezzuto J. M., Kinghorn A. D. (1998). Antioxidant flavonoid glycosides from *Daphniphyllum calycinum*. *Journal of Natural Products*. 61(5), 706-708. **19.** Joo S. J.,

Park H. J., Park J. H., Cho J. G., Kang J. H., Jeong T. S., Kang H. C., Lee D. Y., Kim H. S., Byun S. Y. (2014), Flavonoids from *Machilus japonica* stems and their inhibitory effects on LDL oxidation. *International Journal of Molecular Sciences*. 15(9), 16418-16429. **20.** Mosmann T. (1983), Rapid colorimetric assay for cellular growth and survival: application to proliferation and cytotoxicity assays. *Journal of Immunological Methods*. 65(1-2), 55-63. **21.** Kazuma K., Noda N., Suzuki M. (2003), Malonylated flavonol glycosides from the petals of *Clitoria ternatea*. *Phytochemistry*. 62(2), 229-237. **22.** Halim M. A., Kanan K. A., Nahar T., Rahman M. J., Ahmed K. S., Hossain H., Mozumder N. R., Ahmed M., (2022), Metabolic profiling of phenolics of the extracts from the various parts of blackberry plant (*Syzygium cumini* L.) and their antioxidant activities. *Lwt-Food Science and Technology*, 167(113813), 1-10. **23.** Wang K. J., Yang C. R., Zhang Y. J. (2007), Phenolic antioxidants from Chinese toon (fresh young leaves and shoots of *Toona sinensis*). *Food Chemistry*. 101(1), 365-371. **24.** Sun Y. J., Chen H. J., Xue G. M., Chen H., Zhang Y. L., Li M., Du K., Wang J. M., Feng W. S., (2021), Two new flavonoid glucosides from the fruits of *Sinopodophyllum hexandrum*. *Natural Product Research*. 35(13), 2164-2169. **25.** Ngoc N. T., Quang T. H., Hanh T. T. H., Cuong N. X., Cuong N. T., Ha C. H., Nam N. H., Van M. C., (2022), Phenolic glycosides from the leaves of *Iodes cirrhosa* Turcz. with cytotoxic and antimicrobial effects. *Chemistry & Biodiversity*. 19(9), e202200182.

Journal of Medicinal Materials, 2024, Vol. 29, No. 6 (pp. 329 - 334)

CHEMICAL CONSTITUENTS OF THE DICHLOROMETHANE EXTRACT OF *GANODERMA COCHLEAR*

Vu Thi Hanh Yen¹, Nguyen Van Vinh Ha², Tran Viet Hung², Bui Hong Cuong³,
Pham Thi Huong³, Nguyen Thi Duyen^{4,*}

¹The Representative Office of Pharmascience Inc. Ho Chi Minh City, Vietnam;

²Institute of Drug Quality Control Ho Chi Minh City, Vietnam; ³Hanoi University of Pharmacy, Vietnam;

⁴National Institute of Medicinal Materials (NIMM), Hanoi, Vietnam

*Corresponding author: nguyenduyen6784@gmail.com

(Received September 07th, 2024)

Summary

Chemical Constituents of the Dichloromethane Extract of *Ganoderma cochlear*

From the dichloromethane extract of *Ganoderma cochlear*, five compounds (**1** - **5**) were isolated by column chromatography. Their chemical structures were identified as fornicatin F (**1**), 1-tetracosanoylglycerol (**2**), (22*E*)-ergosta-7,9(11),22-trien-3 β -ol (**3**), polycarpol (**4**), and lucidenic acid N (**5**) based on spectral data and literature references. Compounds **2** - **5** were isolated from *G. cochlear* for the first time.

Keywords: *Ganoderma cochlear*, 1-tetracosanoylglycerol, (22*E*)-ergosta-7,9(11),22-trien-3 β -ol, Lucidenic acid N.

1. Introduction

Ganoderma cochlear (Nees) Merr., belongs to the Ganodermataceae family. The species is popular in Tay Nguyen and is often used as a substitute for *G. lucidum* to enhance immunity and hepatoprotective effects [1]. Up-to-date phytochemical studies have shown over 90 compounds, including mainly triterpenoids, sterols, phenols, and especially alkaloids [2],[3],[4],[5],[6],[7],[8],[9],[10],[11],[12]. Scientific studies *in vitro* have shown the species has valuable effects such as anti-inflammatory [4], hepatoprotective [2], renoprotective [3],[6],[8], neuroprotective [7], anti-oxidant [11], and cytotoxic activity [5],[13],[14]. These activities are mainly attributed to terpenoids and phenolic compounds. However, in Vietnam, there is only one study on the chemical constituents of this mushroom [15]. In this study, we isolated and identified five compounds (**1** - **5**) from the dichloromethane extract of *Ganoderma*

cochlear: fornicatin F (**1**), 1-tetracosanoylglycerol (**2**), (22*E*)-ergosta-7,9(11),22-trien-3 β -ol (**3**), polycarpol (**4**), and lucidenic acid N (Fig.1). Among them, compounds **2** - **5** are reported for the first time from *G. cochlear*.

2. Materials and methods

2.1. Plant materials

The samples were collected in Kon Ka Kinh Park, Gialai, in December 2023. The mushroom was identified as *Ganoderma cochlear* (Nees) Merr., which belongs to the Ganodermataceae family, by Assoc. Prof. Nguyen Phuong Dai Nguyen. A voucher specimen (GC122023) was deposited at the National Institute of Medicinal Materials.

2.2. General experiment procedures

The NMR measurements were conducted using CD₃OD and CDCl₃ as solvents on a Bruker NMR spectrometer with a frequency of 500 or 600 MHz. Tetramethylsilane was used as an internal

standard, and chemical shifts were reported in δ (ppm). Electrospray Ionization Mass Spectrometry (ESI-MS) was performed using an Agilent 1100 series LC-MSD ion trap spectrometer. Column chromatography was performed using *silica gel* (70-230 or 230-400 mesh, Merck) and YMC (ODS-A 12 nm, S-75 μ m, Japan) as the stationary phase. Thin Layer Chromatography (TLC) was carried out on *silica gel* 60 F₂₅₄ plates (Merck). Spots were detected by UV radiation (245 and 365 nm) or by spraying with 10% H₂SO₄ followed by heating.

2.3. Extraction and isolation

The dried and pulverized *G. cochlear* (10.0 kg) was extracted with 240 L 80% ethanol (v/v) for 3 hours at 70 °C, and concentrated under reduced pressure to yield total extract (TGC, 510 g, 5.1%). The total extract was suspended in water and successively extracted with dichloromethane (DCM), ethyl acetate (EtOAc), and *n*-butanol. The solvents were evaporated *in vacuo* to obtain corresponding dichloromethane (DGC, 37.3 g), ethyl acetate (EGC, 102 g), *n*-butanol (BGC, 85.6 g), and water (WGC, 274.5 g) extracts, respectively.

The DGC extract (35 g) was chromatographed on a *silica gel* column, eluting with gradient solvents of *n*-hexane/EtOAc/methanol (50/1/1 - 5/1/1 - 100% MeOH, v/v/v) to give 6 fractions (A-F). Fraction A (3.9 g) was continuously separated on a *silica gel* column, eluting with gradient solvents of *n*-hexane/acetone (15/1 - 1/1, v/v) to afford 3 fractions (A1 - A3). Fraction A1 (985 mg) was crystallized and washed five times with *n*-hexane/methanol (3/1, v/v) to yield compound **1** (21 mg) and a washing solution. Compound **2** (7 mg) was yielded from the concentrated residue of the washing solution (255 mg) by a *silica gel* column with an eluent of *n*-hexane/acetone (5/1, v/v). Fraction A3 (927 mg) was separated on a *silica gel* column, eluting with *n*-hexane/acetone (3/1, v/v) to afford compounds **3** (12 mg) and **4** (14 mg). Fraction C (1.1 g) was further separated on a *silica gel* column, eluting with DCM/MeOH (15/1, v/v) to give 3 fractions (C1 - C3). Compound **5** (12 mg) was obtained from fraction C1 (72 mg) by a YMC column with an eluent of MeOH/water (5/1, v/v).

Compound **1** (fornicatin F): colorless needles. UV (MeOH) λ_{\max} 256 và 201 nm. $[\alpha]_{\text{D}}^{+87.2}$ (*c* 0.1, MeOH). ESI-MS *m/z*: 489.5 [M+H]⁺,

C₂₉H₄₄O₆. ¹H-NMR (600 MHz, CDCl₃) δ_{H} (ppm): 5.07 & 4.84 (2H, s, H-28), 4.27 (1H, br s, H-7), 3.67 (3H, s, 24-OAc), 3.63 (3H, s, 3-OAc), 1.84 (3H, s, H-29), 1.27 (3H, s, H-19), 1.12 (3H, s, H-30), 0.95 (3H, s, H-18), 0.87 (3H, d, *J* = 6.6 Hz, H-21). ¹³C-NMR (125 MHz, CD₃OD) δ_{C} (ppm): 200.0 (C-11), 174.5 (C-24), 174.2 (C-3), 161.3 (C-8), 147.9 (C-4), 137.4 (C-9), 115.0 (C-28), 66.7 (C-7), 52.1 (C-14), 51.6 (3-OAc), 51.5 (24-OAc), 51.4 (C-12), 50.2 (C-17), 45.5 (C-13), 45.1 (C-5), 39.1 (C-10), 35.9 (C-20), 33.4 (C-1), 32.5 (C-6), 31.2 (C-22), 31.0 (C-23), 30.6 (C-15), 29.5 (C-2), 27.3 (C-16), 26.7 (C-30), 24.4 (C-29), 22.6 (C-19), 18.1 (C-21), 17.9 (C-18).

Compound **2** (1-tetracosanoylglycerol): white powder. ESI-MS *m/z*: 443.6 [M+H]⁺, C₂₇H₅₄O₄. ¹H-NMR (600 MHz, CDCl₃) δ_{H} (ppm): 4.20 (1H, dd, *J* = 3.6, 14.4 Hz, H-1' α), 4.16 (1H, dd, *J* = 4.8, 11.4 Hz, H-1' β), 3.90 (1H, br s, H-2'), 3.60 - 3.70 (2H, m, H-3'), 2.35 (2H, t, *J* = 6.6 Hz, H-2), 1.26 - 1.33 (40H, m, H-3→H-22), 1.26 - 1.33 (2H, m, H-23), 0.88 (3H, t, *J* = 6.6 Hz, H-24). ¹³C-NMR (150 MHz, CDCl₃) δ_{C} (ppm): 174.2 (C-1), 70.3 (C-2'), 65.2 (C-1'), 63.4 (C-3'), 34.2 (C-2), 24.9 - 31.9 (C-3 - C-22), 22.7 (C-23), 14.1 (C-24).

Compound **3** ((22*E*)-ergosta-7,9(11),22-trien-3 β -ol): white powder. ESI-MS *m/z*: 395.40 [M-H]⁻, C₂₈H₄₄O. ¹H-NMR (500 MHz, CDCl₃) δ_{H} (ppm): 5.57 (1H, dd, *J* = 3.0, 5.5 Hz, H-11), 5.39 (1H, dd, *J* = 3.0, 5.5 Hz, H-7), 5.23 (1H, dd, *J* = 7.0, 15.0 Hz, H-22), 5.18 (1H, dd, *J* = 7.5, 15.0 Hz, H-23), 3.62 (1H, dd, *J* = 4.5, 10.5 Hz, H-3), 1.04 (3H, d, *J* = 6.5 Hz, H-21), 0.95 (3H, s, H-19), 0.92 (3H, d, *J* = 7.0 Hz, H-28), 0.84 (3H, d, *J* = 7.0 Hz, H-27), 0.83 (3H, d, *J* = 7.0 Hz, H-26), 0.63 (3H, s, H-18). ¹³C-NMR (125 MHz, CDCl₃) δ_{C} (ppm): 141.8 (C-9), 139.8 (C-8), 135.6 (C-23), 132.0 (C-22), 119.6 (C-11), 116.3 (C-7), 70.5 (C-3), 55.8 (C-17), 54.6 (C-14), 46.3 (C-5), 42.9 (C-13), 42.9 (C-24), 40.8 (C-12), 40.4 (C-20), 39.1 (C-4), 38.4 (C-1), 37.1 (C-10), 33.1 (C-25), 32.0 (C-2), 28.3 (C-6), 23.2 (C-16), 21.1 (C-21), 21.1 (C-15), 20.0 (C-27), 19.7 (C-26), 17.6 (C-28), 16.3 (C-19), 12.1 (C-18).

Compound **4** (polycarpol): white amorphous solid. $[\alpha]_{\text{D}}^{+87}$ (*c* 1.25, CHCl₃). ESI-MS *m/z*: 439.35 [M-H]⁻, C₃₀H₄₈O₂. ¹H-NMR (600 MHz, CDCl₃) δ_{H} (ppm): 5.48 (1H, d, *J* = 6.0 Hz, H-7), 5.32 (1H, d, *J* = 6.0 Hz, H-11), 5.15 (1H, t, *J* = 7.2 Hz, H-24), 3.68 (1H, dd, *J* = 6.0, 9.6 Hz, H-15), 3.25 (1H, d, *J* = 4.2, 12.0 Hz, H-3), 1.73 (3H, s, H-

27), 1.64 (3H, s, H-26), 1.10 (3H, s, H-29), 0.99 (3H, s, H-19), 0.92 (3H, s, H-30), 0.91 (3H, d, $J = 6.6$ Hz, H-21), 0.89 (3H, s, H-28), 0.58 (3H, s, H-18). $^{13}\text{C-NMR}$ (150 MHz, CDCl_3) δ_{C} (ppm): 145.9 (C-9), 142.7 (C-8), 134.5 (C-25), 121.0 (C-24), 120.2 (C-7), 116.3 (C-11), 79.0 (C-3), 73.4 (C-15), 50.3 (C-14), 49.1 (C-17), 47.2 (C-5), 43.7 (C-13), 40.5 (C-20), 38.7 (C-4), 37.9 (C-16), 37.4 (C-10), 35.7 (C-12), 34.4 (C-22), 31.5 (C-1), 28.2 (C-28), 27.8 (C-2), 27.3 (C-23), 25.9 (C-27), 25.7 (C-19), 23.0 (C-6), 22.8 (C-21), 18.2 (C-26), 15.8 (C-30), 15.6 (C-18), 11.7 (C-29).

Compound **5** (lucidenic acid N): white power. ESI-MS m/z : 485.3 $[\text{M-H}]^-$, $\text{C}_{27}\text{H}_{40}\text{O}_6$. $^1\text{H-NMR}$

(500 MHz, CD_3OD) δ_{H} (ppm): 4.85 (1H, dd, $J = 9.5, 8.0$ Hz, H-7), 3.17 (1H, dd, $J = 5.0, 12.0$ Hz, H-7), 1.39 (3H, s, H-30), 1.23 (3H, s, H-19), 1.04 (3H, s, H-29), 1.00 (3H, d, $J = 7.0$ Hz, H-21), 0.99 (3H, s, H-18), 0.86 (3H, s, H-28). $^{13}\text{C-NMR}$ (125 MHz, CD_3OD) δ_{C} (ppm): 218.8 (C-15), 200.5 (C-11), 177.6 (C-24), 158.8 (C-8), 144.1 (C-9), 79.0 (C-3), 68.0 (C-7), 60.5 (C-14), 51.5 (C-12), 50.3 (C-5), 47.0 (C-17), 46.7 (C-13), 41.9 (C-16), 39.9 (C-10), 39.7 (C-4), 36.4 (C-20), 36.0 (C-1), 31.9 (C-22), 31.7 (C-23), 28.7 (C-29), 28.3 (C-2), 28.0 (C-6), 24.9 (C-30), 18.9 (C-19), 18.5 (C-21), 17.8 (C-18), 16.2 (C-28).

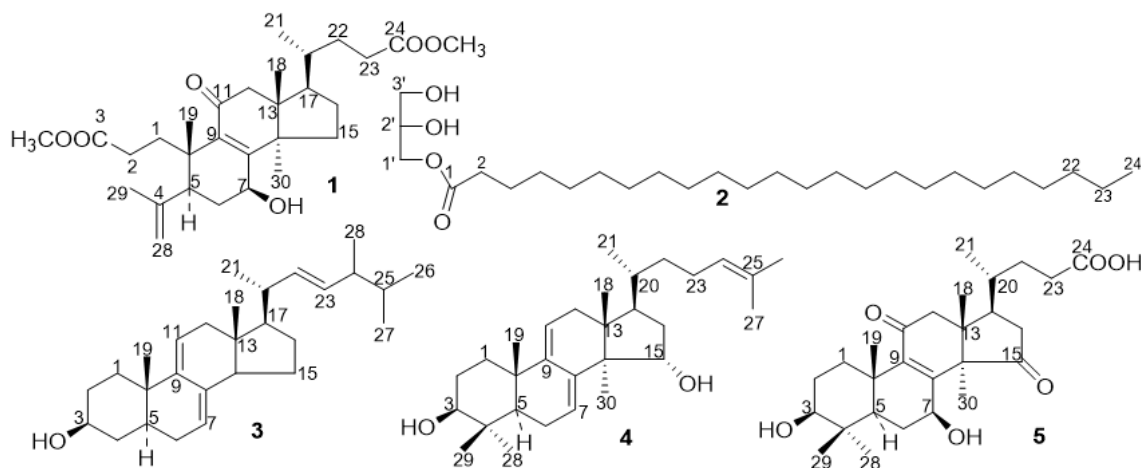


Fig. 1. Chemical structures of compounds (1-5)

3. Results and discussion

Compound **1** was isolated as colorless needles. It had a molecular formula of $\text{C}_{29}\text{H}_{44}\text{O}_6$ based on the ESI-MS spectrum with a peak at m/z 489.5 $[\text{M+H}]^+$. The 1D-NMR spectra of **1** showed the characteristic signals of a 3,4-*seco*-trinorlanostane-triterpenoid. The $^1\text{H-NMR}$ spectrum of **1** showed five methyl groups at δ_{H} 1.84 (3H, s, H-29), 1.27 (3H, s, H-19), 1.12 (3H, s, H-30), 0.95 (3H, s, H-18), and 0.87 (3H, d, $J = 6.6$ Hz, H-21); two methoxy groups at δ_{H} 3.67 (3H, s, 24-OAc) and 3.63 (3H, s, 3-OAc); one hydroxymethine group at δ_{H} 4.27 (1H, br s, H-7); and one methylene group at δ_{H} 4.84 and 5.07 (2H, s, H-28). The $^{13}\text{C-NMR}$ spectrum exhibited 29 carbons: five methyl signals at δ_{C} 26.7 (C-30), 22.6 (C-19), 24.4 (C-29), 17.9 (C-18), and 18.1 (C-21); one hydroxymethine signal at δ_{C} 66.7 (C-7); four olefinic signals at δ_{C} 115.0 (C-28), 147.9 (C-4), 161.3 (C-8), and 137.4 (C-9); and one ketone signal at δ_{C} 200.0

(C-11). Moreover, the $^{13}\text{C-NMR}$ spectrum showed 2 methyl signals at δ_{C} 51.6 and 51.5 and 2 carbonyl signals at δ_{C} 174.5 and 174.2, which indicated the presence of 2 ester groups. The HMBC correlations of H-22 (δ_{H} 2.33 - 2.34 and 2.22 - 2.27), H-23 (δ_{H} 2.34 - 2.36 and 1.26 - 1.36), and methyl (δ_{H} 3.67) with C-24 (δ_{C} 177.5) indicated the ester group at C-24; and the correlations of H-2 (δ_{H} 1.99 - 2.08 and 2.22 - 2.27), H-1 (δ_{H} 2.09 - 2.13), and methyl (δ_{H} 3.63) with C-3 (δ_{C} 174.2) indicated that the remaining ester group was positioned at C-3 (see Fig. 2). Furthermore, the long-range correlations of H-28 (δ_{H} 5.07 and 4.84) with C-5 (δ_{C} 45.1) and C-29 (δ_{C} 24.4) and the correlations of H-5 (δ_{H} 2.13) with C-4 (δ_{C} 147.9), C-6 (δ_{C} 32.5) and C-7 (δ_{C} 66.7) confirmed a 3,4-*seco*-lanostane compound, that is the characteristic structure from *G. cochlear*. The 7β -OH-configuration was assigned based on the coincidence of NMR spectroscopic

data and $[\alpha]_D$ value. Compound **1** was identified as methyl 7 β -hydroxy-11-oxo-3,4-*seco*-25,26,27-trinorlanosta-4(28),8-diene-3,24-diester, and named fornicatin F [2].

Compound **2** was isolated as a white powder. Its molecular formula was determined to be C₂₇H₅₄O₄ based on the ESI-MS spectrum with a peak at m/z 443.6 [M+H]⁺. The ¹H-NMR spectrum of **2** showed a triplet signal for a methyl group at δ_H 0.88 (3H, t, J = 6.6 Hz, H-24); signals of 22 methylene groups at δ_H from 1.26 to 2.35; and five signals at δ_H 4.20 (1H, dd, J = 3.6, 14.4 Hz, H-1' α), 4.16 (1H, dd, J = 4.8, 11.4 Hz, H-1' β), 3.90 (1H, br s, H-2') and 3.60 - 3.70 (2H, m, H-3') corresponding to two oxymethylene and one oxymethine groups. The ¹³C-NMR spectrum displayed 27 carbon signals, including one carbonyl group at δ_C 174.2 (C-1); one oxymethine and two oxymethylene groups at δ_C 70.3 (C-2'), 65.2 (C-1') and 63.4 (C-3'); 22 methylene groups at δ_C from 24.9 to 34.2; and one methyl group at δ_C 14.1 (C-24). The HMBC correlations of H-2 (δ_H 2.34) with C-1 (δ_C 174.2) and C-3 (δ_C 24.9); and H-1' (δ_H 4.20 and 4.16) with C-1 (δ_C 174.2) indicated the ester group at C-1. Compound **2** was identified as 1-tetracosanoylglycerol, based on the above spectroscopic evidence and by comparison to the published literature [16]. Compound **2** is isolated from *G. cochlear* for the first time.

Compound **3** was obtained as a white powder. The ESI-MS spectrum with a peak at m/z 395.4 [M-H]⁻ suggested the molecular formula of **3** as C₂₈H₄₄O. The ¹H-NMR spectrum of **3** showed the presence of six methyl groups at δ_H 1.04 (3H, d, J = 7.0 Hz, H-21), 0.95 (3H, s, H-19), 0.92 (3H, d, J = 7.0 Hz, H-28), 0.84 (3H, d, J = 7.0 Hz, H-27), 0.83 (3H, d, J = 7.0 Hz, H-26), and 0.63 (3H, s, H-18); one hydroxymethine group at δ_H 3.62 (1H, dd, J = 4.5, 10.5 Hz, H-3); four olefinic protons at δ_H 5.57 (1H, dd, J = 3.0, 5.5 Hz, H-11), 5.39 (1H, dd, J = 3.0, 5.5 Hz, H-7), 5.23 (1H, dd, J = 7.0, 15.0 Hz, H-22) and 5.18 (1H, dd, J = 7.5, 15.0 Hz, H-23). The *E*-configuration of the C-22/C-23 double bond was deduced from the coupling constants J = 15.0 Hz of H-22 and H-23 [17]. The ¹³C-NMR spectrum displayed 28 carbon signals, including six methyl signals at δ_C 21.1 (C-21), 20.0 (C-27), 19.7 (C-26), 17.6 (C-28), 16.3 (C-19), and 12.1 (C-18); one hydroxymethine signal at δ_C 70.5; six olefinic signals at δ_C 116.3 (C-7), 139.8 (C-8),

132.0 (C-22), 135.6 (C-23), 141.8 (C-9), and 119.6 (C-11). The HMBC correlations of H-7 (δ_H 5.39) with C-8 (δ_C 139.8) and C-5 (δ_C 46.3); and H-11 (δ_H 5.57) with C-12 (δ_C 40.8), C-10 (δ_C 37.1) and C-9 (δ_C 141.8) indicated that the 2 double bonds were located at C-7/C-8 and C-9/C-11. The HMBC correlations of H-22 (δ_H 5.23) with C-20 (δ_C 40.4) and C-23 (δ_C 135.6); and H-23 (δ_H 5.18) with C-22 (δ_C 132.0) and C-24 (δ_C 42.9) confirmed the remaining double bond at C-22/C-23. Based on the above evidence and by comparison to the published literature [17], compound **3** was identified as (22*E*)-ergosta-7,9(11),22-trien-3 β -ol. This compound is reported for the first time from *G. cochlear*.

Compound **4** was obtained as a white amorphous solid. Its molecular formula was determined to be C₃₀H₄₈O₂ based on the ESI-MS spectrum with a peak at m/z 439.4 [M-H]⁻. The 1D-NMR spectra of **4** showed the characteristic signals of a lanostane-triterpenoid. The ¹H-NMR spectrum of **4** showed 8 methyl groups, including 7 *singlet* signals at δ_H 1.73 (3H, s, H-27), 1.64 (3H, s, H-26), 1.10 (3H, s, H-29), 0.99 (3H, s, H-19), 0.92 (3H, s, H-30), 0.89 (3H, s, H-28), and 0.58 (3H, s, H-18) and 1 *doublet* signal at δ_H 0.91 (3H, d, J = 6.6 Hz, H-21); 2 hydroxymethine signals at δ_H 3.68 (1H, dd, J = 6.0, 9.6 Hz, H-15) and 3.25 (1H, dd, J = 4.2, 12.0 Hz, H-3); 3 olefinic signals at δ_H 5.48 (1H, d, J = 6.0 Hz, H-7), 5.32 (1H, d, J = 6.0 Hz, H-11) and 5.15 (1H, t, J = 7.2 Hz, H-24). The ¹³C-NMR and DEPT showed thirty carbon signals, including 8 methyl groups at δ_C 28.2 (C-28), 25.9 (C-27), 25.7 (C-19), 22.8 (C-21), 18.2 (C-26), 15.8 (C-30), 15.6 (C-18) và 11.7 (C-29); 2 hydroxymethine groups at δ_C 79.0 (C-3) and 73.4 (C-15); 6 olefinic carbons at δ_C 145.9 (C-9), 116.3 (C-11), 120.2 (C-7), 142.7 (C-8), 121.0 (C-24) and 134.5 (C-25). Based on the comparison to the published literature [18], compound **4** was identified as polycarpol. This compound is isolated from *G. cochlear* for the first time.

Compound **5** was isolated as a white powder. The ESI-MS spectrum with a peak at m/z 459.5 [M-H]⁻ suggested the molecular formula of **5** as C₂₇H₄₀O₆. The 1D-NMR spectra of **5** showed characteristic signals of a trinorlanostane-triterpenoid. The ¹H-NMR spectrum of **5** showed 6 methyl signals, including 5 *singlet* signals at δ_H 1.39 (3H, s, H-30), 1.23 (3H, s, H-19), 1.04 (3H, s, H-29), 0.99 (3H, s, H-18) and 0.86 (3H, s, H-28) and

1 doublet signal at δ_{H} 1.00 (3H, d, $J = 7.0$ Hz, H-21); two hydroxymethine signals at δ_{H} 4.85 (1H, dd, $J = 9.5, 8.0$ Hz, H-7) and 3.17 (1H, dd, $J = 5.0, 12.0$ Hz, H-3). The β -configuration of hydroxyl groups (3-OH and 7-OH) was deduced from the coupling constants of H-3 ($J = 5.0, 12.0$ Hz) and H-7 ($J = 9.5, 8.0$ Hz) and was compared with the published data [19]. The ^{13}C -NMR and DEPT showed twenty-seven carbon signals, including 6 methyl groups at δ_{C} 28.7 (C-29), 24.9 (C-30), 18.9 (C-19), 18.5 (C-

21), 17.8 (C-18) and 16.2 (C-28); 2 hydroxymethine groups at δ_{C} 79.0 (C-3) and 68.0 (C-7); one olefinic group at δ_{C} 158.8 (C-8) and 144.1 (C-9); 3 carbonyl groups at δ_{C} 218.8 (C-15), 200.5 (C-11) and 177.6 (C-24). The carbon signals were assigned by comparison to the published literature [19]. Thus, compound **5** was identified as lucidenic acid N [19]. This compound is reported for the first time from *G. cochlear*.

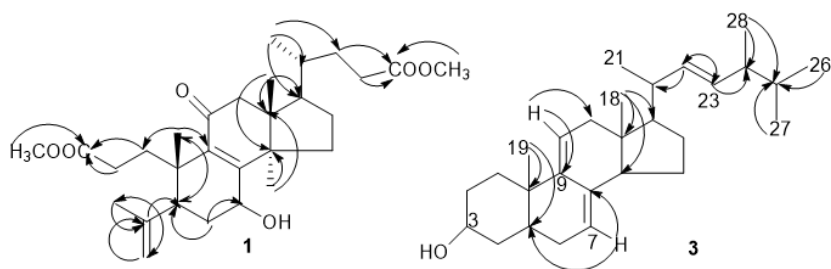


Fig. 2. The HMBC correlations of compounds **1** and **3**

4. Conclusion

Five compounds were obtained from the dichloromethane extract of *G. cochlear*, including fornicatin F (**1**), 1-tetracosanoylglycerol (**2**), (22*E*)-ergosta-7,9(11),22-trien-3 β -ol (**3**), polycarpol (**4**) and lucidenic acid N (**5**). The structures of these compounds were established by spectral data

and literature references. Among them, compounds **2** - **5** were isolated from *G. cochlear* for the first time.

Acknowledgments: We thank MSc. Dang Vu Luong for the NMR and Assoc. Prof. Nguyen Phuong Dai Nguyen for the collection and identification of *Ganoderma cochlear*. We acknowledge the study participants for their gracious help.

References

- Nguyen P. D. N. (2015), The diversity of *Ganoderma* genus in Kon Ka Kinh national park, Tay Nguyen, Vietnam (in Vietnamese), *The 6th national scientific conference on ecology and biological resources in Institute of Ecology and Biological Resource*, 738-742.
- Peng X. R., Liu J. Q., Wang C. F., Li, X. Y., Shu Y., Zhou L., Qiu M. H. (2014), Hepatoprotective effects of triterpenoids from *Ganoderma cochlear*, *Journal of Natural Products*, 77(4), 737-743.
- Wang X. L., Zhou F. J., Dou M., Yan Y. M., Wang S. M., Di L., Cheng Y. X. (2016), Cochlearoids F-K: phenolic meroterpenoids from the fungus *Ganoderma cochlear* and their renoprotective activity, *Bioorganic and Medicinal Chemistry Letters*, 26(22), 5507-5512.
- Peng X. R., Huang Y. J., Lu S. Y., Yang J., Qiu M. H. (2018), Ganolearic acid A, a hexanorlanostane triterpenoid with a 3/5/6/5-fused tetracyclic skeleton from *Ganoderma cochlear*, *Journal of Organic Chemistry*, 83(21), 13178-13183.
- Peng X. R., Wang X., Zhou L., Hou B., Zuo Z. L., Qiu M. H. (2015), Ganocochlearic acid A, a rearranged hexanorlanostane triterpenoid, and cytotoxic triterpenoids from the fruiting bodies of *Ganoderma cochlear*, *RSC Advances*, 5(115), 95212-95222.
- Wang X. L., Wu Z. H., Di, L., Zhou F. J., Yan Y. M., Cheng Y. X. (2019), Renoprotective meroterpenoids from the fungus *Ganoderma cochlear*, *Fitoterapia*, 132, 88-93.
- Peng X. R., Liu J. Q., Wan L. S., Li X. N., Yan Y. X., Qiu M. H. (2014), Four new polycyclic meroterpenoids from *Ganoderma cochlear*, *Organic Letters*, 16(20), 5262-5265.
- Wang X. L., Wu Z. H., Di, L., Zhou F. J., Yan Y. M., Cheng Y. X. (2019), Renoprotective phenolic meroterpenoids from the mushroom *Ganoderma cochlear*, *Phytochemistry*, 162, 199-206.
- Wang X. L., Dou M., Luo Q., Cheng L. Z., Yan Y. M., Li R. T., Cheng Y. X. (2017), Racemic alkaloids from the fungus *Ganoderma cochlear*, *Fitoterapia*, 116, 93-98.
- Lei T., Wang X. -L., Wang Y. -Z., Cheng Y. X. (2015), Two new alkaloids from *Ganoderma cochlear*, *Natural Product Research and Development*, 27(8), 1325-1328.
- Peng X., Liu J., Wang C., Han Z., Shu Y., Li X., Zhou L. Qiu M. (2015), Unusual prenylated phenols with antioxidant activities from *Ganoderma cochlear*, *Food Chemistry*, 171, 251-257.
- Dou M., Li R. T., Cheng Y. X. (2016), Minor compounds from fungus *Ganoderma cochlear*, *Chinese Herbal Medicines*, 8(1), 85-88.
- Qin F. Y., Yan Y. M., Tu Z. C., Cheng Y. X. (2020), (\pm) Ganocochlearols A and B: cytotoxic and COX-2 inhibitory meroterpenoids from *Ganoderma cochlear*, *Natural Product Research*, 34(16), 2269-2275.
- Qin F. Y., Yan Y. M., Tu Z. C., Cheng Y. X. (2018), Meroterpenoid dimers from *Ganoderma cochlear* and their cytotoxic and COX-2 inhibitory activities, *Fitoterapia*, 129, 167-172.
- Nguyen T. D.,

Tran T. T., Hoang D. M., Le T. N., Nguyen P. D. N., Nguyen V. T. (2021), Triterpenoids from the ethyl acetate fraction of *Ganoderma cochlear* (Nees) Merr., *Journal of Medicinal Materials*, 26(6), 277-281. **16.** Hernández G. E., García A., Avalos A. F. G., Rivas G. V. M., Delgadillo P. C., del Rayo C. C. M. (2019), Nuclear magnetic resonance spectroscopy data of isolated compounds from *Acacia farnesiana* (L.) Willd fruits and two esterified derivatives, *Data in Brief*, 22, 255-268. **17.** Huang G. J., Huang S. S., Lin S. S., Shao Y. Y., Chen C. C., Hou W. C., Kuo Y. H. (2010), Analgesic effects and the mechanisms of anti-inflammation of ergostatrien-3 β -ol from *Antrodia camphorata* submerged whole broth in mice, *Journal of Agricultural and Food Chemistry*, 58(12), 7445-7452. **18.** Jung J. H., Pummangura S., Chaichantipyuth C., Patarapanich C., McLaughlin J. L. (1990), Bioactive constituents of *Melodorum fruticosum*, *Phytochemistry*, 29(5), 1667-1670. **19.** Wubshet S. G., Johansen K. T., Nyberg N. T., Jaroszewski J. W. (2012), Direct ¹³C NMR detection in HPLC hyphenation mode: aAalysis of *Ganoderma lucidum* terpenoids, *Journal of Natural Products*, 75(5), 876-882.

Journal of Medicinal Materials, 2024, Vol. 29, No. 6 (pp. 334 - 339)

STEROID AND TRITERPENOID COMPOUNDS ISOLATED FROM *AMANITA PANTHERINA* AND THEIR ANTI-INFLAMMATORY ACTIVITY

To Dao Cuong^{1,*}, Hoang Le Minh¹, Nguyen Phuong Dai Nguyen², Nguyen Huu Kien²,
Nguyen Thi Hoa¹, Truong Thi Viet Hoa¹, Truong Thi Thuy Nhung¹

¹Phenikaa University Nano Institute (PHENA), Phenikaa University, Hanoi, Vietnam;

²Tay Nguyen University, Buon Ma Thuot City, Dak Lak, Vietnam

*Corresponding author: cuong.todao@phenikaa-uni.edu.vn

(Received October 06th, 2024)

Summary

Steroid and Triterpenoid Compounds Isolated from *Amanita pantherina* and their Anti-Inflammatory Activity

Phytochemical research of the ethanolic extract of *Amanita pantherina* sensu Gonnermann & Rabenhorst led to the isolation of six steroids (1–6) and a triterpenoid (7), using various chromatographic separations. Their structures were elucidated to be β -sitosterol (1), stigmasterol (2), cycloeucalenol (3), spinasterol (4), daucosterol (5), stigmasterol 3-*O*- β -D-glucoside (6), and betulin (7) by detailed analysis of NMR spectroscopic records and comparison with those reported. Compound 7 showed the most inhibitory activity (IC₅₀ = 33.4 μ M) against the LPS-induced NO production in macrophage RAW 264.7 cells, followed by compound 3 with an IC₅₀ value of 48.2 μ M. Compounds 1, 2, and 4 exhibited weak inhibitory activity with IC₅₀ values of 92.8, 64.9, and 62.4 μ M, respectively, while compounds 5 and 6 were inactive (IC₅₀ > 100 μ M). This is the first time compounds 3 and 7 have been evaluated for their inhibitory effects on NO production. In addition, compounds 2, 3, and 7 showed weak inhibitory activity against tumor necrosis factor-alpha (TNF- α) with IC₅₀ values of 83.9, 72.8, and 58.1 μ M, respectively.

Keywords: *Amanita pantherina* sensu Gonnermann & Rabenhorst, Sterol, Inflammatory activity, NO production, Cytotoxic, RAW264.7 cells.

1. Introduction

Amanita pantherina sensu Gonnermann & Rabenhorst has fascinated both traditional cultures and modern researchers due to its striking appearance and complex biochemical properties. Historically, it has been used in rituals and conventional medicine. Today, its bioactivity, particularly muscimol and ibotenic acid, has drawn attention to potential therapeutic applications despite its toxicity [1],[2]. In contemporary research, the bioactivity of *A. pantherina* has garnered attention for its potential therapeutic applications. Studies have revealed that this mushroom contains compounds such as alkaloids (muscimol and ibotenic acid) and sterols [3],[4]. Research has highlighted various health

benefits of *A. pantherina*, including its potential neuroactive properties [3]. While primarily recognized for its psychoactive properties, the anti-inflammatory effects of *A. pantherina*, specifically through nitric oxide inhibition, remain underexplored. Given the risks associated with its toxicity, this study focuses on *in vitro* research to evaluate the safety and efficacy of its compounds. Nitric oxide is produced from L-arginine by nitric oxide synthases (NOS), with the inducible form (iNOS) being upregulated by inflammatory stimuli. Elevated NO levels contribute to tissue damage and inflammatory diseases, making iNOS inhibitors of significant interest [5],[6]. Therefore, compounds inhibiting iNOS and reducing NO production greatly interest anti-inflammatory research. This

study elucidates how *A. pantherina* may contribute to anti-inflammatory strategies, linking traditional knowledge with modern scientific research.

2. Materials and Methods

2.1. General experimental procedures

The NMR spectra (^1H - and ^{13}C -NMR) were recorded by the Bruker Avance 500 and 600 MHz spectrometers (Bruker Daltonics, Ettlingen, Germany). *Silica gel* (Si 60 F₂₅₄, 40-63 mesh, Merck, St. Louis, MO, USA), YMC GEL (ODS-A, 12 nm S-150 μm , YMC Co., Ltd., Kyoto, Japan), and Sephadex LH-20 (Sigma-Aldrich, MO, USA) were utilized for column chromatography (CC). Before use, all solvents were redistilled. TLC plates pre-coated, including *Silica gel* 60 F₂₅₄ and RP-C18 F_{254S} (Merck, Darmstadt, Germany), were employed for analytical purposes. Compounds were detected by UV radiation (254 nm and 365 nm) after eluting with the solvent system or spraying with 10% H₂SO₄, followed by heating using a heat gun.

2.2. Plant materials

The fruiting body of *A. pantherina* was collected in February 2023 from Dak Lak province, Vietnam. Botanical identification was performed by Assoc. Prof. Dr. Nguyen Phuong Dai Nguyen at Tay Nguyen University and a voucher specimen (AP-FB-04022023) has been submitted to the Department of Biology, Faculty of Natural Sciences and Technology, Tay Nguyen University.

2.3. Extraction and isolation

The fruiting bodies of *A. pantherina* (0.5 kg) were removed impurities, cut into small pieces, washed, dried, and ground into powder. The dried powder was then extracted using methanol (MeOH, three times, 3 \times 2.0 L) by refluxing. After evaporating the solvent, 50 g of MeOH extract was suspended in hot water and then successfully partitioned to obtain dichloromethane- (CH₂Cl₂, 10.5 g), ethyl acetate- (EtOAc, 12.3 g), and water-soluble (27.2 g) fractions. The CH₂Cl₂ fraction (10.5 g) was subjected to *silica gel* column chromatography (CC) with *n*-hexane - acetone (50:1 - 0:1) to obtain eight fractions (APD1-APD8). Fraction APD2 (1.1 g) was purified via *silica gel* CC and eluted with *n*-hexane - EtOAc (30:1 - 10:1), producing four sub-fractions (APD2.1 to APD2.4). The sub-fraction APD2.3 (250 mg) was processed on an ODS column and

then eluted with acetone - water (2:1 - 5:1), yielding compounds **1** (10.2 mg) and **2** (8.9 mg). The APD3 fraction (450 mg) was also subjected to *silica gel* CC with *n*-hexane - EtOAc (15:1 to 7:1), resulting in three sub-fractions (APD3.1-APD3.3). Sub-fraction APD3.3 (80 mg) was further purified using an ODS column and eluted with acetone - water (3:1 - 5:1), leading to the isolation of compounds **3** (5.2 mg) and **4** (6.5 mg). The APD5 fraction (1.6 g) was also subjected to *silica gel* CC with *n*-hexane:

EtOAc (5:1 - 1:1) to obtain five sub-fractions (APD5.1-APD5.5). Sub-fraction APD5.4 (120 mg) was further purified using an ODS column and then eluted with MeOH - water (2:1 to 4:1), resulting in the isolation of compounds **5** (5.5 mg) and **6** (6.2 mg). The APD7 fraction (4.5 g) was subjected to *silica gel* CC with CH₂Cl₂-EtOAc (10:1 to 1:1), resulting in fourteen sub-fractions (APD7.1-APD7.14). Sub-fraction APD7.7 (65 mg) was further purified using an ODS column and eluted with methanol:water (1:1 - 4:1), leading to the isolation of compound **7** (3.8 mg).

Compound **1**: White powder; ^1H -NMR (500 MHz, CDCl₃) δ_{H} (ppm): 3.51 (1H, m, H-3), 5.35 (1H, t, $J = 4.5$ Hz, H-6), 0.90 (3H, d, $J = 6.4$ Hz, CH₃-21), 0.81 (3H, t, $J = 7.2$ Hz, CH₃-29), 0.83 (3H, d, $J = 6.4$ Hz, CH₃-26), 0.78 (3H, d, $J = 6.4$ Hz, CH₃-27), 0.68 (3H, s, CH₃-18), 0.98 (3H, s, CH₃-19); ^{13}C -NMR (125 MHz, CDCl₃) δ_{C} (ppm): 37.3 (C-1), 40.1 (C-2), 72.2 (C-3), 42.5 (C-4), 141.1 (C-5), 121.8 (C-6), 32.1 (C-7), 31.8 (C-8), 50.5 (C-9), 36.9 (C-10), 21.2 (C-11), 40.2 (C-12), 42.5 (C-13), 57.1 (C-14), 26.5 (C-15), 28.6 (C-16), 56.5 (C-17), 36.6 (C-18), 19.5 (C-19), 34.4 (C-20), 24.4 (C-21), 46.2 (C-22), 23.1 (C-23), 12.3 (C-24), 29.3 (C-25), 20.2 (C-26), 19.5 (C-27), 19.1 (C-28), 11.8 (C-29).

Compound **2**: White powder; ^1H -NMR (500 MHz, CDCl₃) δ_{H} (ppm): 3.53 (1H, m, H-3), 5.37 (1H, br d, $J = 4.5$ Hz, H-6), 5.15 (1H, dd, $J = 3.5$, 15.5 Hz, H-22), 5.02 (1H, dd, $J = 3.5$, 15.5 Hz, H-23), 0.92 (3H, d, $J = 6.5$ Hz, CH₃-21), 0.83 (3H, d, $J = 6.5$ Hz, CH₃-26), 0.81 (3H, d, $J = 6.5$ Hz, CH₃-27), 0.84 (3H, t, $J = 6.5$ Hz, H-29), 0.70 (3H, s, CH₃-18), 1.01 (3H, s, CH₃-19); ^{13}C -NMR (125 MHz, CDCl₃) δ_{C} (ppm): 37.3 (C-1), 31.7 (C-2), 71.8 (C-3), 42.4 (C-4), 140.8 (C-5), 121.6 (C-6), 31.9 (C-7), 32.1 (C-8), 50.2 (C-9), 36.6 (C-10), 21.1 (C-11), 39.7 (C-12), 42.4 (C-13), 56.9 (C-14),

24.4 (C-15), 29.0 (C-16), 56.1 (C-17), 12.1 (C-18), 19.4 (C-19), 40.6 (C-20), 21.1 (C-21), 138.4 (C-22), 129.3 (C-23), 51.3 (C-24), 31.9 (C-25), 21.3 (C-26), 19.0 (C-27), 25.4 (C-28), 12.3 (C-29).

Compound 3: White powder; $^1\text{H-NMR}$ (500 MHz, CDCl_3) δ_{H} (ppm): 4.72 (1H, br s, H-30a), 4.67 (1H, br s, H-30b), 3.22 (1H, m, H-3), 2.24 (1H, m, H-17), 1.04 (3H, d, $J = 6.5$ Hz, CH_3 -27), 1.03 (3H, $J = 6.5$ Hz, CH_3 -26), 0.99 (3H, d, $J = 6.5$ Hz, CH_3 -28), 0.98 (3H, s, CH_3 -18), 0.91 (3H, d, $J = 5.5$ Hz, CH_3 -21), 0.90 (3H, s, CH_3 -29), 0.39 (1H, d, $J = 4.5$ Hz, H-19a), 0.15 (1H, d, $J = 4.5$ Hz, H-19b); $^{13}\text{C-NMR}$ (125 MHz, CDCl_3) δ_{C} (ppm): 31.0 (C-1), 35.0 (C-2), 76.8 (C-3), 44.8 (C-4), 43.5 (C-5), 24.9 (C-6), 25.4 (C-7), 47.1 (C-8), 23.8 (C-9), 29.7 (C-10), 28.3 (C-11), 33.1 (C-12), 45.6 (C-13), 49.1 (C-14), 35.6 (C-15), 27.2 (C-16), 52.4 (C-17), 18.0 (C-18), 27.5 (C-19), 36.4 (C-20), 18.6 (C-21), 35.2 (C-22), 31.5 (C-23), 157.1 (C-24), 34.0 (C-25), 22.2 (C-26), 22.1 (C-27), 14.6 (C-28), 19.3 (C-29), 106.1 (C-30).

Compound 4: White powder; $^1\text{H-NMR}$ (500 MHz, CDCl_3) δ_{H} (ppm): 3.59 (1H, m, H-3), 5.15 (1H, overlapped, H-7), 5.15 (1H, overlapped, H-22), 5.03 (1H, dd, $J = 5.0, 12.5$ Hz, H-23), 1.03 (3H, d, $J = 5.5$ Hz, CH_3 -21), 0.81 (3H, d, $J = 5.5$ Hz, CH_3 -26), 0.80 (3H, d, $J = 5.5$ Hz, CH_3 -27), 0.83 (3H, t, $J = 6.5$ Hz, CH_3 -29); 0.54 (3H, s, CH_3 -18), 0.82 (3H, s, CH_3 -19); $^{13}\text{C-NMR}$ (125 MHz, CDCl_3) δ_{C} (ppm): 37.2 (C-1), 31.6 (C-2), 71.1 (C-3), 38.1 (C-4), 40.5 (C-5), 29.7 (C-6), 117.5 (C-7), 139.6 (C-8), 49.6 (C-9), 34.3 (C-10), 21.6 (C-11), 39.6 (C-12), 43.2 (C-13), 55.2 (C-14), 23.1 (C-15), 28.6 (C-16), 56.0 (C-17), 12.1 (C-18), 13.0 (C-19), 40.8 (C-20), 21.5 (C-21), 138.3 (C-22), 129.4 (C-23), 51.3 (C-24), 31.9 (C-25), 21.2 (C-26), 19.0 (C-27), 25.4 (C-28), 12.3 (C-29).

Compound 5: White amorphous powder; $^1\text{H-NMR}$ (500 MHz, $\text{DMSO-}d_6$) δ_{H} (ppm): 3.43 (1H, m, H-3), 5.32 (1H, s, H-6), 0.93 (3H, d, $J = 6.5$ Hz, CH_3 -21), 0.83 (3H, t, $J = 7.0$ Hz, CH_3 -29); 0.84 (3H, t, $J = 6.5$ Hz, CH_3 -26), 0.81 (3H, d, $J = 6.5$ Hz, CH_3 -27), 0.68 (3H, s, CH_3 -18), 1.00 (3H, s, CH_3 -19), 4.22 (1H, d, $J = 7.5$ Hz, H-1'), 2.90-3.12 (4H, m, H-2'/H-3'/H-4'/H-5'), 3.40 (1H, m, H-6'a), 3.64 (1H, dd, $J = 6.0, 10.0$ Hz, H-6'b); $^{13}\text{C-NMR}$ (125 MHz, $\text{DMSO-}d_6$) δ_{C} (ppm): 36.8 (C-1), 29.3 (C-2), 76.9 (C-3), 38.3 (C-4), 140.4 (C-5), 121.1 (C-6), 31.4 (C-7), 31.3 (C-8), 49.6 (C-9), 36.2 (C-10), 20.6 (C-11), 39.0 (C-12), 41.8 (C-13), 56.2 (C-14), 23.8 (C-15), 27.7 (C-16), 55.4 (C-17), 11.6 (C-18), 18.9 (C-19), 35.4 (C-20), 18.6 (C-21), 33.3 (C-22), 25.5 (C-23), 45.1 (C-24),

28.7 (C-25), 19.7 (C-26), 19.1 (C-27), 22.6 (C-28), 11.7 (C-29), 100.8 (C-1'), 73.4 (C-2'), 76.8 (C-3'), 70.1 (C-4'), 76.7 (C-5'), 61.1 (C-6').

Compound 6: White amorphous powder; $^1\text{H-NMR}$ (600 MHz, Pyridine- d_5) δ_{H} (ppm): 3.95 (1H, m, H-3), 5.34 (1H, br d, $J = 4.8$ Hz, H-6), 5.22 (1H, dd, $J = 9.0, 15.0$ Hz, H-22), 5.06 (1H, dd, $J = 9.0, 15.0$ Hz, H-23), 0.97 (3H, d, $J = 6.6$ Hz, CH_3 -21), 0.91 (3H, d, $J = 6.6$ Hz, CH_3 -27), 0.86 (3H, d, $J = 6.6$ Hz, CH_3 -27), 0.89 (3H, t, $J = 6.6$ Hz, H-29), 0.67 (3H, s, CH_3 -18), 0.94 (3H, s, CH_3 -19), 5.04 (1H, d, $J = 7.5$ Hz, H-1'), 4.55 (1H, d, $J = 2.4, 11.4$ Hz, H-6'a), 4.55 (1H, d, $J = 5.4, 11.4$ Hz, H-6'b), 3.94-4.27 (4H, m, H-2'/H-3'/H-4'/H-5'); $^{13}\text{C-NMR}$ (150 MHz, Pyridine- d_5) δ_{C} (ppm): 37.5 (C-1), 30.3 (C-2), 71.8 (C-3), 42.4 (C-4), 141.0 (C-5), 121.9 (C-6), 32.2 (C-7), 32.1 (C-8), 50.4 (C-9), 37.0 (C-10), 21.1 (C-11), 39.4 (C-12), 40.8 (C-13), 57.0 (C-14), 24.6 (C-15), 29.3 (C-16), 56.1 (C-17), 12.2 (C-18), 19.4 (C-19), 39.9 (C-20), 21.3 (C-21), 138.8 (C-22), 129.5 (C-23), 51.4 (C-24), 32.2 (C-25), 21.5 (C-26), 19.2 (C-27), 25.7 (C-28), 12.5 (C-29), 102.6 (C-1'), 78.6 (C-5'), 78.5 (C-3'), 78.1 (C-2'), 75.4 (C-4'), 62.9 (C-6').

Compound 7: White powder; $^1\text{H-NMR}$ (500 MHz, CDCl_3) δ_{H} (ppm): 4.69 (1H, br s, H-29b), 4.58 (1H, br s, H-29a), 3.81 (1H, d, $J = 11.5$ Hz, H-28a), 3.36 (1H, d, $J = 11.5$ Hz, H-28b), 3.21 (1H, dd, $J = 11.5, 5.5$ Hz, H-3), 1.67 (3H, s, CH_3 -30), 1.02 (3H, s, CH_3 -26), 0.96 (3H, s, CH_3 -27), 0.94 (3H, s, CH_3 -23), 0.84 (3H, s, CH_3 -25), 0.76 (3H, s, CH_3 -24), 0.67 (1H, br d, $J = 9.5$ Hz, H-5); $^{13}\text{C-NMR}$ (125 MHz, CDCl_3) δ_{C} (ppm): 38.9 (C-1), 27.5 (C-2), 79.0 (C-3), 38.8 (C-4), 55.6 (C-5), 18.6 (C-6), 34.6 (C-7), 39.3 (C-8), 50.7 (C-9), 37.4 (C-10), 21.3 (C-11), 25.6 (C-12), 37.2 (C-13), 41.2 (C-14), 27.1 (C-15), 29.7 (C-16), 47.0 (C-17), 48.7 (C-18), 48.1 (C-19), 150.8 (C-20), 29.9 (C-21), 34.3 (C-22), 28.3 (C-23), 15.6 (C-24), 16.5 (C-25), 16.3 (C-26), 14.9 (C-27), 60.7 (C-28), 109.8 (C-29), 19.4 (C-30).

2.4. Cell culture

The RAW 264.7 cells (from American Type Culture Collection, ATCC, USA) were cultured in Dulbecco's Modified Essential Medium (DMEM) supplemented with streptomycin (100 $\mu\text{g}/\text{mL}$), penicillin (100 units/mL), and 10% heat-inactivated fetal bovine serum (FBS, Cambrex, Charles City, IA, USA). The RAW 264.7 cells were maintained in a humidified 5% CO_2 atmosphere at a temperature of 37 $^{\circ}\text{C}$.

2.5. Cell viability assay

The MTS (3-(4,5-dimethylthiazol-2-yl)-5-(3-carboxymethoxyphenyl)-2-(4-sulfophenyl)-2H-tetrazolium) assay was employed to determine the viability of the cells [7]. Briefly, the RAW264.7 cells in DMEM (supplemented with 10% FBS and 1% penicillin-streptomycin) were plated in a 96-well plate. After incubation for 24 hours, the medium was replaced, the compounds (diluted with DMSO at varying concentrations) were added, and continued incubation for 24 hours. 20 μL of MTS was then added to each well and the absorbance was measured at 490 nm by microplate reader.

2.6. NO and TNF- α productions inhibitory activities

Measurement of nitrite in cell culture supernatants to determine the level of NO production. After being seeded in 24-well plates and incubated for 12 h, the RAW 264.7 cells (at a density of 1×10^5 cells/well) were treated with compounds (at concentrations of 1, 3, 10, and 30 μM) in DMEM without FBS. After 1 h treatment,

the RAW 264.7 cells were stimulated with or without 1 $\mu\text{g}/\text{mL}$ of LPS for 24 hours. The Griess reagent was employed to determine the nitrite levels [7]. Briefly, the mixture, including 100 μL of cell culture medium and 100 μL of Griess reagent, was incubated at room temperature for 10 min, and the absorbance was measured at 540 nm by a microplate reader (Biotek, Winooski, VT, USA). A blank sample (fresh culture medium) was employed in each experiment. A sodium nitrite (NaNO_2) standard curve was employed to determine the quantity of nitrite. The amount of TNF- α in the culture supernatant was measured using the ELISA kit (R&D Systems, Minneapolis, MN, USA). N(G)-monomethyl L-arginine (L-NMMA, 1-30 μM) was employed as a positive control in this experiment.

3. Result and Discussion

3.1. Determination of chemical structure

Screening tests of the CH_2Cl_2 soluble fraction from *A. pantherina* extracts led to the isolation of seven secondary metabolites (1–7) through column chromatography.

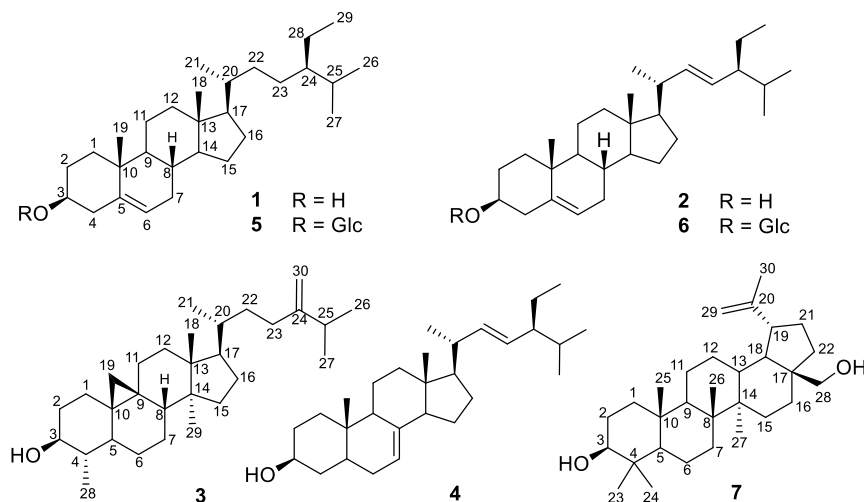


Fig. 1. Structure of the isolated compounds (1-7) from *A. pantherina*.

Compound **3** was isolated as a white powder. The $^1\text{H-NMR}$ spectrum of compound **3** showed signals for protons on a carbon-carbon double bond [δ_{H} 4.72 (1H, br s, H-30a), 4.67 (1H, br s, H-30b)], an oxymethine proton [δ_{H} 3.22 (1H, m, H-3)], and methylene protons [δ_{H} 0.39 (1H, d, $J = 4.5$ Hz, H-19a), 0.15 (1H, d, $J = 4.5$ Hz, H-19b)]. Signals at δ_{H} 1.04 (3H, d, $J = 6.5$ Hz, CH_3 -27), 1.03 (3H, $J = 6.5$ Hz, CH_3 -26), 0.99 (3H, d, $J = 6.5$ Hz, CH_3 -28), 0.98 (3H, s, CH_3 -18), 0.91 (3H, d, J

= 5.5 Hz, CH_3 -21), and 0.90 (3H, s, CH_3 -29) in the $^1\text{H-NMR}$ spectrum of **3** indicate six methyl groups (Fig. 1). The $^{13}\text{C-NMR}$ spectrum displayed 30 carbon signals, including an oxymethine carbon [δ_{C} 76.8 (C-3)], six methyl carbons [C-18/C-21/C-26/C-27/C-28/C-29], and two carbon at δ_{C} 157.1 (C-24) and 106.1 (C-30), suggesting the presence of an olefinic group at C-24 (Fig. 1). It was confirmed by heteronuclear multiple bond correlation (HMBC) correlations from H-30a, H-

30b, CH₃-26, and CH₃-27 to C-24. The HMBC correlation from CH₃-28 to C-3 confirmed the position of the hydroxyl group at C-3. Furthermore, the HMBC correlations from CH₃-18 to C-13, C-14, and C-17, CH₃-21 to C-17 and 20, and CH₃-29 to C-13 and C-14 were also observed. The further detailed analysis of both 1D- and 2D-NMR spectra provides strong evidence for the structure of compound **3**. Thus, compound **3** was identified as cycloeucalenol [8].

Compound **7** was isolated as a white powder. The ¹H-NMR spectrum showed angular methyl protons at δ_H 1.67 (3H, s, CH₃-30), 1.02 (3H, s, CH₃-26), 0.96 (3H, s, CH₃-27), 0.94 (3H, s, CH₃-23), 0.84 (3H, s, CH₃-25), and 0.76 (3H, s, CH₃-24), indicating six methyl groups in the compound. The ¹H-NMR showed the proton of H-3 appeared as a doublet of a doublet at δ_H 3.21 (1H, dd, *J* = 11.5, 5.5 Hz, H-3) and a hydroxymethyl group [δ_H 3.81 (1H, d, *J* = 11.5 Hz, H-28a), 3.36 (1H, d, *J* = 11.5 Hz, H-28b)]. It also showed two olefinic protons at δ_H 4.69 (1H, br s, H-29b) and 4.58 (1H, br s, H-29a) representing the exocyclic double bond (Fig. 1). The ¹³C-NMR spectrum of the compound indicated 30 carbon signals for the terpenoid of lupane skeleton, which includes a carbon bonded to the OH group at C-3 position appearing at δ_C 79.0 ppm, six methyl carbons at δ_C 28.3 (C-23), 15.6 (C-24), 16.5 (C-25), 16.3 (C-26), 14.9 (C-27), and 19.4 (C-30), and a hydroxymethyl carbon at δ_C 60.7 (C-28). The olefinic carbons of the exocyclic double bond appeared at δ_C 150.8 ppm and 109.8 ppm, which are assigned as C-20 and C-29 double bonds of the lupane-type triterpenoid compound (Fig. 1). Thus, the isolated compound was identified as betulin (**7**), which was consistent with the reported literature values [9].

The remaining compounds were identified as β-sitosterol (**1**) [10], stigmasterol (**2**) [10], spinasterol (**4**) [11], daucosterol (**5**) [12], and stigmasterol 3-*O*-β-D-glucoside (**6**) [13] by detailed analysis of NMR spectroscopic records and comparison with those reported.

3.2. NO and TNF-α productions inhibition activities

In the initial experiment, the cytotoxic effects of the seven isolates (**1–7**) were evaluated using the MTS assay [7]. The results indicated that the isolated compounds exhibited no toxicity to the RAW 264.7 cells at concentrations below 100 μM, with cell viability consistently maintained at over 90% (data not shown). Based on these findings, concentrations of 1, 3, 10, and 30 μM were chosen for further experiments to evaluate the effects of the compounds on NO production.

In the second research phase, the anti-inflammatory properties of the seven isolated compounds (**1–7**) were thoroughly evaluated using the Griess reaction assay on the RAW 264.7 cell line [7]. The results showed that compound **7** exhibited the most potent inhibitory activity, with an IC₅₀ value of 33.4 μM, followed by compound **3** with an IC₅₀ value of 48.2 μM, indicating their effectiveness in suppressing inflammatory processes within this cell line. Compounds **1**, **2**, and **4** exhibited weak inhibitory activity with IC₅₀ values of 92.8, 64.9, and 62.4 μM, respectively. In contrast, compounds **5** and **6** demonstrated no significant anti-inflammatory activity (IC₅₀ > 100 μM) (Table 1). In addition, these compounds were further investigated on the LPS-induced TNF-α release. Except for compounds **1** and **4–6**, pretreatment of cells with compounds **2**, **3**, and **7** in several concentrations (1–30 μM) decreased the TNF-α production (Table 1).

Table 1. *In vitro* inhibitory activity of the isolates (**1–7**) on NO and TNF-α productions

Compound	NO (IC ₅₀ , μM) ^a	TNF-α (IC ₅₀ , μM) ^a
1	92.8 ± 3.2	> 100
2	64.9 ± 4.1	83.9 ± 5.2
3	48.2 ± 2.4	72.8 ± 6.0
4	62.4 ± 4.2	> 100
5	> 100	> 100
6	> 100	> 100
7	33.4 ± 1.6	58.1 ± 4.4
L-NMMA ^b	21.5 ± 0.2	14.2 ± 0.8

^a Results are represented as IC₅₀ value (μM); ^b Positive control; The data are expressed as the mean ± SD of three replicates (n = 3).

In the control group without LPS or compounds, NO accumulation increased approximately 9-fold after incubation for 24 hours. When compounds **3** and **7** were tested at concentrations of 1, 3, 10, and 30 μM , they reduced the nitrite accumulation in a dose-dependent manner following LPS-stimulated RAW 264.7 cells (Fig. 2). This finding further highlights the anti-inflammatory effect of compounds **3** and **7**, as they effectively inhibited NO production even in the presence of LPS-induced inflammatory stimulation.

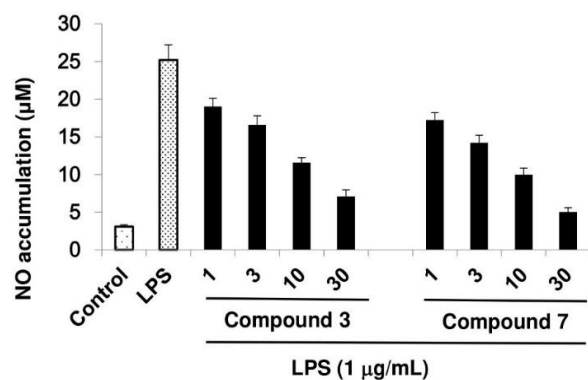


Fig. 2. Inhibition of LPS-induced NO production in RAW 264.7 cells by compounds **3** and **7**. Control values were recorded in the absence of both the compounds and LPS. The results are presented as the mean \pm SD of triplicates ($n = 3$).

4. Conclusion

Seven compounds (**1–7**) were isolated from the fruiting body of *A. pantherina*. Their chemical structures were determined by NMR data and compared with the literature. The anti-inflammatory activity of the isolates (**1–7**) was evaluated by inhibiting LPS-induced NO production in macrophage RAW 264.7 cells. Compound **7** showed the most potent inhibitory activity on NO production with an IC_{50} value of 33.4 μM , followed by compound **3** with an IC_{50} value of 48.2 μM . Compounds **1**, **2**, and **4** showed IC_{50} values of 94.8, 64.9, and 62.4 μM , respectively, while **5** and **6** were inactive ($\text{IC}_{50} > 100 \mu\text{M}$). This is the first time compounds **3** and **7** have been evaluated for their inhibitory effects on NO production. In addition, compounds **2**, **3**, and **7** showed weak inhibitory activity against $\text{TNF-}\alpha$ with IC_{50} values of 83.9, 72.8, and 58.1 μM , respectively. The results suggested that *A. pantherina* and compounds **3** and **7** are promising candidates for further research and potential development as therapeutic agents targeting inflammatory processes.

Acknowledgments: This research is funded by the National Foundation for Science and Technology Development (NAFOSTED) under grant number 108.05-2020.06.

References

- Handl L., Nováček M., Štín R., Čechurová L. (2023), Loss of consciousness and prolonged convulsions due to *Amanita pantherina* intoxication, *Neuroendocrinology Letters*, 44(8), 500-505.
- Vendramin A., Brvar M. (2014), *Amanita muscaria* and *Amanita pantherina* poisoning: two syndromes, *Toxicol*, 90, 269-272.
- Ramawad H. A., Paridari P., Jabermoradi S., Gharin P., Toloui A., Safari S., Yousefifard M. (2023), Muscimol as a treatment for nerve injury-related neuropathic pain: a systematic review and meta-analysis of preclinical studies, *The Korean Journal of Pain*, 36(4), 425-440.
- Yaoita Y., Endo M., Tani Y., Machida K., Amemiya K., Furumura K., Kikuchi M. (1999), Sterol constituents from seven mushroom, *Chemical and Pharmaceutical Bulletin*, 47(6), 847-851.
- Cinelli M. A., Do H. T., Miley G. P., Silverman R. B. (2020), Inducible nitric oxide synthase: Regulation, structure, and inhibition, *Medicinal Research Reviews*, 40(1), 158-189.
- Król M., Kepinska M. (2020), Human nitric oxide synthase—Its functions, polymorphisms, and inhibitors in the context of inflammation, diabetes and cardiovascular diseases, *International Journal of Molecular Sciences*, 22(1), 56.
- Hoang L. M., Hoa T. T. V., Thuy N. T. T., Nguyen H. T., Nguyen P. H., Nguyen N. P. D., Ngu T. N., Truong P. C. H., Tram N. T. T., To D. C. (2024), Nitric oxide inhibitors from the stem bark of *Biancaea decapetala*: An *in vitro* and *in silico* study, *Revista Brasileira de Farmacognosia*, 34(3), 666-672.
- Kikuchi T., Kadota S., Tsubono K. (1986), Studies on the constituents of Orchidaceous plants. IV.¹ Proton and carbon-13 signal assignments of cycloeucaenol-type triterpenes from *Nervilia purpurea* SCHLECHTER by two-dimensional nuclear magnetic resonance spectroscopy, *Chemical and Pharmaceutical Bulletin*, 34(6), 2479-2486.
- Ayatollahi S. A., Shojaii A., Kobarfard F., Nori M., Fathi M., Choudhari M. I. (2009), Terpenes from aerial parts of *Euphorbia splendida*, *Journal of Medicinal Plants Research* 3(9), 660-665.
- Pusparohmana W., Safitry R., Marliana E., Kusuma I. (2020), Isolation and characterization of stigmaterol and β -sitosterol from wood bark extract of *Baccaurea macrocarpa* Miq. Mull. Arg., *Rasayan Journal of Chemistry*, 13(4), 2552-2558.
- Ragasa C. Y., Lim K. (2005), Sterols from *Cucurbita maxima*, *Philippine Journal of Science*, 134(2), 83-87.
- Joe N. P. (2020), Isolation, identification and characterization of daucosterol from root of *Mangifera indica*, *Biomedical Journal of Scientific & Technical Research*, 29(5), 22773-22776.
- Ridhay A., Noor A., Soekamto N. H., Harlim T., van Altena I. (2012), A stigmaterol glycoside from the root wood of *Melochia umbellata* (Houtt) Stapf var. *degrabrata* K., *Indonesian Journal of Chemistry*, 12(1), 100-103.

DETERMINATION OF STRYCHNINE AND BRUCINE BY HPLC FOR BETTER QUALITY CONTROL OF *STRYCHNI SEMEN*

Vu Ngan Binh¹, Pham Thi Thanh Ha¹, Dang Thi Ngoc Lan¹,
Do Thi Bich Diep¹, Nguyen Quynh Chi¹, Do Quyen^{1*},
Huynh Truc Thanh Ngoc², Nguyen Thi Ngoc Dung²,
Sysay Palamy³, Chiobouaphony Phakeovilay³

¹Hanoi University of Pharmacy, Vietnam; ²Faculty of Pharmacy, University of Medicine and Pharmacy at Ho Chi Minh City, Vietnam; ³Faculty of Pharmacy, University of Health Sciences Laos

*Corresponding author: doquyen@hup.edu.vn

(Received September 28th, 2024)

Summary

Determination of Strychnine and Brucine by HPLC for Better Quality Control of *Strychni semen*

In the 5th Vietnamese pharmacopoeial monograph for *Strychni semen*, 19 species of the genus *Strychnos* are accepted as medicinal material, and the quality of *Strychni semen* varies significantly. In this study, a high-performance liquid chromatographic (HPLC) method is used to identify and quantify strychnine and brucine in 12 *Strychni semen* samples collected from different regions in Vietnam and Laos. Based on the alkaloid content in combination with the morphological properties of the analyzed samples, some comments on measures to improve quality control of *Strychni semen* were suggested for the Vietnam market.

Keywords: *Strychnine*, *Brucine*, *Strychni semen*, HPLC, Quality control.

1. Introduction

Strychni semen is a precious traditional medicine of Vietnam, which is included in Vietnamese pharmacopoeia (VP) [1]. This medicinal material was described in other pharmacopoeial monographs such as Pharmacopoeia of the People Republic of China 2020 [2], Hong Kong Chinese Materia Medica Standards - volume 10 (HK) [3], Taiwan Herbal Pharmacopoeia (TP) [4], Korean Pharmacopoeia X (KP) [5], European Pharmacopoeia 11.1 (EP) [6]. *Strychni semen* is made from ripe or dried seeds of the *Strychni* tree. However, both definitions and quality standards in the Vietnamese pharmacopoeia were different from the other pharmacopoeias (Table 1). While in all other pharmacopoeial monographs, the definition of *Strychni semen* specified as seeds from only *Strychnos nux-vomica*, in Vietnamese

pharmacopoeia, *Strychni semen* was defined as seeds from *Strychnos nux-vomica* and other *Strychnos* species. In Vietnam, there are 19 species of the genus *Strychnos*, including 16 species of vines trees, 1 species of a small tree, 2 species of *S. nux-incerica*; *S. nux-blanda*: large tree (stem diameter 20-40 cm). However, different species have significantly different strychnine and brucine contents, leading to variations in the quality of traditional medicine. This leads to difficulties in controlling the quality of *Strychni semen*.

Concerning quality standards, alkaloid content is the crucial criterion. Strychnine and brucine are the two most abundant alkaloids in *Strychni semen* and have an important influence on the effects and toxicity of this medicinal herb. The content limits of strychnine and brucine in different pharmacopoeias were listed in Table 1.

Table 1. Comparison of *Strychni semen* in different pharmacopoeias

Pharmacopoeia	Ref.	<i>Strychnos</i> species	Alkaloid content - analytical method
Vietnamese - VP	[1]	<i>Strychnos</i> species	≥ 1.2% total alkaloid (UV-Vis 262/300 nm)
Chinese - CP	[2]	<i>Strychnos nux-vomica</i>	1.20 - 2.20% strychnine; ≥ 0.8% brucine (HPLC)
Hongkong - HKS	[3]	<i>Strychnos nux-vomica</i>	1.20 - 2.20% strychnine; 0.69 - 1.60% brucine (HPLC)
Taiwan - TP	[4]	<i>Strychnos nux-vomica</i>	1.20 - 2.20% strychnine; ≥ 0.8% brucine (HPLC)
Korean - KP	[5]	<i>Strychnos nux-vomica</i>	≥1.05% strychnine (HPLC)
European - EP	[6]	<i>Strychnos nux-vomica</i>	≥1.5% (strychnine + brucine); 43-67% strychnine (HPLC)

Both strychnine and brucine content limits were mentioned in the quality standards of *Strychni semen* in Chinese, Hong Kong, Taiwan, and European Pharmacopoeias. In the Vietnamese

and Korean Pharmacopoeias, only strychnine content was taken as quality control of this herbal medicine. Since the pharmacological effect and toxicity of strychnine and brucine are different, the

ratio between these two alkaloids was also important, and the upper content limit was also considered in some pharmacopoeias. In the Chinese, Hongkong, and Taiwan pharmacopoeias, the content of strychnine was controlled for both lower and upper limits, but in Vietnamese and Korean pharmacopoeias, only a lower limit was specified. Only the Hong Kong standards for medicinal material set both upper and lower limits for the two substances strychnine and brucine.

Another difference in Vietnamese pharmacopoeia compared to other pharmacopoeias was the analytical technique. High performance liquid chromatographic (HPLC) analysis was used for strychnine and brucine determination in these 5 pharmacopoeial monographs. Only in Vietnamese pharmacopoeia, UV-Vis spectrophotometric analysis was used. Although the dual-wavelength quantitative method in Vietnamese pharmacopoeia also enabled simultaneous determination of strychnine and brucine, the specificity and thus precision and accuracy of the UV-Vis method could not be compared to the HPLC method. On the other hand, due to the acceptance of many *Strychnos* species, the other components in *Strychnos* seeds might interfere with the results of the assay.

Because of these differences in *Strychni semen* specifications in Vietnamese pharmacopoeia compared to all other prestigious pharmacopoeias, it was suggested that the definition in Vietnamese

pharmacopoeia of this herbal material should be revised in terms of *Strychnos* species specified and alkaloid content. However, the monograph can only be revised if more information was collected on the alkaloid content and ratio between strychnine and brucine content among different *Strychnos* species in Vietnam. In this study, strychnine and brucine content were determined in *Strychni semen* samples collected randomly on the market from different regions in Vietnam and compared to samples from China and Laos. Some interesting observations were obtained when comparing the alkaloid content among the *Strychni semen* samples from different species, and when correlating the alkaloid content with the morphological properties of the samples. Based on these observations, some suggestions were raised for better quality control of *Strychni semen*.

2. Materials and methods

2.1. Sample collection

Twelve samples were bought from the market in the north, center, and south of Vietnam, and one from Laos. A Chinese *Strychni semen* sample was bought from an official source (MS11), and a reference medicinal material (MS3) was obtained from the Vietnam National Institute of Drug Quality Control (NIDQC, Hanoi, Vietnam). Table 2 presented sample details and morphological characteristics, recorded with visual observation under normal daylight.

Table 2. Signs and shape characteristics of samples

Sample	Place	Sensory/ Color	Shape characteristics
MS1	DakLak, from market	white with brown patches	distorted, not round, ridged edges, concave inside
MS2	DakLak, collected on site		
MS3	Reference (<i>S. nux-vomica</i>)	grey, brown	evenly round, evenly concave
MS4	Nghe-An, from market	grey white, grey	evenly round, evenly concave
MS5	Hanoi, from company (<i>S. nux-vomica</i>)	grey white, grey	evenly round, evenly concave
MS6	Hochiminh, from company (<i>S. nux-vomica</i>)	many white seeds	round, clear edges
MS7	Hanoi, from market	grey, brown, white	round, oblong, irregular size
MS8	Binh-Dinh, from market	black, dark grey	small, only ¼ normal size
MS9	Lang-Son, from market	white, light brown	oblong seeds
MS10	Hanoi, from market	grey	round, quite even
MS11	China, from company (<i>S. nux-vomica</i>)	grey, white	evenly round, ridges around and concave in the middle
MS12	Laos (<i>S. blanda</i>)	white, light brown	oblong seeds

2.2. Chemicals and instrument

Strychnine reference standard (PRF1001259, 98.0%) was purchased from Biopurify Phytochemicals Ltd (Sichuan, P.R.China);

brucine reference standard (CFS202102, 99.0%) was obtained from ChemFaces (Hubei, P.R.China). Acetonitrile and methanol (HPLC grade), as well as other chemicals at analytical

grade (sodium heptane sulfonate, potassium dihydro phosphate, phosphoric acid, chloroform), were purchased from Merck (Darmstadt, Germany). Analysis was done on the Agilent Technology 1200 series HPLC system with an DAD detector (Agilent, CA, USA).

2.3. Method for standard and sample preparation

Standard preparation

Stock reference standard solutions were prepared in methanol at 250 mg/L for brucine and 500 mg/L for strychnine. These stock solutions were diluted in methanol to obtain the necessary single and mixture standard solutions.

Sample preparation

About 0.6 g of *Strychni semen* powder was accurately weighed into a 50 mL conical flask with a ground stopper, followed by adding 3 mL of 0.1 M NaOH. After 30 minutes, 20 mL of chloroform was added to the conical flask. The entire conical flask was weighed (mass m1), put under reflux extraction for 2 hours and then weighed again. Chloroform was added to obtain the original mass (m1), if necessary. The obtained mixture was filtered through Whatman filter paper with

anhydrous sodium sulfate, and the extract was collected into a 20 mL volumetric flask (A), and filled to volume with chloroform. Exactly 3 mL of the extract was transferred from the flask (A) into a 10 mL volumetric flask (B) and added to volume with methanol to obtain the test sample.

3. Research results

3.1. Morphological properties

All collected samples were identified as *Strychni semen* samples according to the morphological characteristics in Vietnamese pharmacopoeia. Since the samples were collected from the market, species could not be determined for all samples. Only samples bought from pharmaceutical companies or obtained from institutes were determined with species names, as shown in Table 2. Besides, the sample collected onsite from Daklak (MS2) was told to be from a different species than *S. nux-vomica*, but not specified which species. It was observed that samples from different species possessed some different morphological properties (colour, shape as shown in Table 2). Pictures of some typical samples were illustrated in Fig. 1 (the size was marked with a line and number in centimeters).

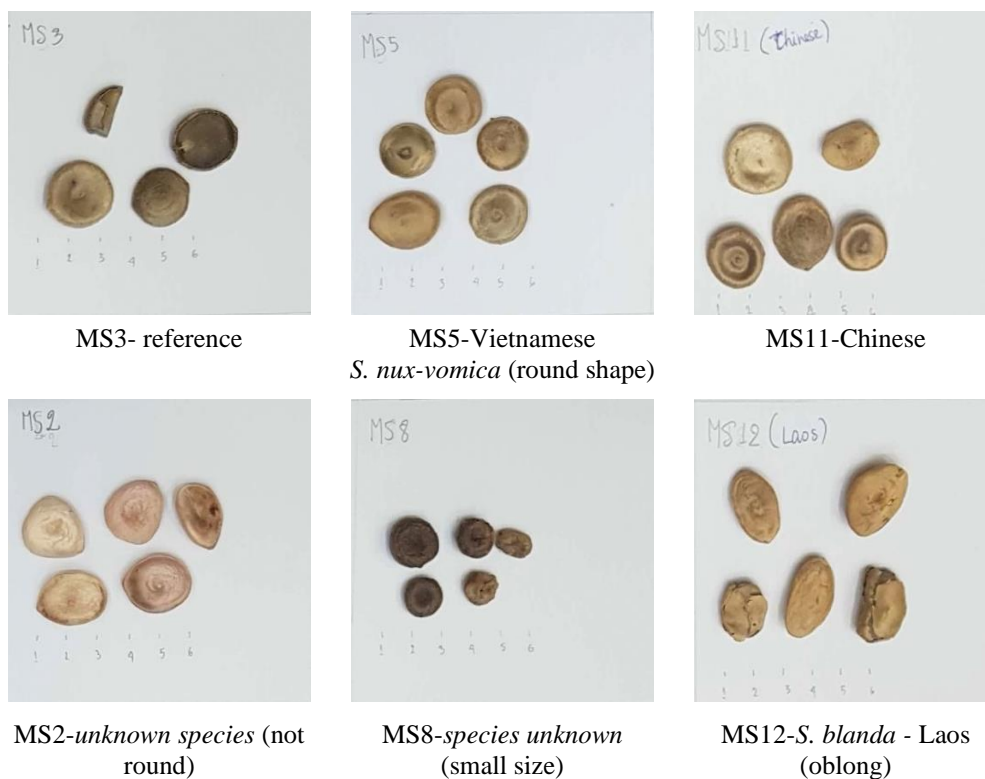


Fig. 1. Pictures of some samples with different morphological properties

3.2. Strychnine and brucine determination by HPLC analysis

Different chromatographic conditions were experimented with, including those from Chinese pharmacopoeia (CP) [2], Hong Kong Chinese Materia Medica Standards (HKS) [3], and European pharmacopoeia (EP) [6]. The chromatographic conditions for the HPLC method in HKS and CP are similar, using a normal C18 column with an isocratic mobile phase containing ion-pairing reagent sodium heptane sulfonate. In the EP monograph, an end-capped ethylene-bridge C18 column with hybrid material was needed for the assay of strychnine and brucine. With the investigated results in terms of peak resolution, analysis time, and simplicity of the analytical procedure, the chromatographic conditions in Chinese pharmacopoeia were chosen.

Chromatographic conditions

An octadecylsilyl column (4.6 x 250 mm; 5 µm) was used as the stationary phase, with the mobile phase consisting of sodium heptane sulfonate 0.01 M in acetonitrile - potassium dihydrogen phosphate 0.02 M adjusted pH to 2.8 with 10% phosphoric acid (21 : 79, v/v) at a flow rate of 1 mL/min was used. Detection was done at 260 nm.

Method validation

The method was validated in terms of system suitability, selectivity, repeatability, and linearity

before application to the collected samples. The national reference medicinal material (MS3) was used for method validation. The system suitability test was done according to the CP monograph. The number of theoretical plates calculated on the strychnine peak was 11000, higher than the required number according to CP (5000). For selectivity, in the MS3 sample, the peaks with retention time corresponding to strychnine and brucine in the reference standard solution were determined as strychnine and brucine peaks, with match ratio and peak purity of higher than 0.999 for both compounds, showing that the chromatographic separation was adequate for quantitation. For linearity, prepare standard solutions of strychnine and brucine in methanol. Carry out analysis with the selected conditions (results in Table 3). The results showed good linearity of strychnine and brucine peak area and concentration within the investigated range, with a correlation coefficient of higher than 0.999 for both compounds. For repeatability, one *Strychni semen* sample was analyzed 6 times separately, and the relative standard deviation (RSD%) was 1.91% and 2.10% for strychnine and brucine content in the sample, respectively. Therefore, the CP method was suitable for application in the *Strychni semen* samples in Vietnam.

Table 3. Results of calibration curve for strychnine and brucine determination

Linearity			
Strychnine		Brucine	
Concentration (µg/ml)	Peak area (mAU.min)	Concentration (µg/ml)	Peak area (mAU.min)
12.152	195.8	5.742	59.4
60.76	1033.5	28.71	328.5
121.52	2001.1	57.42	674.5
243.04	3949.3	114.84	1346.3
303.8	4871.2	143.55	1729.5
y = 16.005x + 37.378 (R = 0.9998)		y = 12.04x - 15.814 (R = 0.9996)	

Analysis of *Strychni semen* samples

The *Strychni semen* samples were prepared as described in section 2.3. Method for sample preparation and extract was analyzed using the selected chromatographic conditions. Results of strychnine and brucine content in the samples were presented in Table 4. These results were compared to Vietnamese pharmacopoeia (VP) limits, presented in Table 4 as complies (C) or not complies (NC) to pharmacopoeial standards. Samples were also compared to Chinese pharmacopoeia (CP), Hong Kong standard (HK), and Korean pharmacopoeia (KP) since the limits are different. Taiwan

pharmacopoeia (TP) had the same limit as Chinese pharmacopoeia, and the European pharmacopoeia standard was meant for homoeopathic preparations, thus these two standards were not included. Since four samples (i.e. MS3, MS5, MS6, and MS11) were *S. nux-vomica*, the comparison to other pharmacopoeias was officially acceptable, and results were marked as capital letters C/NC in Table 4. Other samples (species unknown) were also compared to the other pharmacopoeia standards, but the unofficial results were noted in Table 4 in small letters, in italics. Sample MS12 specified as *S. blanda* was not evaluated according to other pharmacopoeias. To

look more closely at the alkaloid content, the ratio of strychnine/brucine content was also calculated in Table 4. Some typical complied and non-complied

samples are presented in terms of chromatograms in Fig. 2, and as picture in Fig. 3, for better comparison.

Table 4. Strychnine and brucine content in *Strychni semen* samples

Sample	Total (%)	Strychnine (%)	Brucine (%)	Content ratio S/B	Complies to Pharmacopoeias			
					VP	CP	HK	KP
MS1	0.00270	0.00270	+	+	NC	nc	nc	nc
MS2	0.00274	0.00274	+	+	NC	nc	nc	nc
MS3	3.019	1.529	1.490	1.03	C	C	C	C
MS4	2.894	1.561	1.333	1.17	C	c	c	c
MS5	2.243	1.337	0.806	1.66	C	C	C	C
MS6	2.433	1.356	1.077	1.26	C	C	C	C
MS7	1.374	0.901	0.473	1.91	NC	nc	nc	nc
MS8	0.304	0.235	0.069	3.41	NC	nc	nc	nc
MS9	1.713	1.713	-	-	C	nc	nc	c
MS10	1.950	0.790	1.160	0.68	NC	nc	nc	nc
MS11	0.709	0.619	0.090	6.88	NC	NC	NC	NC
MS12	1.135	0.644	0.491	1.31	NC			
MS13	0.653	0.444	0.209	2.12	NC	nc	nc	nc

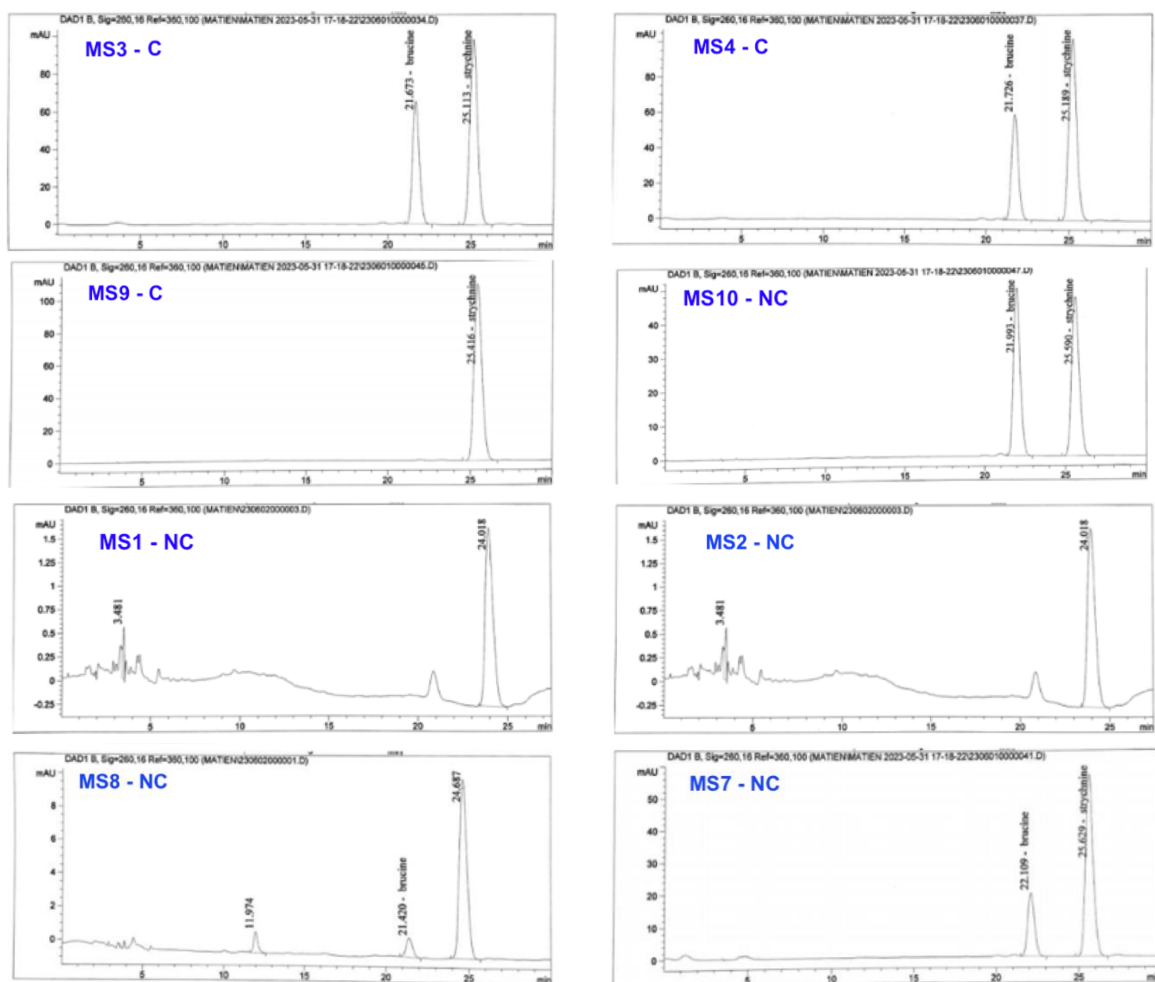


Fig. 2. Chromatograms of strychnine and brucine in *Strychni semen*

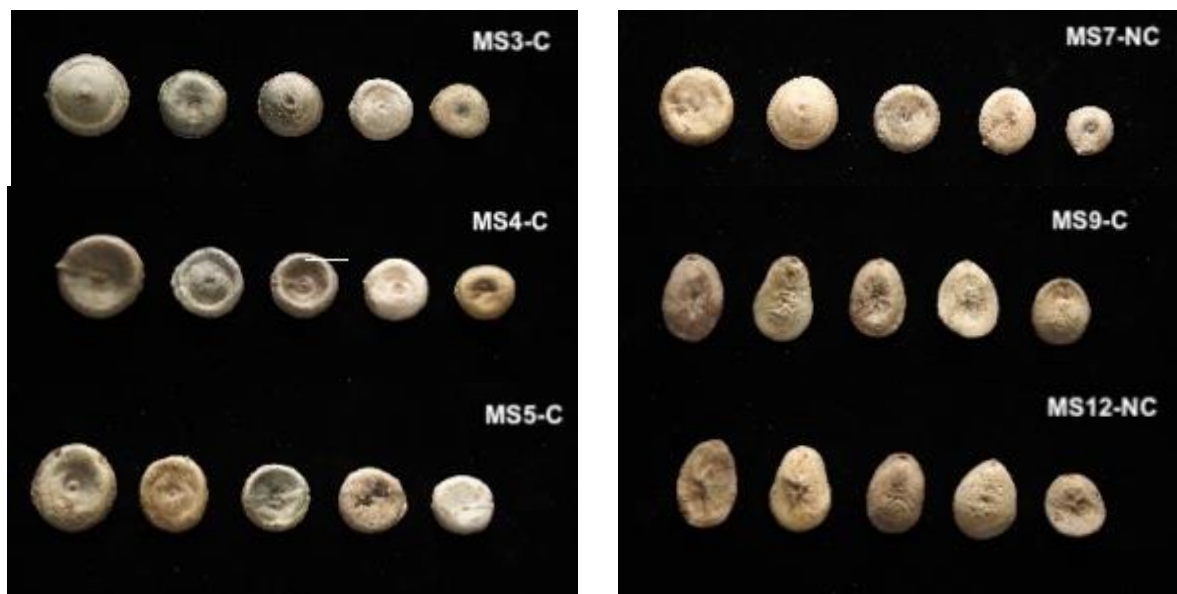


Fig. 3. Shape and size of some *Strychni semen* samples with alkaloid content complied (on the left) and non-complied (on the right) with standards

4. Discussion

Results in Table 4 showed that only 5/12 samples (5/10 Vietnamese samples) complied with Vietnamese Pharmacopoeia. These results again enforced the concern on quality control of *Strychni semen* samples on the market. In most cases, those complying with VP also complied with other pharmacopoeias and vice versa, except sample MS9, which will be discussed further later.

Comments on complied samples

Among 5 complied samples, 3 samples (MS3, MS5, and MS6) were specified as *S. nux-vomica*. Only one *S. nux-vomica* sample (MS11, from China) did not conform to the content limit, and this one also failed other pharmacopoeias' limits, too. Sample MS4 had the same morphological properties as the *S. nux-vomica* samples (similar size, shape, and colour of MS4 versus MS3 and MS5 in Fig. 3), and the strychnine/brucine content ratio was also similar to *S. nux-vomica* samples (chromatograms MS4 vs MS3 in Fig. 2, and values in Table 4). The last complied sample MS9 was not supposed to be *S. nux-vomica*. Firstly, it was the only sample that hardly contained brucine (Table 4). As observed in Fig. 2, the brucine peak was not detected on the chromatogram. Therefore, although the alkaloid content complied with VP and KP, but failed to comply with CP and HK (also failed with TP and EP). The morphological properties of MS9 were somewhat similar to MS12 (*S. blanda*), as shown in Fig. 3, but the S/B

ratio was not similar. So MS9 might be from another *Strychnos* species.

Comments on non-complied samples

Some samples had very low alkaloid content: total content of strychnine and brucine < 0.5% for MS1, MS2, MS8, and brucine peaks in MS1 and MS2 were even not quantifiable. While collecting MS2 on-site in Daklak, it was even revealed that this *Strychni semen* sample was supposed to be from a different species than *S. nux-vomica*, and it usually possessed very low toxicity. Five samples showed very low total alkaloids (<1%), only <50% of the required total content for *S. nux-vomica* in CP, HK, and TP): MS1, MS2, MS8, MS11, and MS13. After processing, the alkaloid content would be even lower, efficacy could hardly be expected. Not only the total content was low, the S/B ratio for MS11 was much higher than the normal range for *S. nux-vomica* (0.64 to 1.56, calculated from the range of % strychnine 43-67% for *S. nux-vomica* stated in EP). These samples might be from other species.

Although MS11 was stated as *S. nux-vomica* (MS11), the assay result did not support this fact, because of the very high S/B ratio (6.88). This sample was imported from China from a pharmaceutical company. The appearance of this sample was totally fine (Fig. 1) with typical *S. nux-vomica* morphological properties. The low quality can only be discovered by an alkaloid content assay. This could be a typical example of the problem in Vietnam market has been facing for

many years: importing low-quality herbal materials.

Only 2 samples (MS7, MS10) with morphological properties similar to *S. vomica* (MS7 in Fig. 3) failed to meet the content requirement, but the total content of alkaloid was still higher than 1.2% (the limit for strychnine in VP), similarly to what observed with sample MS12 *S. blanda* (1.14%).

Comments on the Strychnus species mentioned in Vietnamese pharmacopoeia

Although the number of samples was very limited in this study, some observations could be obtained to support the suggestion that the diversified source of *Strychni semen* materials to all 19 *Strychnus* species in Vietnam had resulted in difficulties in controlling *Strychni semen* quality for users, buyers and even sellers of this herbal material. If the VP monograph limited the source of *Strychni semen* to only *S. nux-vomica* as other pharmacopoeias, it could be an economic loss, for sure. Because we could not exploit a variety of other *Strychnos* species that also contain a good amount of alkaloid. Therefore, it would be ideal for the *Strychni semen* monograph to specify the names of the *Strychnos* species with high potential as herbal materials.

However, in order to reach this optimal solution, many other studies had to be performed to evaluate the economic as well as the scientific potential of the most important *Strychnos* species in Vietnam. Until that time, maybe the option of limiting the source would be a better choice for better quality control of *Strychni semen* as herbal material.

Comments on alkaloid content in Vietnamese pharmacopoeia

At present, all manufacturers of drugs and dietary supplements (that might contain *Strychni semen*) are required to run under GMP guidelines. The HPLC systems have become a common instrument in the laboratory of these manufacturers. Therefore, the UV-Vis method used in Vietnamese pharmacopoeia should be updated to the HPLC method. Apart from the

HPLC methods from pharmacopoeias that were investigated in this study, other HPLC-DAD methods were also found in national [7] and international [8] publications. However, the HPLC method used in this study - the official method from Chinese pharmacopoeia - proved to be feasible for applications in Vietnam. It was a simple method, easy to perform, and provided repeatable results within an acceptable analysis time. The content limit was suggested to include both strychnine and brucine content in the requirements because the strychnine/brucine content ratio might bring along information on species.

5. Conclusion

In Vietnam, 19 *Strychnos* species are available throughout the country. Therefore the sources of materials for *Strychni semen* are diversified, and the quality of this herbal medicine also varies significantly. In the Vietnam Pharmacopoeia V, the monograph on *Strychni semen* only referred to the genus *Strychnos* in general. Hereby, we proposed to quality control only the *Strychnos nux-vomica* species in the Vietnamese Pharmacopoeia. In this study, 12 *Strychni semen* samples were collected from the north, the center, and south of Vietnam. The HPLC analysis of the strychnine and brucine content of the samples revealed the situation of low-quality samples on the market with a high ratio: of 5/10 Vietnamese *Strychni semen* samples did not comply with Vietnamese pharmacopoeial standards. Observations on the complied and non-complied samples also supported this proposal. However, since the number of samples was very limited in this study, this could only be considered as the first step for further studies supporting this proposal.

Acknowledgment: *The authors would like to express sincere thanks to the Fondation Pierre Fabre for creating the Mekong Pharma Network "Quality of Herbal Health Product" among pharmacy universities in Vietnam, Laos, and Cambodia, which facilitated the collaboration in this study.*

References

1. Ministry of Health (2017), *5th Vietnamese Pharmacopoeia*, 1240-1241.
2. Chinese Pharmacopoeia Commission (2020), *Pharmacopoeia of The People's Republic of China 2020*.
3. Department of Health (2020), *Hong Kong Chinese Materia Medica Standards 2020*.
4. Ministry of Health and Welfare Taiwan (2019), *3rd Edition Taiwan Herbal Pharmacopoeia*.
5. Ministry of Food and Drug Safety (2024), *12th edition Korean Pharmacopoeia*.
6. Council of Europe (2023), *11th European Pharmacopoeia*.
7. Giang Thị Kim Liên, Trần Ngọc Đông, Nguyễn Thị Hoàng Anh (2018), Nghiên cứu phương pháp chiết và xác định hàm lượng brucine và strychnine từ hạt mã tiền chế bằng HPLC, *Tạp chí Khoa học và Công nghệ Đại học Đà Nẵng*, 9(130), 71-75.
8. Jiang X., Tian J. X., Wang M., Tian Y., Zhang Z. J. (2019), Analysis of dihydroindole-type alkaloids in *Strychnos nux-vomica* unprocessed and processed seeds by high-performance liquid chromatography coupled with diode array detection and mass spectrometry, *Journal of Separation Sciences*, 42(22), 3395-3402.

QUALITY EVALUATION OF *PHELLODENDRON AMURENSE* COLLECTED IN VIETNAM USING HPLC-DAD AND QAMS METHODS

Nguyen Thi Ha Ly¹, Do Thi Hang², Nguyen Minh Khoi^{1,*}

¹National Institute of Medicinal Materials (NIMM), Hanoi, Vietnam;

²Phuc Yen Regional General Hospital, Vinh Phuc, Vietnam

*Corresponding author: Khoinguyenimm6@gmail.com

(Received September 26th, 2024)

Summary

Quality Evaluation of *Phellodendron amurense* Collected in Vietnam Using HPLC-DAD and QAMS Methods

A simple and sensitive high-performance liquid chromatography (HPLC-DAD) method has been developed to quantify phellodendrine, palmatine chloride, and berberine chloride in *Phellodendron amurense* collected in Vietnam. Based on this method, a quantitative analysis of multiple components with a single marker (QAMS) was carried out and the relative correction factors (RCFs) were calculated to determine the contents of phellodendrine and palmatine chloride according to berberine chloride (used as an internal standard). The RCF values of phellodendrine and palmatine chloride were 2.79 and 0.30, respectively, according to the internal standard. The accuracy of the QAMS method was verified by comparing it with the results of the external standard method (ESM), as well as the feasibility of the method applied to quality control of *Phellodendron amurense*. The %RSD of f values in different injection volumes were from 3.76% to 3.98%. The accuracies of QAMS were from 90% to 110% and no significant difference in results was found between the content of phellodendrine and palmatine chloride analyzed by QAMS and external standard method. The findings from QAMS indicated that it was a convenient and precise approach for identifying multiple components, particularly when certain genuine standard substances were inaccessible. It can potentially be utilized for controlling the quality of *Phellodendron amurense*.

Keywords: *Phellodendron amurense*, Berberin, HPLC, QAMS.

1. Introduction

The well-known traditional remedy *Phellodendri amurensis* cortex was developed from the dried bark of *Phellodendron amurense* Rupr. [1]. *Phellodendri amurensis* cortex has been shown through contemporary pharmacological studies to possess a range of biological activities, such as anti-inflammatory [3], anti-tumor [2], anti-microbial, anti-oxidant, and anti-herpes simplex virus [4], as well as hypoglycemic and neuroprotective properties [5]. Multiple constituents contribute to the effects of *Phellodendri amurensis* cortex; however, only palmatine chloride and berberine chloride were determined according to Chinese Pharmacopoeia 2015 [6], Hong Kong Chinese Materia Medica Standards [7], and Vietnamese Pharmacopoeia 2017 [1]. Despite being the active components of the cortex of *Phellodendri amurensis*, they are also present in certain other species. To guarantee the medication's effectiveness, it is crucial to set up comprehensive quality control procedures for *Phellodendri amurense*. The quantitative analysis of multiple components by single-marker (QAMS) method allows to determination of the concentrations of multiple components simultaneously and requires only a single reference standard. To some extent, this method could also significantly reduce the cost and time

of the analysis process [8],[9],[10],[11],[12]. Thus, QAMS has been widely accepted and applied in the quality control of herbal medicine. This study selects three alkaloids, including phellodendrine, palmatine chloride, and berberine chloride, as markers for the simultaneous determination of *Phellodendri amurensis* cortex quality control in Vietnam using the HPLC-DAD method. The purpose of this study was to develop a QAMS method for simultaneously determining phellodendrine, palmatine chloride, and berberine chloride in *Phellodendri amurensis* cortex samples collected in Vietnam. Berberine chloride was used as an internal standard substance, and the RCF of other compounds was established. The developed method could simultaneously determine the contents of active components in 10 *Phellodendri amurensis* cortex samples collected in Vietnam, which provides a theoretical scientific basis for the comprehensive quality control and evaluation of *Phellodendri amurensis* cortex and its products.

2. Experimental

2.1. Materials

The *Phellodendri amurensis* cortex sample (PAC-1) was collected in 4/2023 in Sa Pa (Lao Cai province, Vietnam). The samples were identified by Prof. Dr. Pham Thanh Huyen (NIMM). These samples were cleaned, dried in the

oven at (60°C) and ground into powder before using in this study. Some *Phellodendri amurensis* cortex samples (**PAC2-PAC10**) were purchased on the market.

2.2. Chemicals

Methanol and acetonitrile of HPLC grade were purchased from Merck (Germany). All other solvents were of analytical grade. Phellodendrine (CAS 6873-13-8; Lot: CFS202301, 99.5%); palmatine chloride (CAS: 10605-02-4, Lot: CFS202201, 98%) and berberine chloride (CAS: 633-65-8; Lot: CFS202202, 98%) were purchased from Chemfaces (China).

2.3. Preparation of standard solutions

Standard stock solutions of the three compounds (phellodendrine, palmatine chloride, and berberine chloride) were prepared by dissolving the primary standard in methanol. The stock solutions were then diluted to establish calibration curves in the ranges of 0.5 - 125 µg/mL for phellodendrine, 0.25 - 50 µg/mL for palmatine chloride, and 13 - 1300 µg/mL for berberine chloride. The stock and working solutions were stored at 4°C.

Mixed standard solution: each reference stock solution was accurately, put into a 5 mL volumetric flask, and then methanol was added to the scale, and mixed thoroughly; the concentrations of phellodendrine, palmatine chloride, and berberine chloride were 25 µg/mL, 25 µg/mL, and 65 µg/mL, respectively. The solutions were stored at 4°C in a refrigerator and filtered through a 0.45 µm membrane filter before injection.

2.4. Preparation of sample solution

Weigh accurately 0.2 g of the powdered sample and put it into a 50-mL centrifugal tube, then add accurately 10 mL of methanol and weigh. Sonicate the mixture for 30 min and weigh again. Add an appropriate amount of methanol to compensate for

the weight loss. Mix and centrifuge at about 3000 x g for 5 min. Filter through a 0.45 µm filter [6],[7].

2.5. Instrument and Chromatographic Conditions

The HPLC system (Shimadzu, Japan) used for the analysis consisted of a binary pump LC-30AD, a SIL-30AC autosampler, a CTO-10AS column oven, and a diode-array detector (SPD-M20A). Quantitative estimation was performed with LabSolutions software programs. The separation of compounds was performed on an Agilent C₁₈ column (250 x 4.6 mm, 5 µm). The mobile phase was a mixture of acetonitrile (ACN) and 0.1% trifluoroacetic acid. The elution program was optimized and conducted as follows: 0-20 min (10-90% ACN); 20-30 min (90% ACN); 30-35 min (90-10% ACN); 35-40 min (100% ACN). The solvent flow rate was kept at 0.8 mL/min. The injection volume was 10 µL. Detection was set at a wavelength of 270 nm [1],[14],[15].

2.6. External standard method (ESM)

The analytical method was developed and validated for system suitability, specificity, calibration curve, accuracy, precision, detection limit, and quantitation limit following the current ICH guidelines [13].

2.7. QAMS method

Methods for calculating the relative retention time (RRT) and the relative correction factor (RCF, *f*) have been previously reported [8],[9],[10],[11],[12]. First, berberine chloride was selected as the internal standard, and a multipoint method was used to calculate *f* values for phellodendrine and palmatine chloride. The content of the multi-marker components measured by QAMS was compared with results from ESM, to validate the methods of QAMS.

The formula for calculating the RRT and RCF:

$$RRT_X = \frac{T_{Rx}}{T_{Rs}} \quad (1)$$

where

T_{Rs}, A_s, and C_s are the retention time, peak area, and concentration of the internal standard substance (berberine chloride);

T_{Rx}, A_x và C_x are the retention time, peak area, and concentration of the analyzed compound.

$$RCF = \frac{A_s \times C_x}{A_x \times C_s} \quad (2)$$

The RCF value was evaluated by analyzing the mixed standard solution under some different conditions in terms of sample injection volume (2-10 µL), types of HPLC C₁₈ chromatography columns from 3 different brands (Agilent, Phenomenex, and Vertical) and analyzed on 2 different HPLC systems.

2.8. Calculation

The content of the measured component in *Phellodendri amurensis* cortex samples by the ESM method was calculated as follows:

$$X_{\text{ESM}}(\%) = \frac{C_t \times V \times P \times 100}{m \times 100 \times (100 - a)} \times 100 \quad (3)$$

where C_t : the concentration of analyzed compounds in the sample solution from the calibration curve equation (mg/mL);

V : volume of the sample solution (mL);

m : weight of sample taken to prepare the sample solution (mg);

a : the moisture of sample (%);

P : the purity of the standard compound (%).

The concentration of the measured component by QAMS was calculated as follows:

$$C_x = \frac{f_x \times A_x \times C_s}{A_s} \quad (4)$$

where A_x and C_x are the peak area and the concentration of the analyte in the test sample;

A_s và C_s are the peak area and the concentration of the internal standard substance;

f_x is the RCF value.

3. Results and Discussion

3.1. Validation HPLC-DAD method for quantification of phellodendrine, palmatine chloride, and berberine chloride in *Phellodendri amurensis* cortex

3.1.1. Specificity:

The experiment was performed with the blank, standard, and *Phellodendri amurensis* cortex sample solutions according to the analytical procedure. The retention times of phellodendrine, palmatine chloride, and berberine chloride were 12.6 min, 17.1 min, and 17.6 min, respectively. The peak of each compound was confirmed by comparing the retention time and UV spectrum of each marker constituent. The obtained results are shown in Fig. 1 and Table 1.

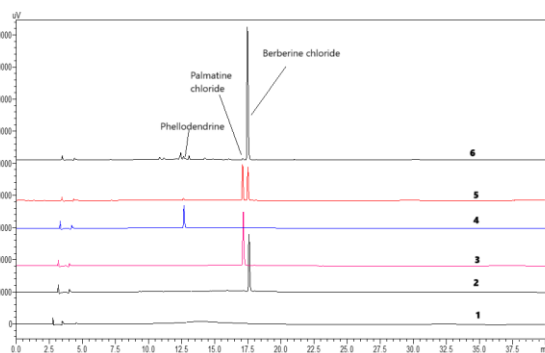


Fig. 1. HPLC-DAD chromatograms of the blank, standard, and *Phellodendri amurensis* cortex sample solutions (1-blank sample; 2-berberine chloride; 3-palmatine chloride; 4-phellodendrine; 5- mixed standard solution sample; 6- *Phellodendri amurensis* cortex sample)

Table 1. Parameters of peaks of three components

	Phellodendrine	Palmatine chloride	Berberine chloride
Retention time (t_R , min)	12.6	17.1	17.6
Resolution (R_s)	2.11	1.98	2.89
Tailing factor (T_f)	1.23	1.18	1.25
Number of Theoretical Plates (N)	83709	97228	121096
Purity of peak	0.999	0.993	0.999
The similarity of the UV spectrum	0.997	0.998	0.999

3.1.2. Linearity, LOD, and LOQ:

The calibration curves of three components were established by using the peak area (y) as the vertical axis and the concentration of the analyte

(x) as abscissa, respectively. All the correlation coefficients (R) were more than 0.999 for the concentration range, indicating acceptable linearity.

Table 2. Regression, equations, correlation coefficients, linearity ranges, limits of detection, and limits of quantification for three components

Compounds	Regression equation*	R^2	Linearity range ($\mu\text{g/mL}$)	LOD ($\mu\text{g/g}$)	LOQ ($\mu\text{g/g}$)
Phellodendrine	$y = 5126.6x + 1968.2$	0.9999	0.5 - 125	0.03	0.09
Palmatine chloride	$y = 47279x + 10888$	0.9999	0.25 - 50	0.01	0.04
Berberine chloride	$y = 17188x - 191368$	0.9992	13 - 1300	0.01	0.04

*In the regression equation $y = ax + b$, where y refers to the peak area and x refers to the concentration of the substance ($\mu\text{g/mL}$).

Furthermore, the limit of detection (LOD) and the limit of quantification (LOQ) were calculated by diluting sample solutions until signal-to-noise ratios of 3 and 10, respectively. LOD and LOQ of three substances were also calculated as shown in Table 2.

3.1.3. System suitability:

It can be observed from Table 3 that the RSD% of retention time and peak area were all under 2%. These indicate that the developed method conforms to system suitability criteria.

Table 3. System suitability testing (n = 6)

Parameter	Phellodendrine 25 µg/mL		Palmatine chloride 25 µg/mL		Berberine chloride 65 µg/mL	
	Mean	RSD(%)	Mean	RSD(%)	Mean	RSD(%)
Retention time, t_R (min)	12.64	0.16	17.11	0.16	17.58	0.15
Peak area (mAu.s)	127659.8	1.36	1192262	0.26	1057784	0.34

3.1.4. Precision:

The intra- and inter-day precision was summarized in Table 4.

Table 4. The evaluated results of precision (intra-day and inter-day)

Time	Code	Weight (g)	Content (%)		
			Phellodendrine	Palmatine chloride	Berberine chloride
Day 1	M1	0.2011	0.60	0.15	7.45
	M2	0.2042	0.60	0.15	7.35
	M3	0.2006	0.61	0.14	7.41
	M4	0.2024	0.59	0.15	7.41
	M5	0.2014	0.60	0.15	7.42
	M6	0.1932	0.59	0.15	7.68
		Mean (n=6)	0.60	0.15	7.45
		RSD% (n=6)	1.23	1.02	1.55
Day 2	M7	0.2003	0.58	0.14	7.48
	M8	0.1908	0.55	0.15	7.86
	M9	0.2001	0.58	0.14	7.50
	M10	0.1957	0.59	0.15	7.66
	M11	0.1938	0.58	0.15	7.74
	M12	0.1922	0.57	0.15	7.80
		Mean (n=12)	0.59	0.15	7.56
		RSD% (n=12)	2.88	1.41	2.32

The evaluation was performed by calculating the relative standard deviation (RSD%). The criterion of acceptance was RSD% <3.7% for the mean contents of three compounds phellodendrine, palmatine chloride, and berberine chloride, respectively. The results showed that the method had good precision.

3.1.5. Accuracy:

The accuracy was evaluated by adding a

known amount of three standards at four different levels (20%, 80%, 100%, and 120%) to the sample. Each experiment was repeated three times. Conduct HPLC-DAD analysis of spiked and unspiked samples, determine the amount of standard added based on the calibration curve equations, and calculate the recovery efficiency compared to the actual amount of standard added.

Table 5. The results of evaluating the accuracy (n=3)

Compound	Level	Recovery rate (%)
Phellodendrine	20% spiked	97.8 ± 0.6
	80% spiked	105.8 ± 1.2
	100% spiked	101.4 ± 1.7
	120% spiked	98.3 ± 0.9
Palmatine chloride	20% spiked	96.4 ± 0.5
	80% spiked	102.4 ± 3.4
	100% spiked	104.7 ± 2.5
	120% spiked	100.7 ± 4.4
Berberine chloride	20% spiked	99.9 ± 1.0
	80% spiked	96.2 ± 0.7
	100% spiked	96.2 ± 0.5
	120% spiked	97.3 ± 0.3

The results in Table 5 showed that the recovery rates of the three compounds were in the range of 96.2% -105.8%. The recovery values were 97.8-105.8% for phellodendrine, 96.4-104.7% for palmatine chloride, and 96.2-99.9% for berberine chloride. The results indicated that the accuracy of the developed method was acceptable.

3.2. QAMS method for quantification of phellodendrine, palmatine chloride, and berberine chloride in *Phellodendri amurensis cortex*

3.2.1. Determine RCF value according to different sample injection volumes:

Berberine chloride was selected as the internal standard, and the values of RCF (*f*) for the other two markers were computed in different concentrations according to Equation 2 mentioned in Section 2.7. The average RCF value of each compound is shown in Table 6.

Table 6. RCF values of two markers according to different sample injection volumes

Injection volumes	Phellodendrine 25 µg/mL			Palmatine chloride 25 µg/mL			Berberine chloride 65 µg/mL	
	Peak area	Concentration (µg/ml)	RCF	Peak area	Concentration (µg/ml)	RCF	Peak area	Concentration (µg/ml)
2	63278	11.96	2.60	477985	9.88	0.28	765675	55.68
3	78318	14.89	2.67	716639	14.93	0.29	859176	61.12
4	103531	19.81	2.73	955075	19.97	0.30	935482	65.56
5	127813	24.55	2.77	1194386	25.03	0.30	996999	69.14
6	164160	31.64	2.82	1438524	30.20	0.31	1085619	74.30
7	182894	35.29	2.86	1673909	35.17	0.31	1198897	80.89
8	209113	40.41	2.87	1917524	40.33	0.31	1215285	81.84
9	221606	42.84	2.90	2155463	45.36	0.32	1320972	87.99
10	247161	47.83	2.93	2387111	50.26	0.32	1426821	94.15
TB			2.79			0.30		
RSD%			3.98			3.76		

3.2.2. Determination of RRT and RCF values on different columns:

Table 7. RRT and RCF values of two markers according to different columns

Compounds		Berberine chloride	Phellodendrine		Palmatine chloride			
Instrument	Column	RT (min)	RT (min)	RRT	RCF	RT (min)	RRT	RCF
HPLC-DAD	A	17.50	12.63	0.72	2.79	17.09	0.98	0.31
		17.49	12.62	0.72	2.80	17.09	0.98	0.31
		17.49	12.62	0.72	2.80	17.09	0.98	0.31
	B	15.49	11.82	0.76	2.80	15.25	0.98	0.30
		15.49	11.88	0.77	2.81	15.25	0.98	0.31
		15.49	11.88	0.77	2.77	15.25	0.98	0.30
	C	19.03	14.12	0.74	2.80	18.64	0.98	0.30
		18.99	14.11	0.74	2.79	18.61	0.98	0.30
		18.97	14.10	0.74	2.77	18.58	0.98	0.30
Mean				0.74	2.79		0.98	0.30
RSD%				2.55	0.47		0.34	0.49

Column A (Eclipse Plus C₁₈ Agilent, 4.6x250 mm, 5µm); Column B (Phenomenex: Luna® 5µm C₁₈, 4.6x250 mm, 5 µm); Column C (VertiSep TM UPS C₁₈ HPLC Column, 4.6x250 mm, 5µm).

3.2.3. Determination of RRT and RCF values on different HPLC instruments:

Table 8. RRT and RCF values of two markers according to different HPLC instruments

Compounds		Berberine chloride	Phellodendrine		Palmatine chloride			
Instrument		RT (min)	RT (min)	RRT	RCF	RT (min)	RRT	RCF
HPLC-DAD 1		17.50	12.63	0.72	2.79	17.09	0.98	0.31
		17.49	12.62	0.72	2.80	17.09	0.98	0.31
		17.49	12.62	0.72	2.80	17.09	0.98	0.31
HPLC-DAD 2		12.18	9.10	0.75	2.80	0.97	0.97	0.31

Compounds	Berberine chloride	Phellodendrine			Palmatine chloride		
		12.19	9.01	0.74	2.81	0.97	0.97
	12.22	9.12	0.75	2.81	0.97	0.97	0.31
Mean			0.73	2.80		0.98	0.31
RSD%			2.05	0.27		0.56	0.00

The results of determining the RRT and RCF values of each substance phellodendrine (RRT = 0.74 and RCF = 2.79), palmatine chloride (RRT = 0.98; RCF = 0.30) compared to the berberine chloride standard showed good repeatability (RSD values < 3%) when using different stationary phases and different HPLC chromatography systems. This proves that the research method is

stable and has good repeatability.

3.3. Analysis of samples and comparison of the results between QAMS and ESM methods

The contents of each component in 10 samples of *Phellodendri amurensis* cortex were calculated by QAMS and ESM, respectively. The results are shown in Table 9.

Table 9. Content of berberine chloride, phellodendrine, and palmatine chloride in 10 samples of *Phellodendri amurensis* cortex determined by QAMS and ESM (n=3)

Code	Method	Content (%)			P-value*
		Berberine chloride	Phellodendrine	Palmatine chloride	
PAC-1	ESM	7.92	0.71	0.11	0.295
	QAMS		0.68	0.10	
PAC-2	ESM	7.62	0.56	0.07	0.500
	QAMS		0.54	0.07	
PAC-3	ESM	5.76	0.84	0.17	0.374
	QAMS		0.79	0.16	
PAC-4	ESM	4.25	0.22	0.05	0.795
	QAMS		0.20	0.06	
PAC-5	ESM	6.16	0.36	0.02	0.545
	QAMS		0.35	0.01	
PAC-6	ESM	6.43	0.41	0.02	0.205
	QAMS		0.39	0.01	
PAC-7	ESM	5.21	0.28	0.03	0.500
	QAMS		0.27	0.03	
PAC-8	ESM	3.22	0.19	0.06	0.662
	QAMS		0.18	0.05	
PAC-9	ESM	5.32	0.55	0.23	0.206
	QAMS		0.54	0.21	
PAC-10	ESM	4.98	0.86	0.13	0.295
	QAMS		0.83	0.12	

3.5. Discussion

Vietnamese Pharmacopoeia V and Chinese Pharmacopoeia stipulated that the berberine chloride content in *Phellodendri amurensis* cortex must not be less than 0.33% [1],[6]. Hong Kong Chinese Materia Medica Standards Office stipulates that the berberine chloride content in *Phellodendri amurensis* cortex must not be less than 0.33% and the palmatine chloride content must not be less than 0.18% [7]. The results showed the mean contents of 3.22 - 7.92%, 0.18 - 0.86%, and 0.01 - 0.23%, for the berberine

chloride, phellodendrine, and palmatine chloride, respectively. The results obtained in this study showed that all samples of *Phellodendri amurensis* cortex met the berberine chloride content criteria, however, only one sample (**PAC-9**) met the palmatine chloride content criteria. Sample **PAC-1** has the highest berberine chloride content (7.92%), higher than the *Phellodendri amurensis* cortex samples purchased on the market (**PAC-2** to **PAC-9**). The highest phellodendrine content is 0.86% in sample **PAC-10**, the lowest is 0.2% in sample **PAC-4**.

It was found that the percentage difference between these two methods was less than $\pm 5.0\%$. Using Minitab 16 software, a paired sample *T*-test was performed on two contents of ten samples measured by QAMS and ESM. The results revealed that there were no significant variations between the results of two different determination methods (P-value > 0.05), indicating that the established approach was accurate and dependable. QAMS is a multi-component analysis method based on one standard substance, which has been applied in many studies on medicinal herbs, with advantages such as being able to analyze multiple substances simultaneously but only using a single standard substance, helping to reduce analysis time and costs [8],[9],[10],[11],[12]. In Vietnam, there are few studies on the simultaneous quantification of berberine chloride, palmatine chloride, and phellodendrine in herbs. In particular, there have been no studies applying the QAMS method to simultaneously quantify these substances according to a standard substance. The results obtained in this study contribute a new method in the field of standardizing the quality of *Phellodendri amurensis* cortex.

4. Conclusion

In this study, a method named QAMS was established to evaluate the quality of *Phellodendri amurensis* cortex using HPLC-DAD equipment. In this method, berberine chloride was used as the internal standard to determine the RCF between berberine chloride and other markers (phellodendrine, palmatine chloride). According to the obtained results, QAMS was accurate and feasible for quality evaluation, and there was no significant difference in the content results obtained by QAMS and ESM. Ten samples of *Phellodendri amurensis* cortex were determined, and the results showed that the mean contents of 3.22-7.92%, 0.18-0.86%, and 0.01-0.23%, for the berberine chloride, phellodendrine, and palmatine chloride, respectively. There were no significant variations between the results of two different determination methods QAMS and ESM (P-value >0.05). The obtained results indicated that the established QAMS method can be accurately, economically, simply, and quickly applied to the multiple components analysis of *Phellodendri amurensis* cortex.

References

1. Ministry of Health (2017), Vietnamese Pharmacopoeia, *Medical Publishing House, Hanoi, Vietnam*, Vol. II: 1184-1185.
2. Kumar R., Das M., Ansari K. M. (2012), Nexrutine(R) inhibits tumorigenesis in mouse skin and induces apoptotic cell death in human squamous carcinoma A431 and human melanoma A375 cells, *Carcinogenesis*, 33, 1909-1918.
3. Kim J. H., Huh J. E., Baek Y. H., Lee J. D., Choi D. Y., Park D. S. (2011), Effect of *Phellodendron amurense* in protecting human osteoarthritic cartilage and chondrocytes, *Journal of Ethnopharmacology*, 134, 234-242.
4. Wang W., Zu Y., Fu Y., Reichling J., Suschke U., Nokemper S. (2009), *In vitro* antioxidant, antimicrobial and anti-herpes simplex virus type 1 activity of *Phellodendron amurense* Rupr. from China, *The American Journal of Chinese Medicine*, 37, 195-203.
5. Xian Y. F., Lin Z. X., Su Z. R., Chen J. N., Lai X. P. (2013), Comparison the neuroprotective effect of Cortex *Phellodendri Chinensis* and Cortex *Phellodendri amurensis* against beta-amyloid-induced neurotoxicity in PC12 cells, *Phytomedicine*, 20, 187-193.
6. Pharmacopoeia of the people's republic in China (2015), Cortex *Phellodendri Amurensis*, Vol.IA, 336-337.
7. HongKong Chinese Materia Medica Standards Office, Cortex *Phellodendri Amurensis*, Vol. I: 22-30.
8. Zhang Y., Li Q., Feng Y., Yang L., Wang Q., Guo Y. and Qiu D. (2021), Simultaneous Determination of Eight Chemical Components in *Angelicae Sinensis Radix* and Its Herbal Products by QAMS, *Journal of Analytical Methods in Chemistry*, 2021, 7178982.
9. Zhang J., Chen L., Qiu J., Zhang Y., Wang L., Jiang L., Jiang Y., Liu B. (2020), Simultaneous Determination of Six Chromones in *Saposhnikovia Radix* via Quantitative Analysis of Multicomponents by Single Marker. *Journal of Analytical Methods in Chemistry*, 2020, 7867046.
10. Zhua C., Lia X., Zhang B., Lin Z. (2017), Quantitative analysis of multi-components by single marker—a rational method for the internal quality of Chinese herbal medicine, *Integrative Medicine Research*, 6(1), 1-11.
11. Li Y., Zhang Y., Zhang Z., Hu Y., Cui X., Xiong Y. (2019), Quality Evaluation of *Gastrodia Elata Tubers* Based on HPLC Fingerprint Analyses and Quantitative Analysis of Multi-Components by Single Marker, *Molecules*, 24(8), 1521.
12. Chen L. M., Gao H. M., Hu X. H., Zhu J. J., Feng W. H., Yan L. H., Liu X. Q., Zhang Y. X., Wang Z. M. (2019), Establishment of QAMS method with dehydroandrographolide as internal reference substance for quality control of *Andrographis Herba*. *China Journal of Chinese Material Medica*, 44(4), 730-739.
13. ICH Harmonized Tripartite guidelines. Validation of analytical procedures: Text and methodology Q2(R2). 2023, 1-32.
14. Akowuah G.A., Okechukwu P.N., Chiam N.C. (2014), Evaluation of HPLC and Spectrophotometric Methods for Analysis of Bioactive Constituent Berberine in Stem Extracts of *Coscinium fenestratum*, *Acta Chromatographica*, 26(2), 243-254.
15. Xu K., He G., Qin J., Cheng X., He H., Zhang D., Peng W. (2018), High-efficient extraction of principal medicinal components from fresh *Phellodendron bark (cortex phellodendri)*, *Saudi Journal of Biological Sciences*, 25, 811-815.

DEVELOPMENT AND VALIDATION OF QUANTITATIVE ANALYSIS OF L-DOPA FROM *MUCUNA PRURIENS*

Le Thi Loan¹, Dang Minh Tu¹, Dang Viet Hau¹, Nguyen Thi Thu Trang¹, Luong Thi Lan¹,
Ha Van Oanh², Nguyen Van Tai^{1,*}

¹National Institute of Medicinal Materials (NIMM), Hanoi, Vietnam;

²Hanoi University of Pharmacy, Vietnam

*Corresponding author: nguyenvantai1111@gmail.com

(Received February 28th, 2024)

Summary

Development and Validation of Quantitative Analysis of L-Dopa from *Mucuna pruriens*

Mucuna pruriens is an important medicinal plant used for the treatment of Parkinson's disease and many others in ancient traditional Indian medicine. This study reports a simple and rapid high performance liquid chromatography (HPLC) method for the quantification of L-dopa in *Mucuna pruriens* seeds. Methanol/water/hydrochloric acid (70:30:0.1) was used as the extraction solvent. The chromatographic condition was performed on the Agilent Zorbax Eclipse plus C₁₈ column (250 x 4.6 mm, 5 μm), the mobile phase was 0.1% acetic acid/methanol (99:1), flow rate 0.8 mL/min, and the ultraviolet (UV) detector was set at 280 nm. The method has been validated, showing that it is selective, specific, accurate, and suitable for the quantification of L-dopa in *Mucuna* seeds. The recovery was 99.89 - 101.49%, and relative standard deviation (RSD) values of the repeatability and intermediate precision were less than 2%. The limit of quantification of L-dopa was 0.12 μg/mL, corresponding to 0.07 mg/g in samples. This method was used to determine the L-dopa content in 5 samples of *Mucuna pruriens* seeds and showed the L-dopa content ranging from 5.20 ± 0.02% to 5.92 ± 0.10% by weight of dried medicinal herbs.

Keywords: *Mucuna pruriens*, L-dopa, Levodopa, HPLC.

1. Introduction

Mucuna pruriens (L.) DC. is a climbing legume distributed across Africa and Asia. The seeds of the plant contain a high amount (3- 6%) of L-dopa [1],[2]. L-dopa is also known as L-3,4-dihydroxyphenylalanine, an aromatic amino acid, which is biosynthesized via L-tyrosine. It is a precursor molecule of the neurotransmitters dopamine, norepinephrine, and epinephrine. Nowadays, the compound is used for the clinical treatment of Parkinson's disease, a neurodegenerative disorder, which substantiates its prolonged use in traditional Indian medicine. The control of crucial human body functions can be affected by a lack or excess of L-dopa and its metabolites. Treatment of L-dopa in Parkinson's patients is often individualized [3], the initial dose is 125 mg x 2 times/day, may be increased by 100-750 mg every 3-7 days, maximum 8 g/day [4]. Consequently, it is necessary to monitor the concentration of L-dopa in *Mucuna* seeds as well as in all plant matrices destined for human consumption.

There have been several publications on methods to quantify L-dopa in *Mucuna* seeds and products containing it. L-dopa's low molecular weight and polar nature generally make its determination by reversed-phase liquid chromatography challenging. In addition, L-dopa

aqueous solutions are unstable and degrade naturally over time, so the extraction procedure also requires special attention. Vachani et al. [5] and Sundaram et al. [6] reported the HPTLC methods for quantitation of L-dopa in polyherbal formulations containing *M. pruriens* seeds. Pulikkalpura et al. [7] reported studies on quantification and degradation of L-dopa in *M. pruriens* seeds by HPTLC. Soumyanath et al. [8] quantified L-dopa in *M. pruriens* seeds and its formulations by HPLC. British Pharmacopoeia and the United States Pharmacopoeia describe methods for L-dopa determination in tablets or capsules [9],[10].

In Vietnam, *M. pruriens* has also been reported to appear in some places. However, up to now, there have been no studies on the L-dopa content in *Mucuna* seeds in Vietnam. Here, we report a validated HPLC method according to the International Conference on Harmonization guidelines for the quantification of L-dopa content in *M. pruriens* seeds collected in Vietnam.

2. Materials and methods

2.1. Plant material

Mucuna pruriens were collected in Bac Giang province. The scientific name of the samples was identified by Master Dang Minh Tu - Center of Medicinal Material Resources, Institute of Medicinal Materials, based on botanical

characteristics and compared with the taxonomic keys of the genus *Mucuna* [11]. Specimens were kept at the Center of Medicinal Material

Resources - Institute of Medicinal Materials. Fresh samples were dried at 50°C, ground, and stored in sealed plastic bags until use.

Table 1. Samples of information

No.	Sample name	Collection location	Time collection
1	DM1	Son Dong, Bac Giang	12/2021
2	DM2	Luc Nam, Bac Giang	11/2022
3	DM3	Luc Nam, Bac Giang	12/2022
4	DM4	Luc Nam, Bac Giang	10/2023
5	DM5	Luc Nam, Bac Giang	12/2023

2.2. General experimental procedures

Standard material: Levodopa (Chengdu Biopurify), Lot No. 14022406, purity 98,0%.

Solvents, reagents: methanol, acetic acid, phosphoric acid, hydrochloric acid (HPLC grade)

Instruments: HPLC analysis was performed on a Shimadzu system, consisting of a binary pump LC-20AD, a SIL-20A autosampler, a CTO-20A column oven, and a UV-Vis detector SPD-20A.

2.3. Methods

Moisture of samples was determined according to the method of Vietnam Pharmacopoeia V, Appendix 9.6.

The method of sample extraction and chromatographic conditions were investigated and modified based on the methods of P. Siddhuraju and the United States Pharmacopeia [10], [12].

Sample treatment:

Sample preparation: Standard stock solution of L-dopa was prepared by dissolving it in methanol: water: hydrochloric acid (70: 30: 0.1, v/v/v), then diluted to establish calibration curves in ranges of 19.88 - 397.60 µg/mL. The stock and working solutions were stored at 4°C.

Sample extraction: sample preparation factors were investigated including extraction solvents (0.1% HCl solution, methanol, 70% methanol, 50% methanol, 0.1% HCl in methanol, 0.1% HCl in 50% methanol, 0.1% HCl in 70% methanol and 1.0% HCl in 70% methanol), extraction method (ultrasonic and heat reflux methods), extraction time (1 - 3 hours), the ratio of the mass of the sample to the volume of the solvent (g/mL) (1/125, 1/250, 1/500). Select the test sample preparation

method to get the highest content of L-dopa.

HPLC condition: The separation of the compound was performed on an Agilent Zorbax Eclipse plus C₁₈ column (250 x 4.6 mm, 5 µm). The column temperature was maintained at 40°C. The mobile phase was a mixture of methanol and 0.1% acetic acid in water (1: 99, v/v). The flow rate was kept at 0.8 mL/min. The injection volume was 5 µL. Detection was set at a wavelength of 280 nm.

Method validation: the method was validated according to ICH guidelines [13].

Application: samples were treated and analysed according to the developed method. The concentration of analytes in the samples is calculated based on the calibration curve.

3. Results and Discussion

3.1. Method development

The chromatographic conditions were performed on the Agilent Zorbax Eclipse plus C₁₈ column (250 x 4.6 mm, 5 µm). The column temperature was maintained at 40°C. The detection was set at 280 nm.

Selection of mobile phase programs

Three mobile phase program including: (1) methanol and 0.1% trifluoroacetic acid in water (1: 99, v/v) at flow rate of 0.8 mL/min; (2) methanol and 0.1% phosphoric acid in water (1: 99, v/v) at flow rate of 0.6 mL/min; (3) methanol and 0.1% acetic acid in water (1: 99, v/v) at flow rate of 0.8 mL/min were tested. The results showed that with the mobile phase program 1 and the mobile phase program 2, the peaks of L-dopa were broadened (Fig. 1). With the mobile phase consisting of methanol and 0.1% acetic acid in water, the peaks were symmetric and sharp.

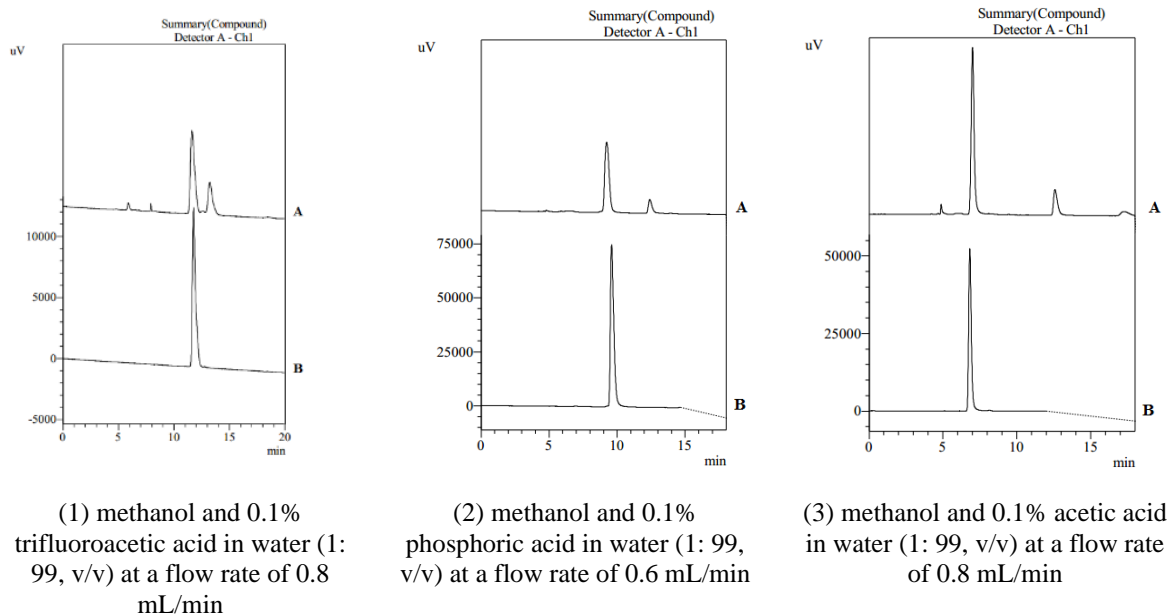


Fig. 1. Chromatograms for selection of mobile phase programs (A: sample solution; B: standard)

Selection of injection volume

Simultaneously, 2 levels of sample injection volume were also investigated. The results showed that when the injection volume was 5 μ l, the peaks shape had a better shape than when the injection volume was 10 μ l.

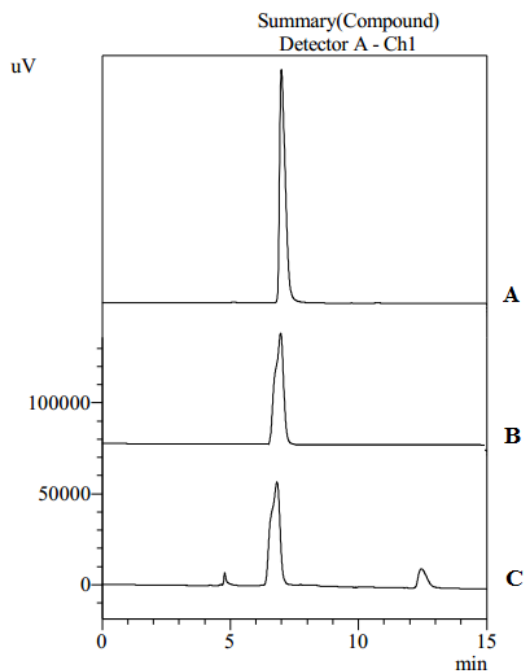


Fig. 2. Chromatograms for selection of injection volume (A: standard solution 5 μ l; B: standard solution 10 μ l; C: sample solution 10 μ l)

Therefore, the selected chromatographic conditions analysis of L-dopa in *Mucuna* seeds were: Agilent Zorbax Eclipse plus C₁₈ column (250 x 4.6 mm, 5 μ m); the mobile phase consisted of methanol and 0.1% acetic acid in water (1: 99, v/v) at flow rate of 0.8 mL/min; the column temperature was maintained at 40°C; the detection was set at 280 nm; the injection volume was 5 μ l.

3.2. Optimization of extraction conditions

The results are presented in Table 2. showed that acidic solvents (methanol, 70% methanol containing 0.1% HCl) have higher L-dopa extraction efficiency than corresponding neutral pH solvents (methanol, 70% methanol). Furthermore, the experimental process showed that when using neutral pH solvents, the extract is not stable and quickly changes color, even when stored in cold conditions (2-8°C) for 3 days. Meanwhile, using an acidic extraction solvent, the color of the extract is more stable, even when stored at room temperature for up to 7 days. This result is consistent with the literature [12].

The solvents 70% methanol containing 0.1% HCl and 70% methanol containing 1.0% HCl were shown to be better extraction solvents, reaching $5.21 \pm 0.02\%$ and $5.20 \pm 0.2\%$ respectively. There was no significant difference in the efficiency of extracting L-dopa from medicinal herbs when

increasing the concentration of HCl in the extraction solvent from 0.1% to 1.0%. Besides, at both levels of HCl concentration used, the medicinal extracts are color stable under normal or cold conditions.

This result is consistent with published results

on the method of quantifying L-dopa in medicinal herbs 0.1 M HCl, MeOH: 0.1 M HCl (70:30) [14],[15],[16], 0.1 M HCl : EtOH (1:1) [17], HCOOH : EtOH (1:1) [12]. So, 70% methanol containing 0.1% HCl was chosen as the extraction solvent from the *Mucuna* seeds.

Table 2. The results of extraction conditions optimization (n = 3)

Extraction solvents (m= 0.2000 g, 100 mL solvents, reflux in 90 min.)		Methods and times of extraction (m= 0.2000 g, 100 mL of 0.1% HCl in 70% methanol)	
Solvents	L-dopa (%)	Conditions	L-dopa (%)
0.1% HCl solution	5.02 ± 0.02	Sonication 10 min.	4.71 ± 0.05
50% Methanol	5.05 ± 0.02	Sonication 15 min.	4.98 ± 0.06
0.1% HCl in 50% methanol	5.11 ± 0.09	Sonication 30 min.	5.09 ± 0.03
70% Methanol	5.11 ± 0.02	Sonication 60 min.	5.02 ± 0.03
0.1% HCl in 70% methanol	5.21 ± 0.02	Reflux 60 min.	5.05 ± 0.01
Methanol	4.89 ± 0.09	Reflux 90 min.	5.21 ± 0.03
0.1% HCl in methanol	5.09 ± 0.03	Reflux 120 min.	5.21 ± 0.01
1.0 % HCl in 70% methanol	5.20 ± 0.02	Reflux 150 min.	5.21 ± 0.02
		Reflux 180 min.	5.17 ± 0.03
Ratio of sample/solvent (m/v, g/mL) (m= 0.2000 g, 0.1% HCl in 70% methanol, reflux in 90 min.)			
Conditions	L-dopa (%)	Conditions	L-dopa (%)
0.2000 g/25 mL	4.90 ± 0.05	0.2000 g/100 mL	5.20 ± 0.02
0.2000 g/50 mL	5.11 ± 0.04	0.2000 g/50 mL, 2 times	5.21 ± 0.02

Other factors of sample preparation conditions, including extraction methods, extraction time, and ratio of sample/solvent, were also investigated.

From the results, the sample preparation procedure was selected as follows: weigh accurately 0.2000g of seed powder, add 100mL 0.1% HCl in 70% methanol, reflux for 1.5 hours, cool to room temperature, filter and transfer the filtrate to a 100-mL volumetric flask, make up to the mark with 0.1% HCl in 70% methanol. The solution was filtered through a 0.45 µm membrane filter before HPLC analysis.

3.3. Method validation

Specificiation

The experiment was performed with the blank, standard, and sample solutions according to the analytical procedure. The obtained chromatograms are shown in Fig. 3.

The results showed that there was no peak in the blank sample at the retention times of the targeted peaks in the standard solution. The obtained chromatograms showed clear separation peaks and low background noise. Therefore, the analytical method was specific for the determination of the targeted marker.

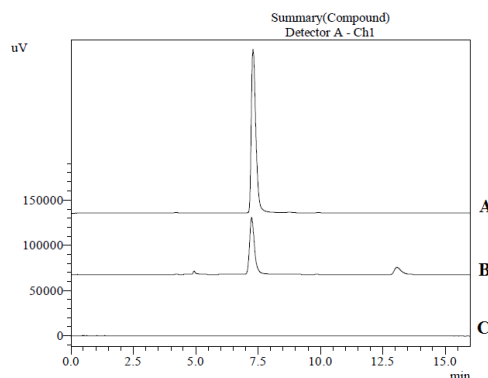


Fig. 3. Chromatograms for specificity study (A: standard; B: sample solution; C: blank)

System suitability

Table 3. System suitability testing

No	Retention time (min.)	Peak area (mAu.s)
1	7.437	666416
2	7.497	664118
3	7.422	661140
4	7.453	656679
5	7.298	665378
6	7.416	655072
7	7.525	652013
Mean	7.435	660116.6
SD	0.073	5588.0
RSD (%)	0.98	0.85

Table 3 shows that the RSD % of retention time and peak area were all under 2%. These indicated that the developed method conforms to system suitability criteria.

Linearity

Different concentrations of L-dopa were prepared and injected into the HPLC system. The calibration curve was constructed by plotting the peak areas versus the concentrations of the analyte. The result showed satisfactory linearity in the concentration ranges of 19.88 - 397.60 µg/mL for L-dopa. The typical calibration curve equation of L-dopa was $y = 6747x - 17272$, with the P-value of y-intercept less than 0.05. Linear correlation value $R^2 = 0.9999$. Therefore, it can be concluded that this developed method conforms the linearity.

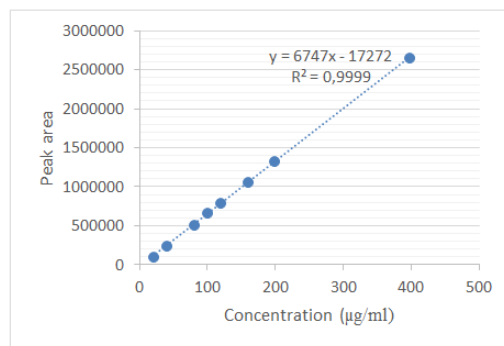


Fig. 4. Illustrating the linearity between L-dopa concentration and its corresponding peak area *Precision*

The results of the repeatability and intermediate precision study are presented in Table 4. The average content of L-dopa is 5.20% and the RSD all under 2.0%. The result was in good agreement with acceptable values for validation of the analytical procedure.

Table 4. The precision results

No.	L-dopa content (%)		Average: 5.20% RSD: 0.40%
	Day 1	Day 2	
1.	5.22	5.20	
2.	5.19	5.21	
3.	5.25	5.18	
4.	5.19	5.17	
5.	5.21	5.22	
6.	5.19	5.19	
Average (%)	5.21	5.20	
SD (%)	0.02	0.02	
RSD (%)	0.44	0.36	

Accuracy

Weigh accurately approximately 1.00 mg, 2.00 mg, and 3.00 mg of L-dopa, then dissolved each in 50 mL of 0.1% HCl in 70% methanol to obtain solutions with a corresponding concentration of approximately 20.00, 40.00, and 60.00 µg/mL. These solutions were added

to 0.1000 g of the known samples, then extraction and analysis were performed. The results in Table 5 show that recovery rates of L-dopa were in the range of 95-105%. The recovery values were from 99.34 to 100.74%, indicating that the accuracy of the method was acceptable.

Table 5. The accuracy testing results

Amount added (µg/mL)	Amount found (µg/mL)	Recovery (%)	M ± SD (%)
19.80	20.04	101.21	100.74 ± 0.81
20.20	20.44	101.20	
20.20	20.16	99.80	
40.00	39.65	99.12	99.81 ± 0.60
40.20	40.28	100.20	
40.40	40.44	100.11	
61.00	60.45	99.10	99.34 ± 0.46
60.60	60.52	99.87	
60.80	60.22	99.05	

LOD and LOQ

The limits of detection (LOD) and the limits of quantification (LOQ) were calculated by diluting sample solutions until signal-to-noise ratios of 3 and 10, respectively. LOD and LOQ were estimated to be 0.128 µg/mL and 0.4224 µg/mL for L-dopa, corresponding to 0.07 mg/g and 0.23 mg/g in samples.

The analytical method for the determination of L-dopa in *Mucuna* seeds met the requirements of systematic suitability, selectivity, linearity, precision, and accuracy according to ICH criteria. Therefore, this method could be used to analyze L-dopa in *Mucuna* seeds.

3.4. Applications

The proposed method was applied for the determination of L-dopa in 5 samples *Mucuna* seeds. Each sample was analyzed in triplicate to determine the meant content (%). The results are summarized in Table 6.

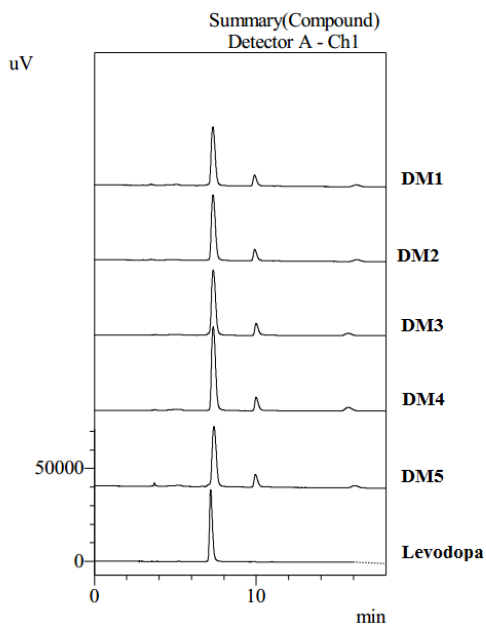


Fig. 5. Chromatograms of samples

Table 6. L-dopa content in the *Mucuna pruriens* seeds

No.	Sample name	Moisture (%)	Weight (g)	Peak area (mAu.s)	Concentration (µg/mL)	Content (%)	M ± SD (%)
1	DM1	9.08	0.2154	672562	101.61	5.19	5.20 ± 0.01
			0.2198	689422	104.05	5.21	
			0.2188	684372	103.32	5.19	
2	DM2	9.79	0.2137	757923	113.96	5.91	5.80 ± 0.22
			0.2078	739813	111.34	5.94	
			0.2152	714330	107.65	5.55	
3	DM3	10.03	0.2102	740915	111.50	5.90	5.94 ± 0.06
			0.2009	720446	108.54	6.00	
			0.2055	724797	109.17	5.90	
4	DM4	9.12	0.2186	790182	118.63	5.97	5.92 ± 0.10
			0.2114	764344	114.89	5.98	
			0.2070	724737	109.16	5.80	
5	DM5	9.85	0.2105	741043	111.52	5.88	5.82 ± 0.07
			0.2124	743934	111.94	5.85	
			0.2305	795228	119.35	5.74	

Discussion

The validation results showed that the developed method is selective, specific, accurate, and suitable for the quantification of L-dopa in *Mucuna* seeds. According to published studies, the LOD of L-dopa ranges from approximately 10 ng/mL to 15 µg/mL [18]. The analytical method of Kasture and colleagues published in 2014 has a LOD/LOQ of 0.115/0.348 µg/mL [17]. Meanwhile, Baranowska's method has a lower LOD/LOQ, 10 and 30 ng/mL, respectively [19]. Thus, the developed method has a relatively low

detection limit and quantitation limit, suitable for quantifying L-dopa in *Mucuna* seeds.

Quantitative results show that the studied samples have L-dopa marker content ranging from 5.20 ± 0.02% to 5.92 ± 0.10% by weight of dried seeds.

This result is consistent with published literature. Modi et al. [2], Behara et al. [20], and Raina et al. [1] estimated 5.60, 4.83, and 3.29-5.44%, respectively of L-dopa in *M. pruriens* seeds by HPTLC. In 2003, L. Capo-Chichi and colleagues researched and announced that the L-

dopa content in *Mucuna cochinchinensis* seeds in Colombia was 5.4% [21]. Research by Perumal Siddhuraju in 2001 showed that the L-dopa content in the seeds of *Mucuna pruriens* var. *utilis* was 4.96% [22]. Bhumika G. Rathod and colleagues in 2014 developed a method and determined the L-dopa content in *Mucuna pruriens* from 3.84 - 5.095% [15]. In 2016, author Deokar G. and his colleagues researched and published the L-dopa content in *Mucuna pruriens* seeds quantified by the HPLC method with a content ranging from 3.9 - 6.2% [23]. According to Patil, the L-dopa content in *Mucuna sanjappae* seeds reached 7.3% [24]. A study by Fernandez-Pastor and colleagues in 2019 showed that the amount of L-dopa in the seeds of *Mucuna pruriens* ranged from 3.0-3.2% [25].

The L-dopa content in *Mucuna* seeds depends on the species and collection area. However, our results showed that *Mucuna pruriens* seeds in Vietnam have quite high concentrations, up to more than 5%. This is interesting information,

suggesting that *Mucuna pruriens* seeds in Vietnam can be a potential source of raw materials to provide L-dopa naturally for humans. These can be considered initial results, providing important suggestions for further research to develop the medicinal source of *Mucuna pruriens* seeds in Vietnam.

4. Conclusion

In this study, the method for quantifying L-dopa in *Mucuna* seeds by HPLC has been developed and validated, showing that the method is selective, specific, accurate, and suitable for the quantification of L-dopa in *Mucuna* seeds. In addition, the quantitative results showed that the *Mucuna pruriens* seeds samples collected at Bac Giang province had L-dopa content ranging from $5.20 \pm 0.02\%$ to $5.92 \pm 0.10\%$ by weight of dried.

Acknowledgment: *This work was supported by the project: "Research on chemical composition and preparation of 01 reference substance of Mucuna pruriens seeds" We acknowledge the study participants for their gracious help.*

References

1. Raina A. P., Khatri R. (2011), Quantitative determination of L-DOPA in seeds of *Mucuna pruriens* germplasm by high performance thin layer chromatography, *Indian Journal of Pharmaceutical Sciences*, 73(4), 459.
2. Modi K. P., Patel N. M., Goyal R. K. (2008), Estimation of L-Dopa from *Mucuna pruriens* L INN and formulations containing *M. pruriens* by HPTLC Method, *Chemical and Pharmaceutical Bulletin*, 56(3), 357-359.
3. Marsot A., Guilhaumou R., Azulay J. P., Blin O. (2017), Levodopa in Parkinson's disease: a review of population pharmacokinetics/pharmacodynamics analysis, *Journal of Pharmacy & Pharmaceutical Sciences*, 20, 226-238.
4. Ministry of Health (Vietnam) (2022), *Vietnamese National Drug Formulary. 3rd*, Hanoi.
5. Vachhani U. D., Trivedi M. N., Bajaj A., Shah C. (2011), A HPTLC method for quantitative estimation of L-dopa from *Mucuna pruriens* in polyherbal aphrodisiac formulation, *Research Journal of Pharmaceutical, Biological and Chemical Sciences*, 2, 389-396.
6. Sundaram U., Gurumoorthi P. (2012), Validation of HPTLC method for quantitative estimation of L-Dopa from *Mucuna pruriens*, *International Research Journal of Pharmacy*, 3, 300-304.
7. Pulikkalpara H., Kurup R., Mathew P. J., Baby S. (2015), Levodopa in *Mucuna pruriens* and its degradation, *Scientific Reports*, 5(1), 11078.
8. Soumyanath A., Denne T., Peterson A., Shinto L. (2012), P01. 36. Assessment of commercial formulations of *Mucuna pruriens* seeds for Levodopa (L-DOPA) content, *BMC Complementary and Alternative Medicine*, 12, 1.
9. Commission B. P. (2021), British pharmacopoeia (BP) 2022. *The Stationery Office on Behalf of the MHRA, London*.
10. Convention U. S. P. (2017), *The United States Pharmacopeia 2018 : USP 41; The national formulary: NF 36*, 2392-2395.
11. Press M. B. G. (2010), Flora of China volume 10 Fabaceae.
12. Siddhuraju P., Becker K. (2001), Rapid reversed-phase high performance liquid chromatographic method for the quantification of L-Dopa (L-3, 4-dihydroxyphenylalanine), non-methylated and methylated tetrahydroisoquinoline compounds from *Mucuna* beans, *Food Chemistry*, 72(3), 389-394.
13. Guideline I. H. T. (2005), Validation of analytical procedures: text and methodology, *Q2 (R1)*, 1(20), 05.
14. Dhanani T., Singh R., Shah S., Kumari P., Kumar S. (2015), Comparison of green extraction methods with conventional extraction method for extract yield, L-Dopa concentration and antioxidant activity of *Mucuna pruriens* seed, *Green Chemistry Letters and Reviews*, 8(2), 43-48.
15. Rathod B. G., Patel N. M. (2014), Development of validated RP-HPLC method for the estimation of L-Dopa from *Mucuna pruriens*, its extracts and in Aphrodisiac formulation, *International Journal of Pharmaceutical Sciences and Research*, 5, 508-513.
16. Pavón-Pérez J., Oviedo C. A., Elso-Freudenberg M., Henríquez-Aedo K., Aranda M. (2019), LC-MS/MS method for L-DOPA quantification in different tissues of *Vicia faba*, *Journal of the Chilean Chemical Society*, 64(4), 4651-4653.
17. Kasture V., Sonar V. P., Patil P. P., Musmade D. (2014), Quantitative Estimation of L-Dopa from Polyherbal Formulation by using RP-HPLC, *American Journal of PharmTech Research*, 4, 408-414.
18. Tesoro C., Lelario F., Ciriello R., Bianco G., Di Capua A., Acquavia M. A. (2022), An Overview of Methods for L-Dopa Extraction and Analytical Determination in Plant Matrices, *Separations*, 9(8), 224.
19. Baranowska I., Płonka J. (2015), Simultaneous determination of biogenic amines and methylxanthines in foodstuff—sample preparation with HPLC-DAD-FL analysis, *Food Analytical Methods*, 8, 963-972.
20. Behera A., Sankar D. G., Si S. C. (2010), Development and validation of an HPTLC-densitometric method for determination of levodopa in seeds of *Mucuna pruriens* and its capsule dosage form, *Eurasian Journal of Analytical Chemistry*, 5(2), 126-

136. **21.** Capo-Chichi L., Eilittä M., Carsky R., Gilbert R., Maasdorp B. (2003), Effect of genotype and environment on L-dopa concentration in *Mucunas* (*Mucuna sp.*) Seeds, *Tropical and Subtropical Agroecosystems*, 1(2-3), 319-328. **22.** Siddhuraju P., Becker K. (2001), Rapid reversed-phase high performance liquid chromatographic method for the quantification of L-Dopa (L-3,4-dihydroxyphenylalanine), non-methylated and methylated tetrahydroisoquinoline compounds from *Mucuna* beans, *Food Chemistry*, 72(3), 389-394. **23.** Deokar G., Kakulte H., Kshirsagar S. (2016), Phytochemistry and pharmacological activity of *Mucuna pruriens*: A review, *Pharmaceutical and Biological Evaluations*, 3(1), 50-59. **24.** Patil R. R., Gholave A. R., Jadhav J. P., Yadav S. R., Bapat V. A. (2015), *Mucuna sanjappae* Aitawade et Yadav: a new species of *Mucuna* with promising yield of anti-Parkinson's drug L-Dopa, *Genetic Resources and Crop Evolution*, 62(1), 155-162. **25.** Fernandez-Pastor I., Luque-Muñoz A., Rivas F., Medina-O'Donnell M., Martinez A., Gonzalez-Maldonado R., Haidour A., Parra A. (2019), Quantitative NMR analysis of L-Dopa in seeds from two varieties of *Mucuna pruriens*, *Phytochemical Analysis*, 30(1), 89-94.

Journal of Medicinal Materials, 2024, Vol. 29, No. 6 (pp. 361 - 366)

ANTI-AGGREGATORY AND ANTI-COAGULANT ACTIVITIES OF *POLYGONUM CUSPIDATUM* EXTRACTS

Le Hong Luyen*, Nguyen Thi Van Anh

University of Science and Technology of Hanoi, Vietnam Academy of Science and Technology,
Hanoi, Vietnam

*Corresponding author: le-hong.luyen@usth.edu.vn

(Received October 25th, 2024)

Summary

Anti-Aggregatory and Anti-Coagulant Activities of *Polygonum cuspidatum* Extracts

Polygonum cuspidatum, also called Côt khí củ in Vietnam, is a well-known traditional plant with many approved pharmacological effects. In the current study, various extracts from *P. cuspidatum* rhizomes were tested for their anti-thrombotic activity on human blood for the first time. The platelet aggregation triggered by collagen was measured in human platelet-rich plasma. The blood clotting time was determined using three factors of the coagulation system: activated partial thromboplastin time (APTT), prothrombin time (PT), and thrombin time (TT). The results showed that the ethyl acetate extract (PC-EA) displayed the most potent inhibitory effect against collagen-induced platelet aggregation, with the percentage of inhibition increasing from 28.03% at 0.2 mg/mL to 82.38% at 0.8 mg/mL. Moreover, this extract also expressed a more potent anti-coagulant activity than the *n*-hexane and ethanol extracts ($p < 0.05$). In addition, PC-EA was the only sample that prolonged the blood clotting time in a dose-dependent manner for both APTT and TT assays. However, this extract could slightly extend the PT at 0.8 mg/mL with 13.57 ± 0.48 s compared to 12.13 ± 0.17 s of DMSO 0.1% used as the negative control ($p < 0.05$). The ethanol fraction from 0.4 mg/mL possessed considerably higher APTT and TT values than the negative control, meanwhile, the *n*-hexane display no effects on the blood coagulation by any pathways. In conclusion, the ethyl acetate was the most active fraction from *P. cuspidatum*. Therefore, this extract could provide a source of promising phytoconstituents used in further prevention and treatment of thrombosis-associated diseases.

Keywords: *Polygonum cuspidatum*, Anti-aggregatory activity, Anti-coagulant activity, Thrombosis.

1. Introduction

The World Health Organization (WHO) stated that cardiovascular diseases (CVD) are the leading cause of death globally [1]. Thrombosis, or the formation of blood clots in blood arteries, is the main source of CVD [2]. The main antithrombotics include antiplatelet drugs aiming to reduce platelet aggregation and anticoagulant agents focusing on the suppression of blood clot development. Conventional antithrombotic medications are powerful, however, also linked to several negative consequences [3]. Therefore, seeking new effective antithrombotic agents from natural resources with fewer side effects is required for further treatment of CDV.

Polygonum cuspidatum Sieb. et Zucc (*P.*

cuspidatum), belonging to the family Polygonaceae, is a well-known medicinal plant largely growing in many Asia countries. In the literature, many pharmacological effects *in vitro* and *in vivo* of this plant have been approved including the anti-inflammatory effect [4], anticancer activity [5], neuroprotective effect [6], and hepatoprotective effect [7]. Moreover, previous studies documented that several polyphenolic compounds such as resveratrol, polydatin, quercetin, emodin, and their derivatives were the key active phytoconstituents in *P. cuspidatum* [8]. A few reports on the cardioprotective action of polydatin have been published, justifying its ability to prevent heart failure and cardiac hypertrophy caused by

pressure overload [9] or to lower the expression of angiotensin and avoid damage from cardiac ischemia [10]. Another study by Gavriil et al. demonstrated that the consumption of a supplement containing *P. cuspidatum* extract decreased significantly the platelet-activating factor-triggered platelet aggregation [11]. However, the inhibitory effect related to the thrombosis-associated diseases of *P. cuspidatum* and its components was still limited.

Therefore, the present study aimed to evaluate the anti-thrombotic effect of *Polygonum cuspidatum* extracts for the first time. This activity is composed of two primary assays investigated on human plasma: the anti-aggregatory and anticoagulant effects.

2. Material and Methods

2.1. Chemicals

Aspirin, collagen, heparin, and dimethyl sulfoxide (DMSO) were purchased from Sigma-Aldrich. Blood clotting reagents including APTT, PT, and TT were obtained from Dade Behring Marburg GmbH (Marburg, Germany).

2.2. Plant material

Dried roots of *Polygonum cuspidatum* were harvested in Thai Nguyen province in February 2023. The plant was identified by Dr. Nguyen Quoc Binh, Vietnam National Museum of Nature, Vietnam Academy of Science and Technology.

One gram of *P. cuspidatum* root powder was soaked twice using sonication for 30 minutes with 10 mL of each solvent with increasing polarity: *n*-hexane (HX), ethyl acetate (EA), and ethanol 80% (ET). The corresponding extracts (PC-HX, PC-EA, and PC-ET) were completely evaporated under reduced pressure and then stocked at 4°C before testing.

2.3. Blood samples preparation

The study received approval from the Ethics Committee of the School of Medicine and Pharmacy at Vietnam National University, Hanoi, Vietnam (document number 02/2020/CN-HĐĐĐ). Healthy participants in the study, aged 18 to 35 years, are nonsmokers, free of any medications for at least three weeks, and have fasted overnight at least 8 hours before the test. Whole blood (10 mL) after drawing from venous was put into test tubes containing 3.2% sodium citrate as the anticoagulant agent. After that, the blood samples were centrifuged for 10 minutes

respectively at 500 rpm and then at 3000 rpm to collect platelet-rich plasma (PRP) and platelet-poor plasma (PPP), according to the protocol in the Department of Hemostasis, National Institute of Hematology and Blood Transfusion. All plasma samples were utilized up to three hours after collection.

2.4. Antiplatelet aggregation assay

This experiment was done following the technique of Le et al. [12]. 50 µL of PC-HX, PC-EA, and PC-ET (at a range of concentrations from 0.2 to 0.8 mg/mL in DMSO 0.1%) and 450 µL of PRP were slightly mixed and incubated for 3 min at 37°C. Then, the platelet aggregation was produced by adding 1 µL of collagen at 2 µg/mL. The percentage of aggregation of the negative control (X) and samples (Y) was measured by a Chrono-Log 530 VS aggregator (USA). The inhibition of platelet aggregation (%I) was calculated as follows:

$$\%I = (1 - Y/X) \times 100\%$$

The experiment used DMSO at 0.1% and aspirin at 0.1 mg/mL as the negative and positive controls, respectively.

2.5. Anticoagulant assay

Mixtures containing 50 µL of plant extracts at varying concentrations (final at 0.2, 0.4, and 0.8 mg/mL) and 450 µL of PPP were made, then incubated for five minutes at 37°C. Subsequently, clotting reagents (APTT, PT, and TT) were then added to measure the time that plasma has started to clot. APTT and PT values respectively represent the clotting time produced by the intrinsic and extrinsic pathways, while TT refers to the common pathway in which, fibrinogen was transformed into fibrin to form a blood clot. DMSO 0.1% was used as the negative control. Heparin at 0.2 IU/mL (for APTT and TT parameters) or 2 IU/mL (for PT parameter) was used as the positive control.

All experiments were carried out in triplicate with three different blood samples.

2.6. Data analysis

Results were expressed as the means ± standard deviation. Data were statistically compared using one-way ANOVA tests, and Tukey post-tests in the GraphPad 9.5.0 software. Pearson correlation was analyzed to determine the statistical relationship between concentrations and activities of samples.

3. Results and discussion

3.1. Anti-aggregatory activity of *P. cuspidatum* extracts

The inhibitory effect of different *P. cuspidatum* extracts on collagen-induced aggregation were demonstrated in Fig. 1. It is noted that all samples exhibited a dose-dependent manner activity from 0.2 to 0.8 mg/mL (Pearson correlation, $r > 0.95$, $p < 0.05$). Among the three fractions, PC-EA was shown to express the highest anti-aggregatory effect, followed by PC-ET and PC-HX. In more detail, at 0.8 mg/mL, the percentage of inhibitions obtained by PC-EA, PC-ET, and PC-HX was 82.38%, 48.61%, and 17.82% respectively.

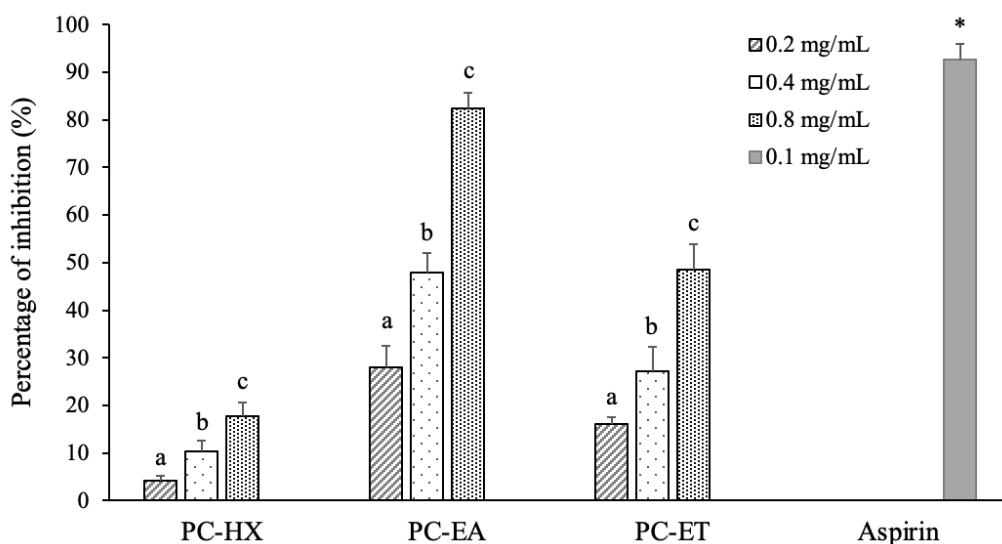


Fig. 1. Inhibitory effect of *P. cuspidatum* extracts on collagen-induced aggregation

PC-HX: the *n*-hexane extract, PC-EA: the ethyl acetate extract, PC-ET: the ethanol extract, aspirin: the positive control.

Different letters indicate significant differences among concentrations of the sample fraction,

*: $p < 0.05$: significant difference between aspirin and other samples.

3.2. Anti-coagulant effect of *P. cuspidatum* extracts

Like the anti-aggregatory effect, three fractions of *P. cuspidatum* were tested for their anti-coagulant activity at three concentrations of 0.2, 0.4, and 0.8 mg/mL. In this experiment, the blood clotting time was determined by three factors corresponding to three pathways: APTT is a functional measure of the intrinsic pathway of the coagulation system, PT is the time taken to form a blood clot in the extrinsic pathway with the presence of sufficient calcium, while TT measures the time when fibrinogen convert into fibrin in the solid state under the action of thrombin [12]. In the

However, all these values were remarkably smaller than aspirin at 0.1 mg/mL used as the positive control ($p < 0.05$).

In 2003, a group of Korean scientists found similar results as indicated in the present study by proving that the ethyl acetate extract from *P. cuspidatum* was able to prevent collagen-induced platelet aggregation more effectively than other extracts [13]. In addition, polydatin, a main bioactive compound isolated from *P. cuspidatum*, was shown to possess a promising anti-platelet aggregation activity [14]. However, a very limited report was published in the literature on the anti-aggregatory effect of *P. cuspidatum* and its phytoconstituents.

APTT and TT tests, heparin served as the positive control was used at the concentration of 0.2 IU/mL, which was able to prolong the clotting time by 1.5-2 times compared to the negative control. In addition, many previous studies have shown that heparin also influences the extrinsic pathway by increasing the activity of coagulation inhibitors on this pathway [15],[16]. Therefore, after examining several concentrations (including 0.2 IU/mL), the authors found that heparin at a concentration of 2 IU/mL showed the ability to significantly prolong the clotting time in the PT test. Similar results of heparin on the three coagulation pathways were also demonstrated in

several recent articles published by Le et al. [12],[17],[18].

Effect of *P. cuspidatum* extracts on activated partial thromboplastin time (APTT)

In Table 1, it is seen that PC-HX at all concentrations did not prolong the clotting time compared to the negative control ($p > 0.05$). In contrast, PC-EA expressed a strong anti-coagulant activity from 0.2 mg/mL to 0.8 mg/mL when APTT increased from 34.40 s to 40.81s, respectively. Meanwhile, PC-ET showed significantly higher APTT than DMSO 0.1% only from 0.4 mg/mL (34.15 s) to 0.8 mg/mL (38.71 s). In general, the ethyl acetate fraction possessed the most remarkable anti-aggregatory effect, followed by the ethanol fraction and the *n*-hexane fraction. This finding is also consistent with the result obtained by Nguyen et al. when they investigated similar experiments on *Canna generalis* extracts [17].

Effect of *P. cuspidatum* extracts on prothrombin time (PT)

In this assay, most of the samples tested were not able to extend the clotting time compared to the negative control (PT 12.13 s, $p > 0.05$). Only PC-EA at 0.8 mg/mL displayed a significant anti-coagulant effect through the extrinsic pathway (PT 13.57s, $p < 0.05$ compared to DMSO 0.1%). However, the clotting time of this extract was still considerably shorter than the one of the positive control, heparin with 31.21 s.

Effect of *P. cuspidatum* extracts on thrombin time (TT)

Similar to APTT and PT assays, PC-HX expressed no extending effect on blood coagulation's common pathway since it was not able to prolong TT compared to the negative control at all three concentrations tested ($p > 0.05$). Meanwhile, PC-ET only displayed an anti-coagulant activity at 0.8 mg/mL (TT, 18.49 ± 1.25

s vs. 14.31 ± 1.03 s of DMSO 0.1%, $p < 0.05$). Particularly, PC-EA extended the blood clotting time in a dose-dependent manner with TT rising from 13.63 s at 0.2 mg/mL to 21.60 s at 0.8 mg/mL (Pearson correlation, $r > 0.90$, $p < 0.05$). The positive control, heparin at 0.2 IU exhibited remarkably a longer TT (32.30 ± 1.30) than all samples tested ($p < 0.05$).

Taking into consideration all the results mentioned above, it is worth noting that the ethyl acetate extract was shown to be the most active fraction of *P. cuspidatum* in inhibiting both platelet aggregation and blood coagulation. In our previous documents, the ethyl acetate fraction from different medicinal plants such as *Kaempferia parviflora* [12], *Canna generalis* [17], *Canna edulis* [18], or *Canna warszewiczii* [19], was also more potent than other fractions. In addition, several compounds isolated from the ethyl acetate extract of those plants were justified to be very potent in preventing platelet aggregation and prolonging the blood clotting time. For instance, the active compounds composed of 5,7,4'-trimethoxyflavone and 5-hydroxy-3,7,4'-trimethoxyflavone from *K. parviflora*; 4-ketopinoresinol and indole-3-carboxylic acid from *C. generalis*; epimedokoreanone A and nepetidine B from *C. edulis*. In the current study, *P. cuspidatum* could serve as a source of phytoconstituents having potential in the treatment of thrombosis-associated diseases. In the upcoming studies, molecular docking analysis will be investigated to predict the potential interactions between the main components in *P. cuspidatum* and target receptors in the blood coagulation pathways. The results will help find the bioactive compounds from this plant and their mechanism of action.

Table 1. Anti-coagulant activity of *P. cuspidatum* extracts

Sample	Concentration (mg/mL)	APTT (s)	PT (s)	TT (s)
PC-HX	0.2	28.70 ± 1.08 (#)	11.76 ± 0.59 (#)	14.65 ± 0.52 (#)
	0.4	29.63 ± 0.24 (#)	12.08 ± 0.81 (#)	14.38 ± 0.64 (#)
	0.8	31.05 ± 0.69 (#)	12.16 ± 0.29 (#)	14.59 ± 0.50 (#)
PC-EA	0.2	34.40 ± 2.11 (*) (#)	12.20 ± 0.92 (#)	13.63 ± 0.87 (#)
	0.4	37.27 ± 1.35 (*) (#)	12.76 ± 0.59 (#)	17.72 ± 1.31 (*) (#)
	0.8	40.81 ± 1.04 (*) (#)	13.57 ± 0.48 (*) (#)	21.60 ± 1.47 (*) (#)

Sample	Concentration (mg/mL)	APTT (s)	PT (s)	TT (s)
PC-ET	0.2	31.05 ± 0.59 (#)	12.90 ± 1.16 (#)	14.75 ± 0.89 (#)
	0.4	34.15 ± 1.16 (*)(#)	11.60 ± 0.47 (#)	15.26 ± 0.38 (#)
	0.8	38.71 ± 1.73 (*)(#)	12.01 ± 0.85 (#)	18.49 ± 1.25 (*)(#)
DMSO	0.1%	30.95 ± 1.17 (#)	12.13 ± 0.17 (#)	14.31 ± 1.03 (#)
Heparin	0.2 IU	47.01 ± 1.90		32.30 ± 1.30
	2 IU		31.21 ± 0.82	

APTT: activated partial thromboplastin time, PT: prothrombin time, TT: thrombin time, PC-HX: the *n*-hexane extract, PC-EA: the ethyl acetate extract, PC-ET: the ethanol extract, DMSO: the negative control, heparin: the positive control, *: $p < 0.05$ compared to the negative control, #: $p < 0.05$ compared to the positive control.

4. Conclusion

Different extracts from *Polygonum cuspidatum* were evaluated for their anti-aggregatory and anti-coagulant activities for the first time. It was shown that the ethyl acetate fraction possessed the highest inhibitory effect against collagen-induced platelet aggregation. In addition, this extract was able to prevent blood coagulation through all tested pathways by elongating APTT, PT, and TT values in comparison with the negative control. The ethanol extract only extended two factors APTT and TT, while the *n*-hexane did not provide any changes in the blood clotting time. In conclusion,

the ethyl acetate exhibited better anti-thrombotic activity than the ethanol and the *n*-hexane extracts. Therefore, further investigation on the ethyl acetate extract needs to be carried out to seek active phytochemicals and their mechanism of action in the treatment of cardiovascular diseases related to blood clot formation.

Acknowledgments: This study was supported by the Biopharma-Environmental Assessment & Monitoring (BEAM) group, University of Science and Technology of Hanoi, Vietnam Academy of Science and Technology.

References

1. WHO, Cardiovascular diseases (CVDs), Accessed: Jan. 08, 2022. [Online]. Available: [https://www.who.int/news-room/fact-sheets/detail/cardiovascular-diseases-\(cvds\)](https://www.who.int/news-room/fact-sheets/detail/cardiovascular-diseases-(cvds)).
2. Mackman N. (2008), Triggers, targets and treatments for thrombosis, *Nature*, 451, 914-918.
3. Mackman N., Bergmeier W., Stouffer G. A., Weitz J. I. (2020), Therapeutic strategies for thrombosis: new targets and approaches, *Nature Review Drug Discovery*, 19 (5), 333-352.
4. Liu B., Li S., Sui X., Guo L., Liu X., Li H., Gao L., Cai S., Li Y., Wang T., Piao X. (2018), Root extract of *Polygonum cuspidatum* Siebold & Zucc. ameliorates DSS-induced ulcerative colitis by affecting NF- κ B signaling pathway in a mouse model via synergistic effects of polydatin, resveratrol, and modin, *Frontiers in Pharmacology*, 9, 347, 1-14.
5. Zhao J., Pan B., Zhou X., Wu C., Hao F., Zhang J., Liu L. (2022), *Polygonum cuspidatum* inhibits the growth of osteosarcoma cells via impeding Akt/ERK/EGFR signaling pathways, *Bioengineered*, 13 (2), 2992-3006.
6. Liu F., Li F. S., Feng Z. M., Yang Y. N., Jiang J. S., Li L., Zhang P. C. (2015), Neuroprotective naphthalene and flavan derivatives from *Polygonum cuspidatum*, *Phytochemistry*, 110, 150-159.
7. Zhao X. J., Chen L., Zhao Y., Pan Y., Yang Y. Z., Sun Y., Jiao R. Q., Kong L. D. (2019), *Polygonum cuspidatum* extract attenuates fructose-induced liver lipid accumulation through inhibiting Keap1 and activating Nrf2 antioxidant pathway, *Phytomedicine*, 63, 152986.
8. Ke J., Li M.-T., Xu S., Ma J., Liu M. Y., Han Y. (2023), Advances for pharmacological activities of *Polygonum cuspidatum* - A review, *Pharmaceutical Biology*, 61 (1), 177-188.
9. Ding W., Dong M., Deng J., Yan D., Liu Y., Xu T., Liu J. (2014), Polydatin attenuates cardiac hypertrophy through modulation of cardiac Ca^{2+} handling and calcineurin-NFAT signaling pathway, *American Journal of Physiology-Heart and Circulatory Physiology*, 307(5), H792-802.
10. Dong M., Liao S., Chen Y., Zheng N., Ma J., Xiao Z., Liu Y., Ding W., Liu J. (2017), Trans-polydatin protects the mouse heart against ischemia/reperfusion injury via inhibition of the renin-angiotensin system (RAS) and Rho kinase (ROCK) activity, *Food Function*, 8, 2309-2321.
11. Gavriil L., Detopoulou M., Petsini F., Antonopoulou S., Fragopoulou E. (2019), Consumption of plant extract supplement reduces platelet activating factor-induced platelet aggregation and increases platelet activating factor catabolism: a randomised, double-blind and placebo-controlled trial, *The British Journal of Nutrition*, 121(9), 982-991.
12. Le H. L., Nguyen V. H., Nguyen T. D., Nguyen T. V. A., Le D. H. (2023), Potential antiaggregatory and anticoagulant activity of *Kaempferia parviflora* extract and its methoxyflavones, *Industrial Crops and Products*, 192, 116030.
13. Jeon W. K., Kim J. H., Lee A. Y., Kim H. K. (2003), Inhibition of whole blood platelet aggregation from traditional medicines, *Korean Journal of Oriental Medicine*, 9 (2), 55-67.
14. Du Q. H., Peng C., Zhang H. (2013), Polydatin: A review of pharmacology and pharmacokinetics, *Pharmaceutical Biology*, 51 (11), 1347-1354.
15. Per M. S., Ulrich A., Metre L. L. (1988), Heparin induces release of extrinsic: Coagulation pathway inhibitor (EPI), *Thrombosis Research*, 50 (6), 803-813.
16. Anne K. L., Ulrich A., Rita S. (1991), The anticoagulant effect in heparinized blood and plasma resulting from interactions with extrinsic pathway inhibitor, *Thrombosis Reserach*, 1991, 64 (2), 155-168.
17. Le H. L., Nguyen T. M. H., Vu T. T., Nguyen T. T. O., Ly H. D. T., Le N. T., Nguyen V. H., Nguyen T. V. A. (2022), Potent antiplatelet aggregation, anticoagulant and

antioxidant activity of aerial *Canna x generalis* L.H Bailey & E.Z Bailey and its phytoconstituents, *South African Journal of Botany*, 147, 882-893. 18. Nguyen T. M. H., Le H. L., Ha T. T., Bui B. H., Le N. T., Nguyen V. H., Nguyen T. V. A. (2020), Inhibitory effect on human platelet aggregation and coagulation and antioxidant activity of *C. edulis* Ker Gawl rhizome and its secondary metabolites, *Journal of Ethnopharmacology*, 263, 113136. 19. Nguyen T. V. A., Ly H. D. T., Vu T. T., Nguyen T. T., Le H. L. (2018), Novel finding on anticoagulant activity of *Canna warszewiczii* extracts, *Asian Journal of Pharmacognosy*, 2(2), 5-10.

Journal of Medicinal Materials, 2024, Vol. 29, No. 6 (pp. 366 - 370)

POTENTIAL ACTIVITIES OF ARTEMISIA VULGARIS METHANOL EXTRACT AGAINST NTERA-2 CANCER STEM CELLS

Trieu Ha Phuong^{1,3}, Tran Le Nam Khanh¹, Nguyen Thi Cuc¹, Nguyen Thi Nga^{1,3}, Do Thi Phuong¹, Le Hoang Ngan Ha¹, Nguyen Thi Giang An⁴, Nguyen Trung Nam¹, Do Thi Thao^{1,2,*}

¹Institute of Biotechnology, Vietnam Academy of Science and Technology

²Graduate University of Science and Technology, Vietnam Academy of Science and Technology

³University of Science and Technology of Ha Noi, Vietnam Academy of Science and Technology

⁴Faculty of Biology, College of Education, Vinh University

*Corresponding author: thaodo@ibt.ac.vn

(Received August 14th, 2024)

Summary

Potential Activities of *Artemisia vulgaris* Methanol Extract Against NTERA-2 Cancer Stem Cells

Cancer stem cells are the major cause of tumor initiation and metastasis, which can lead to drug resistance and recurrence in cancer patients. The search for natural chemicals that can inhibit the development of cancer stem cells is of interest to many scientists. *Artemisia vulgaris* L. (in Vietnamese named Ngai cuu) is known for traditional medicine to treat diseases such as diabetes, antiseptic, stomach aches, and cancer prevention. This study aims to evaluate the biological effect of methanol extract from *A. vulgaris* on the NTERA-2 cancer stem cell line. The activity of the extract was illustrated through cytotoxicity assay using the 3-(4,5-Dimethylthiazol-2-yl)-2,5-Diphenyltetrazolium Bromide (MTT) method on monolayer and three-dimension cell culture models and *in vitro* migration assay. The extract of *A. vulgaris* exhibited inhibitory activity on NTERA-2 cells with an IC₅₀ value of 18.31 µg/mL and reduced spheroid formation at the concentration of 500 µg/mL. Besides, this extract significantly reduced cell migration ability at the concentration of IC₅₀ and 2xIC₅₀. Consequently, *A. vulgaris* crude methanol extract presented obvious effects on NTERA-2 cancer stem cells, providing a new direction for investigating natural compound ingredients of this plant for more efficient cancer treatment.

Keywords: *Artemisia vulgaris*, NTERA-2, Cytotoxicity, Tumorsphere formation assay, Scratch assay.

1. Introduction

Cancer stem cells (CSCs) are a subpopulation of tumor cells with characteristics of both stem cells and cancer cells: proliferation, self-renewal, and differentiation. CSCs are thought to be associated with tumor recurrence and metastasis. Although chemotherapy and radiation can suppress large cancer populations and shrink tumors, those are not sufficient to eliminate thoroughly CSC populations. Therefore, residual CSCs would initiate and develop new tumors. The most effective strategy for cancer treatment was to combine drugs that target non-CSC and CSC tumor cells, respectively [1]. The discovery of new chemotherapy drugs to prevent tumor recurrence is necessary to overcome drug resistance caused by CSCs.

Artemisia vulgaris L. (AV), a popular species belonging to the *Artemisia* genus from the Asteraceae family, distributes widely in natural

habitats worldwide, particularly in tropical countries such as China, Indonesia, Vietnam... [2]. This plant contains various rich chemical compositions such as sterols, flavonoids, phenolic acids, and coumarins which are responsible for many biological activities. In ancient times, *Artemisia vulgaris* L. has been traditionally used to treat menstruation- and pregnancy-related ailments, heal wounds, gout, leg tiredness, and fever [3]. At present, a lot of scientific researchers have proved that this species possesses antioxidant [4], antihypotensive [5], anticancer [6], anti-inflammatory [7], antifungal [8], and antibacterial activities [9].

However, no reports exhibit the biological effect of the crude methanol extract from *Artemisia vulgaris* L. (VAM) on cancer stem cells. Therefore, in this project, we study the potential effects of VAM against proliferation, stemness, and migration properties of NTERA-2 pluripotent

human embryonal carcinoma *in vitro*.

2. Materials and methods

2.1. Research materials

The pluripotent human embryonal carcinoma cell line NTERA-2 was kindly provided by Prof. P. Wongtrakoongate, Mahidol University, Thailand. The plant was collected in Que Phong district, Nghe An province, Vietnam in April 2021. The plant identification was performed by Dr. Nguyen The Cuong, Institute of Ecology and Biological Resources, Vietnam Academy of Science and Technology (VAST). The AV01 voucher sample was deposited at the Institute of Biotechnology, VAST. The fresh aerial parts of the plant were shadow-dried, chopped, and grinded. The 100 grams of dried powder was crudely extracted using 99.8% methanol at 50°C under sonicated conditions. The solvent was then thoroughly removed by a rotary evaporator to obtain 68.2 grams of VAM extract.

2.2. Cell culture

NTERA-2 cells were cultured using DMEM medium (Dulbecco's modified Eagle's medium), supplemented with 10% fetal bovine serum, 1% Penicillin-Streptomycin, 1% MEM non-essential

amino acids, 1% HEPES 1M in 37°C, 5% CO₂ incubator.

2.3. Anti-proliferative assay

The inhibitory effect of the extract on NTERA-2 was evaluated by the 3-(4,5-Dimethylthiazol-2-yl)-2,5-Diphenyltetrazolium Bromide (MTT) assay. NTERA-2 cells (3x10⁴/mL) were pre-cultured in 96-well plates for 24 h, then treated with VAM extract at various concentrations of 0.8, 4, 20, and 100 µg/mL for a further 48 h. The cells added with DMSO 0.5% were the negative control (NC). Subsequently, 20 µL MTT dye (5 mg/mL) was added to each well and incubated for 4 h in a CO₂-humidified incubator. Then, the medium was removed, and the formazan was dissolved in DMSO. The absorbance was read by a microplate reader (BioTek, Elx800) at 540 nm. The data were analysed and shown as the percentage of cell survival, and the IC₅₀ value was calculated by TableCurve2Dv4. The percentage of cell survival was determined by the following formula:

$$\% \text{ Cell viability} = \frac{\text{OD}(\text{treated sample})}{\text{OD}(\text{untreated sample})} \times 100\%$$

2.4. Tumorsphere assay

In 96-well ultrathin surface plates, cells were cultured to form tumorspheres. A total of 5000 cells/well were grown in DMEM medium throughout two days to form a stable tumorsphere. After 48h, the spheres were treated with the VAM extract at a concentration range from 0.8 to 500 µg/mL and incubated at 48h at 37°C. Tumorsphere size was observed under a microscope and analysed by using ImageJ software. Then, NTERA-2 cell proliferation in spheres was evaluated through MTT assays.

2.5. Migration assay

NTERA-2 cells (10⁵ cells/well) were cultivated in a 24-well plate in DMEM medium and incubated at 37°C and 5% CO₂ overnight. A sterilized 20-200 µL pipet tip was used to scratch each well. Detached cells were removed by washing with PBS buffer, then adding medium

with VAM at several concentrations (0.5xIC₅₀, IC₅₀, and 2xIC₅₀) to each well. The scratch area was taken image at day 0 (0 h) via microscope. After the 24-hour-incubation, the closure area was observed under the microscope to acquire the images at 24 h. The results were determined and analysed by using ImageJ software. The percentage of closure was calculated by the following formation: % Closure = (Area_{0h} - Area_{24h})/Area_{0h} * 100.

2.6. Statistical analysis

The data was calculated by GraphPad Prism 5.0 software, which utilized the unpaired t-test and one-way analysis of variance to determine statistical significance.

3. Results

3.1. The effect of the crude methanol extract from *Artemisia vulgaris* L. on NTERA-2 cell viability

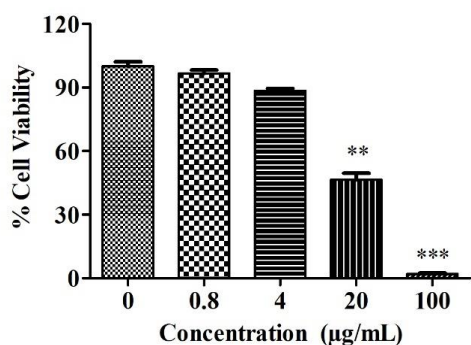


Fig. 1. Anti-proliferation effect of VAM extract at several concentrations on NTERA-2 cells. **P < 0.01, ***P < 0.001

In Fig. 1, there was a reduction in the percentage of cell viability in a dose-dependent manner when NTERA-2 cells were treated with VAM extract. After 48 h of incubation, VAM extract at concentrations of 20 µg/mL, and 100

µg/mL significantly inhibited cell survival with a percentage of inhibition of about $53.58 \pm 3.13\%$ and $99.04 \pm 0.86\%$, respectively. In contrast, treatment with 0.8 and 4 µg/mL did not significantly suppress NTERA-2 cell proliferation. The value of half maximal inhibitory concentration (IC_{50}) was calculated at 18.31 µg/mL.

3.2. Reducing NTERA-2 tumorsphere

VAM extract was further evaluated for inhibitory effect on 3-dimensional tumorspheres (3D) of NTERA-2 with five concentrations of 500, 100, 20, 4, and 0.8 µg/mL. Treatment with 500 µg/mL of VAM extract for 48h destroyed NTERA-2 tumorspheres. In addition, NTERA-2 cell viability in spheroid form was significantly reduced by treating VAM extract at 100 and 500 µg/mL.

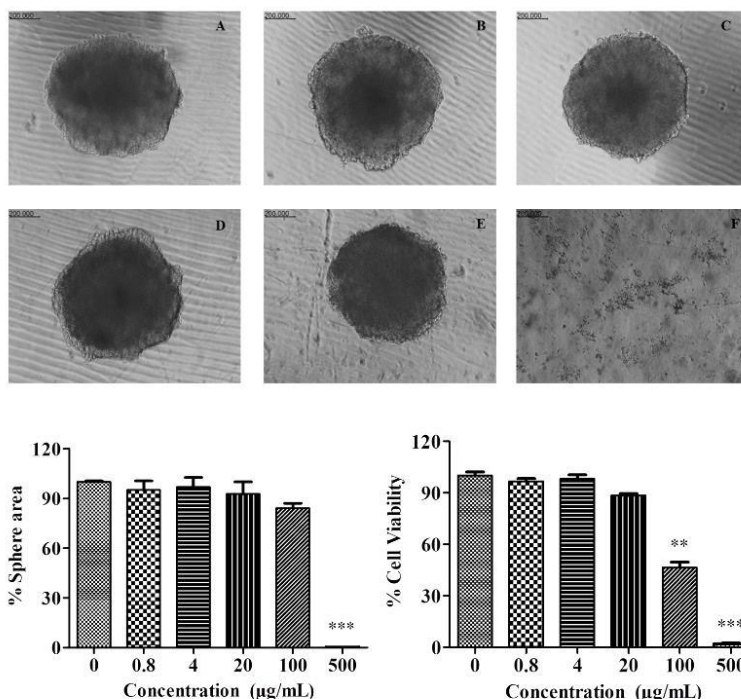


Fig. 2. The inhibitory effect of VAM extract on tumorsphere was accessed through the size of sphere area and cell viability on spheroid form with (A) DMSO 0.5% as untreated control; (B, C, D, E, F) VAM extract 0.8; 4; 20; 100; 500 µg/mL. **P < 0.01, ***P < 0.001

3.3. Preventing NTERA-2 migration

Subsequently, the impact of this extract on the migration of NTERA-2 cells was examined using a scratch assay with three concentrations: $0.5 \times IC_{50}$, IC_{50} , and $2 \times IC_{50}$. The outcomes of the scratch assay presented that VAM extract at

concentrations of IC_{50} and $2 \times IC_{50}$ significantly prevented the cell migration with the percentage of closure area of $25.89 \pm 3.03\%$ and $0.75 \pm 0.20\%$, compared with negative control as 34.95% after 24 hour-treatment (Fig. 3).

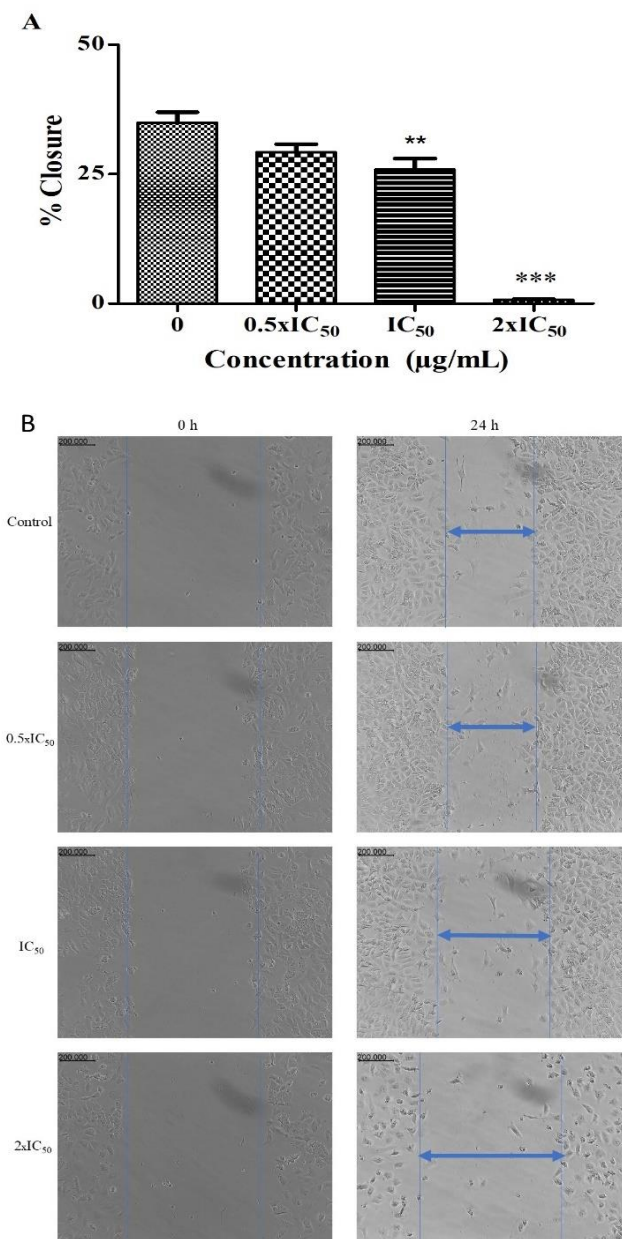


Fig. 3. (A) Evolution of the scratch closure in the control group and treated groups. The closure area was covered by cells after exposure to different concentrations of VAM extract for 24 hours. (B) The images of cell migration were taken on day 0 and after 24 h. **P < 0.01, ***P < 0.001.

4. Discussion

From this study, the data showed that the methanol extract from *A. vulgaris* suppressed NTERA-2 cancer stem cell proliferation with an IC₅₀ value of 18.31 µg/mL. As reported, the extract of *Artemisia vulgaris* L. had a positive effect on HepG2 hepatocarcinomas and HaCaT keratinocytes with IC₅₀ of 13.36 ± 0.45 and 27.30 ± 3.71 µg/mL, respectively [10]. In another research, *Artemisia alba*, a species belonging to

the *Artemisia* genus, whose acetone extracts inhibited SW-480 colon cancer cells with IC₅₀ about 240.12 ± 25.49 µg/mL [11]. In addition, the dichloromethane extract of *A. diffusa*, *A. santolina*, and *A. ciniformis* also prevented HT-29 cell growth [12]. According to Long Li *et al.*, the *Artemisia absinthium* crude extract showed a reduction in cell viability in breast cancer cells with an IC₅₀ value of 25 µg/mL [13].

Besides evaluating cytotoxicity effect through

two-dimensional (2D) cultures, VAM extract was further investigated stemness-suppressing ability via tumorspheroidal assay. The results indicated that VAM reduced spheroid forming, a unique characteristic of CSCs [14]. According to the report of Tin et al., in 2013, it was also demonstrated that artemisinin, derived from sweet wormwood (*Artemisia annua*), has an inhibitory effect on the tumorspheres derived from breast cancer stem cells [15].

The process of metastasis involves tumor cells moving away from the primary tumor site, with cancer stem cells (CSCs) potentially playing a key role in enabling this movement [16]. Concerning our results, 2xIC₅₀ of the crude extract might prevent NTERA-2 cell migration compared to the control after 24 h of incubation. Besides, the methanol extract from *A. vulgaris* also demonstrated a reduction in HCT-15 colon cancer

cell migration capacity, as stated by G Lian et al., [17]. Additionally, a different study showed that certain plants belonging to the same genus, including *Artemisia dracuncululus*, *Artemisia annua*, and *Artemisia absinthium*, could have wound healing potential on HaCat cell line with wound closure rates of 89.65 ± 2.18%, 98.55 ± 0.64%, and 97.84 ± 1.98%, respectively [18].

5. Conclusion

In conclusion, the crude methanol extract of *Artemisia vulgaris* demonstrated anti-cancer potential against NTERA-2 cancer stem cells by inhibiting their survival, reducing stemness characteristics by preventing tumorsphere formation as well as suppressing cell migration *in vitro*.

Acknowledgment: This work was funded under the Grant number TĐTĐBG0.03/21-23 from the Vietnam Academy of Science and Technology.

References

1. Meerson A., Khatib S., Mahajna, J. (2021). Flavonoids targeting cancer stem cells for augmenting cancer therapeutics. *International Journal of Molecular Sciences*, 22(23), 13044.
2. Abad M. J., Bedoya L. M., Apaza L., Bermejo P. (2012). The *Artemisia* L. genus: a review of bioactive essential oils. *Molecules*, 17(3), 2542-2566.
3. Ekiert H., Pajor J., Klin P., Rzepiela A., Ślesak H., Szopa A. (2020). Significance of *Artemisia vulgaris* L. (Common Mugwort) in the history of medicine and its possible contemporary applications substantiated by phytochemical and pharmacological studies. *Molecules*, 25(19), 4415.
4. Temraz A., El-Tantawy W. H. (2008). Characterization of antioxidant activity of extract from *Artemisia vulgaris*. *Pakistan Journal of Pharmaceutical Sciences*, 21(4), 321-6.
5. Tigno X. T., de Guzman F., Flora A. M. T. V. (2000). Phytochemical analysis and hemodynamic actions of *Artemisia vulgaris* L. *Clinical hemorheology and microcirculation*, 23(2, 3, 4), 167-175.
6. Erel Ş. B., Şenol S. G., Köse F. A., Ballar P. (2011). *In vitro* cytotoxic properties of six *Artemisia* L. species. *Turkish Journal of Pharmaceutical Sciences*, 8(3), 247-52.
7. El-Tantawy W. H. (2015). Biochemical effects, hypolipidemic and anti-inflammatory activities of *Artemisia vulgaris* extract in hypercholesterolemic rats. *Journal of Clinical Biochemistry and Nutrition*, 57(1), 33-38.
8. Obistioiu D., Cristina R. T., Schmerold I., Chizzola R., Stolze K., Nichita I., Chiurciu V. (2014). Chemical characterization by GC-MS and *in vitro* activity against *Candida albicans* of volatile fractions prepared from *Artemisia dracuncululus*, *Artemisia abrotanum*, *Artemisia absinthium* and *Artemisia vulgaris*. *Chemistry Central Journal*, 8, 1-11.
9. Blagojević P., Radulović N., Palić R., Stojanović G. (2006). Chemical composition of the essential oils of Serbian wild-growing *Artemisia absinthium* and *Artemisia vulgaris*. *Journal of Agricultural and Food Chemistry*, 54(13), 4780-4789.
10. Maki P., Thongdeeying P., Itharat A., Pipatrattanaseree W., Davies N. M. (2023). Cytotoxic Activity Against Liver Cancer and Cholangiocarcinoma Cells of *Artemisia vulgaris* L. extract and cirsimaritin, its isolated compound. *Asian Medical Journal and Alternative Medicine*, 23(1), 17-24.
11. Jakovljević M. R., Milutinović M., Djurdjević P., Todorović Ž., Stanković M., Milošević-Djordjević O. (2023). Cytotoxic and apoptotic activity of acetone and aqueous *Artemisia vulgaris* L. and *Artemisia alba* Turra extracts on colorectal cancer cells. *European Journal of Integrative Medicine*, 57, 102204.
12. Taghizadeh Rabe S. Z., Mahmoudi M., Ahi A., Emami S. A. (2011). Antiproliferative effects of extracts from Iranian *Artemisia* species on cancer cell lines. *Pharmaceutical Biology*, 49(9), 962-969.
13. Li L., Wang J., Miao S., Ma S., Shi X., Wen A. (2020). Apoptosis induction and reactive oxygen species generation by *Artemisia absinthium* L. leaf extract in MCF-7 breast carcinoma cells. *Pharmacognosy Magazine*, 16(69), 422-427.
14. Yakisich J. S., Azad N., Venkatadri R., Kulkarni Y., Wright C., Kaushik V., Iyer A. K. V. (2016). Formation of tumorspheres with increased stemness without external mitogens in a lung cancer model. *Stem Cells International*, 2016(1), 5603135.
15. Tin II A. S. (2013). *Development of a Breast Cancer Stem Cell Model and the Inhibitory Regulation of Small Molecule Phytochemicals on Various Stages of Human Breast Cancer Cells*. University of California, UC Berkeley Electronic Theses and Dissertations, <https://escholarship.org/uc/item/0fw3v9x3>.
16. Shiozawa Y., Nie B., Pienta K. J., Morgan T. M., Taichman R. S. (2013). Cancer stem cells and their role in metastasis. *Pharmacology & Therapeutics*, 138(2), 285-293.
17. Lian G., Li F., Yin Y., Chen L., Yang, J. (2018). Herbal extract of *Artemisia vulgaris* (mugwort) induces antitumor effects in HCT-15 human colon cancer cells via autophagy induction, cell migration suppression and loss of mitochondrial membrane potential. *Journal of BUON.: official journal of the Balkan Union of Oncology*, 23(1), 73-78.
18. Minda D., Ghiulai R., Banciu C. D., Pavel I. Z., Danciu C., Racoviceanu R., Soica C., Budu O. D., Mutean D., Diaconeasa Z., Dehelean C. A., Avram, S. (2022). Phytochemical profile, antioxidant and wound healing potential of three *Artemisia* species: *in vitro* and *in vivo* evaluation. *Applied Sciences*, 12(3), 1359.

ACUTE ORAL TOXICITY AND ANTI-INFLAMMATORY EFFECT OF THE STANDARDIZED EXTRACT FROM *VITEX TRIFOLIA* L. FRUITS

Do Thi Hong Khanh^{1,2}, Bui Thanh Tung¹, Pham Thi Nguyet Hang^{1,2,*}, William R. Folk³

¹University of Medicine and Pharmacy, Vietnam National University;

²National Institute of Medicinal Materials (NIMM), Hanoi, Vietnam;

³University of Missouri, USA

*Corresponding author: nguyethangpt@nimmm.org.vn

(Received November 18th, 2024)

Summary

Acute Oral Toxicity and Anti-Inflammatory Effect of the Standardized Extract from *Vitex trifolia* L. Fruits

Recent studies suggest that the decline in ovarian function and estrogen levels during menopause cause increased proinflammatory cytokines and oxidative stress associated with these symptoms and perhaps progressive central nervous system (CNS) damage. Our previous studies have shown that a *Vitex trifolia* L. *n*-butanol extract improved cognitive deficit and ameliorated the atrophy of the uterus in ovariectomized mice, as a menopause model. The purpose of this study is to determine acute oral toxicity in mice and evaluate the anti-inflammatory properties of the standardized extract from the fruits of *V. trifolia* (VTE) collected in Vietnam. The acute toxicity study showed that the VTE had an LD₅₀ value of 26.0 g/kg BW. Our results indicated that in the carrageenan-induced paw edema rat model, VTE at a dose of 150 mg/kg significantly inhibited paw edema at 4 and 6 hours. In addition, VTE at both doses of 150 mg/kg and 300 mg/kg significantly decreased the volume of inflammatory exudate, the number of leukocytes, and the protein content in the exudate in the carrageenan and formaldehyde-induced peritonitis model. Taken together, these results suggest that VTE exhibits potent acute anti-inflammatory effects. Further research is required to assess the potential for preventing or treating CNS-related inflammatory conditions.

Keywords: *Vitex trifolia* fruit extract, Acute oral toxicity, Anti-inflammatory.

1. Introduction

Vitex trifolia L. is endemic to regions of southeast Asia, China, Japan, Korea, India, Africa, Australia, and other Pacific countries, where it is used in traditional medicines and dietary supplements for a variety of health conditions. The Vietnamese name for *Vitex trifolia* is “Mãn kinh”, which means “menopause”, for it is often used to treat symptoms experienced during or after menopause, including those associated with the CNS such as anxiety, headache, depression and reduced cognitive function [1],[2],[3],[4]. Recent studies suggest that the decline in ovarian function and estrogen levels during menopause cause increased proinflammatory cytokines and oxidative stress associated with these symptoms and perhaps progressive CNS damage [5],[6],[7].

V. trifolia extracts modulate proinflammatory cytokines and oxidative stress through multiple targets and signaling pathways [1],[2],[3]. Our previous studies have shown that a *V. trifolia* *n*-butanol extract improved cognitive deficit and ameliorate the atrophy of the uterus in ovariectomized mice, as a menopause model

[8],[9]. Our recent experiments (unpublished) and studies by others indicate that *V. trifolia* extracts (VTE) exhibit estrogen-like activity [1],[2],[3]. However, virtually all such studies have used VTEs whose components have not been characterized, nor have the plant materials been collected in Vietnam, where they are widely used in medicines and dietary supplements [10],[11].

Fructus Viticis was used in traditional medicines of China, Korea, and Japan and perhaps elsewhere *V. trifolia* may be mixed with *V. trifolia* Steenis subsp. *litoralis* or even *V. rotundifolia* [1],[2],[10],[12],[13],[14]. *V. trifolia* sp. and *V. rotundifolia* are sometimes considered to be synonymous - however, their phenotypes, growth properties, genetic markers and chemical constituents are distinct [2],[13],[15],[16],[17],[18]. Therefore, the present study aims to determine the acute oral toxicity in mice and evaluate the anti-inflammatory properties in the hind paw edema model and peritonitis model in rats of the standardized VTE analyzed by HPLC.

2. Materials and Methods

2.1. Plant materials and extraction

The fruits of *Vitex trifolia* L. were collected in Nghe An, Vietnam, and identified by Dr. Pham Thanh Huyen from the National Institute of Medicinal Materials (NIMM). The voucher specimens of these plants were deposited at the Herbarium of the Medicinal Material Resources Center (NIMM), Vietnam. The standardized extract VTE was prepared as follows: The dried plant sample (1 kg) was coarsely ground and extracted twice by reflex with 50% aqueous ethanol for 3 hours and 1.5 hours, respectively.

The extracts were then combined and filtered, and the solvent was evaporated under reduced pressure at 60°C to give a liquid extract. The liquid extract was then vacuum dried at a temperature of 60°C, with a pressure of 50 mmHg. The final extract had a moisture content of less than 5% and a yield of 14%. High Performance Liquid Chromatography (HPLC) chromatograms of VTE and standards are shown in Fig. 1 and indicate agnuside and casticin are major components. According to the analysis method, the content agnuside and casticin in the VTE were not less than 0.7% and 0.2%, respectively.

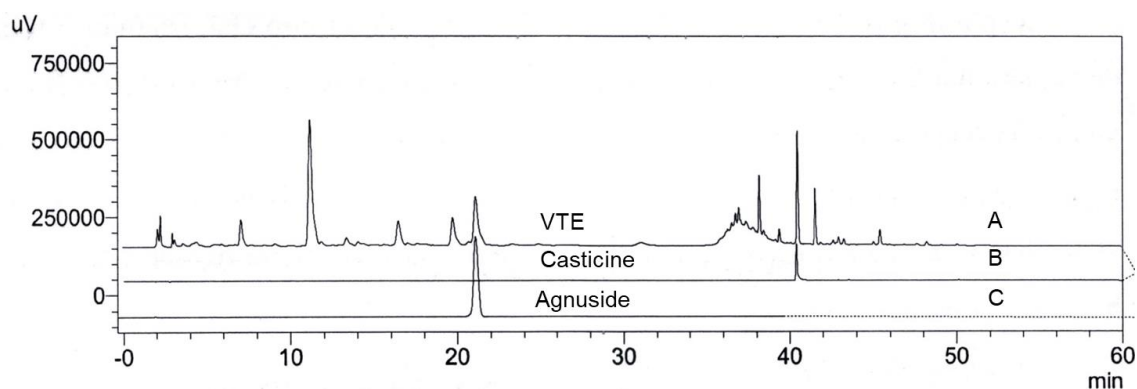


Fig. 1. Characterization of VTE by HPLC.

HPLC/UV profiles of VTE (A), Casticine (B; RT= 40.2 min) and Agnuside (C; RT =20.9 min)

2.2. Animals

For acute oral toxicity studies, male and female *Swiss albino* mice (weight 18-20 g) were purchased from the National Institute of Hygiene and Epidemiology, Hanoi, Vietnam. For anti-inflammatory evaluation, Wistar rats of both sexes (weight 180-200 g) were obtained from the Vietnam Military Medical Academy. The animals were acclimated to the laboratory animal room for at least one week before any procedures were performed. Food and water were available ad libitum. Housing conditions were maintained at 22 ± 1°C with 12-hour light-dark cycles.

2.3. Acute oral toxicity in mice and determination of LD₅₀

For the acute oral toxicity test [19], mice were fasted for approximately 12 hours, with free access to water, prior to oral administration (0.2 ml/10 g body weight) of VTE (up to 42.5 g/kg, po.). Behavioral expressions and signs of toxicity were observed in the animals two hours post-treatment. Mortality within the first 24 hours was recorded for each group, and surviving animals

were monitored for an additional seven days for signs of delayed toxicity. The median lethal dose (LD₅₀) was estimated using the Behrens-Karber method and calculated as following:

$$LD_{50} = LD_{100} - \frac{\sum(d \times z)}{n}$$

Where:

LD₅₀: the dose that causes the death of 50% of the test animals

LD₁₀₀: the lowest dose that causes the death of 100% of the test animals

d: the difference between two consecutive doses

z: the average number of mice dead between two consecutive doses

n: the number of test mice per group

2.4. Evaluation of anti-inflammatory activities in rats

2.4.1. Hind paw edema induced by carrageenan:

For the carrageenan-induced hind paw edema test [20],[21], rats were placed into 4 groups (n=10

rats/group). The control group (#1) and the reference group (#2) received normal water and ibuprofen (30 mg/kg, Traphaco JSC, Vietnam), respectively, and the test groups (#3 and #4) were treated with 150 and 300 mg/kg body weight of VTE. Water, VTE, and ibuprofen were administered orally (1 mL/100 g body weight) for five consecutive days. On day 5, one hour after treatment, each rat received subcutaneously a subplantar injection of 0.05 mL freshly prepared 1% carrageenan solution (BDH Chemicals Ltd., Poole, England) suspended in sterile physiological saline into the right hind paw. Paw volume was measured by a digital water plethysmometer (Ugo Basile, model 7140, Italy), before the treatment (V_0) and 2, 4, 6, and 24 h after carrageenan injection (V_t). The increase in volume of edema was determined for each rat.

The increase in paw volume for each rat was calculated using the following equation:

$$\Delta V\% = \frac{V_t - V_0}{V_0} \times 100$$

Where:

V_0 is the paw volume before inducing inflammation;

V_t is the paw volume after inducing inflammation at t h.

The anti-inflammatory effect is evaluated by the ability to inhibit edema (I%)

$$I\% = \frac{\Delta \bar{V}_c\% - \Delta \bar{V}_t\%}{\Delta \bar{V}_c\%} \times 100$$

Where:

$\Delta \bar{V}_c\%$ is the average increase in paw volume in the control group;

$\Delta \bar{V}_t\%$ is the average increase of paw volume in the treated group at t h.

2.4.2. Peritonitis induced by carrageenan and formaldehyde:

Rats were placed into 4 groups and

administered water, extracts, or ibuprofen for five days as described above. On day 5, rats were injected with carrageenan (0.5% w/v) and formaldehyde (1.5% v/v) suspended in sterile physiological saline with a volume of 1 mL/100 g body weight [22]. Twenty-four hours later the rats were sacrificed and the peritoneal cavity of each was opened to collect exudate, whose volume and protein concentration and leucocytes count were determined. Protein concentration was determined using a colorimetric method based on the Biuret reaction principle. In brief, the exudates were centrifuged to separate the supernatants, which were then transferred into specific cuvettes and analyzed using an Atellica® CH Analyzer (Siemens Healthcare Diagnostics Inc., USA) following the manufacturer's instructions. Simultaneously, the leukocyte count was assessed with an XN-2000™ Automated Hematology Analyzer (Sysmex, Japan).

2.5. Statistical analysis

Statistical analyses were conducted using IBM SPSS Statistics version 23.0 software, and data are presented as the mean \pm standard deviation (SD). One-way analysis of variance (ANOVA) or a t-test, where only two conditions were compared, was used to examine the significant differences among groups. Differences of $p < 0.05$ were considered significant.

3. Results

3.1. Acute toxicity

Following the oral administration of varying doses of VTE ranging from 17.41 to 42.5 g/kg (BW) to mice, the mortality and dose response were documented, as outlined in Table 1. Accordingly, the LD₅₀ value was estimated at 26.0 g/kg BW based on the Behrens-Karber's method.

Table 1. Mortality percentage after 24 hours from oral administration of various doses of VTE

Group	Dose (g/kg)	n	Mortality	d	z	d x z
1	17.41	10	0			
2	21.76	10	1	4.4	0.5	2.18
3	27.20	10	8	5.4	4.5	24.48
4	34.00	10	9	6.8	8.5	57.80
5	42.50	10	10	8.5	9.5	80.75
$\Sigma (d \times z)$						165.21

3.2. Anti-inflammatory effect of VTE on rat paw edema assay

Carrageenan injection induced inflammation in the rat's hind paw, which increased paw diameter and reached a maximum by 4 hours. Administration of ibuprofen significantly reduced inflammation in the hind paw at almost all time points, including at 2, 4, and 6 hours. At 24 hours, ibuprofen tended to decrease the rat paw thickness but not significantly compared to the control

group. While VTE at a dose of 150 mg/kg also significantly inhibited paw edema at 4 and 6 hours, VTE at a dose of 300 mg/kg decreased the rat paw thickness only at 4 hours. At other time points, VTE at doses of 150 and 300 mg/kg slightly inhibited inflammation in the hind paw but not significantly compared to the control group. Collectively, these results suggest that VTE possesses relatively strong acute anti-inflammatory activity in the rat paw edema assay.

Table 2. Effect of VTE and ibuprofen on rat paw edema induced by carrageenan

Group	V ₂		V ₄		V ₆		V ₂₄	
	% Edema compared to V ₀	Edema inhibition (%)	% Edema compared to V ₀	Edema inhibition (%)	% Edema compared to V ₀	Edema inhibition (%)	% Edema compared to V ₀	Edema inhibition (%)
1	39.33 ± 11.58	-	54.35 ± 20.22	-	52.48 ± 17.33	-	3.73 ± 4.60	-
2	21.22 ± 9.54*	46.05	36.98 ± 8.90*	31.96	36.74 ± 9.48*	29.99	2.70 ± 6.63	27.61
3	32.42 ± 15.68	17.47	36.33 ± 14.36*	33.16	34.57 ± 17.31*	34.13	2.86 ± 2.72	23.32
4	41.92 ± 9.02	-6.58	33.90 ± 16.33*	37.63	38.70 ± 14.80	26.26	1.66 ± 1.39	55.50

Group 1: Control, Group 2: Ibuprofen 30 mg/kg, Group 3: VTE 150 mg/kg, Group 4: VTE 300 mg/kg. **p* < 0.05 compared to Group 1 (Control group)

3.3. Anti-inflammatory effect of VTE on peritonitis induced by carrageenan and formaldehyde

Rats were treated with saline, VTE, or ibuprofen for five consecutive days before

peritonitis induction. The exudate volume, protein concentration, and leucocyte count in exudate were determined and the results are presented in **Table 3** and **Fig. 2**.

Table 3. Effect of VTE and ibuprofen on exudate volume in peritonitis model induced by carrageenan and formaldehyde

Group	Exudate volume (mL/100g)
Group 1: Control	3,92 ± 1,01
Group 2: Ibuprofen 30 mg/kg	3,04 ± 0,70*
Group 3: VTE 150 mg/kg	3,00 ± 0,71**
Group 4: VTE 300 mg/kg	1,42 ± 0,43***^Δ

*, ***p* < 0.05; 0.01 compared to Group 1, respectively, ^Δ*p* < 0.05 compared to Group 2

The data indicate that the administration of ibuprofen (30 mg/kg) significantly decreased the leukocyte migrations (13.91 ± 3.78 leukocytes/mL), exudate volume (3.04 ± 0.70 mL/100 g), and protein content (4.66 ± 0.17 mg/mL) compared with the control group (23.08 ± 5.78 leukocytes/mL, 3.92 ± 1.01 mL/100 g, and 7.73 ± 2.46 mg/mL for leukocyte count, exudate volume, and protein content, respectively). Administration of VTE also significantly affected these parameters. Specifically, the results for groups pretreated with VTE at doses

of 150 mg/kg and 300 mg/kg were 17.24 ± 3.23 and 16.58 ± 3.47 leukocytes/mL, 3.00 ± 0.71 mL/100 g and 1.42 ± 0.43 mL/100 g, and 5.40 ± 0.73 mg/mL and 4.90 ± 0.20 mg/mL for leukocyte count, exudate volume, and protein content, respectively. Intriguingly, the exudate volume in the group administered 300 mg/kg of VTE was even significantly lower than that in the group treated with ibuprofen, indicating the potent anti-inflammatory effect of VTE in the peritonitis model.

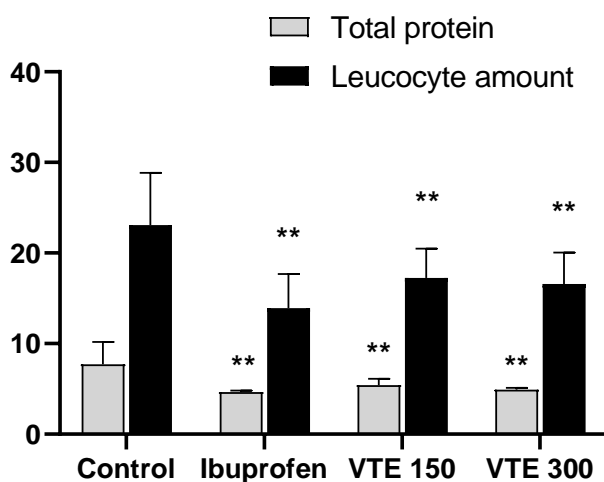


Fig. 2. Effect of VTE and ibuprofen on leukocytes/mL and protein content (mg/mL) in the exudate in the carrageenan and formaldehyde-induced peritonitis model
 ** $p < 0.01$ compared to Group 1 (control group)

4. Discussion

Vitex trifolia L. has long been used in traditional medicines and dietary supplements, however, no prior studies have evaluated the composition, safety, and anti-inflammatory properties of VTE from Vietnamese sources. In this study, the acute anti-inflammatory effects of VTE were evaluated by the carrageenan-induced paw edema model [23],[24] and the peritonitis model. In both models, ibuprofen decreased paw edema at 2, 4, and 6 hours in the paw edema model, and significantly reduced indicators (leukocyte count, protein content) in the peritonitis model compared to the control group. In the present study, VTE at both doses of 150 mg/kg and 300 mg/kg significantly reduced the paw edema volume at the time points of 4 hours and 6 hours post-inflammation induction. In addition, VTE at both doses of 150 mg/kg and 300 mg/kg also significantly decreased the volume of inflammatory exudate, the number of leukocytes, and the protein content in the exudate in the peritonitis model.

Our findings resemble previous studies regarding the anti-inflammatory activities *in vivo* of extracts of leaves of *V. trifolia*. According to Parvathi Annamalai et al. (2022), the methanol extract of *V. trifolia* leaves at doses of 100 mg/kg and 200 mg/kg significantly inhibited carrageenan-induced paw edema and effectively reduced leukocyte infiltration. Moreover, *V.*

trifolia leaves significantly inhibited the tissue levels of interleukin (IL)-1 β , IL-6, and tumor necrosis factor (TNF)- α induced by carrageenan, as well as the levels of cytokine-induced neutrophil chemoattractants CINC-2/C-X-C (CXCL3) and CINC-3/CXCL2 in tissue and serum, while significantly upregulating anti-inflammatory cytokine IL-10 levels. Additionally, *V. trifolia* leaves significantly reduced carrageenan-induced I κ B α degradation and NF- κ B p65 nuclear translocation, providing insights into its molecular mechanism mediated through the downregulation of the NF- κ B signaling pathway [1],[2],[3],[25].

Other *in vitro* studies have also provided evidence regarding the anti-inflammatory effect of *V. trifolia*. Specifically, Hai-Ning Wee et al. (2020) investigated the effects of various extracts of *V. trifolia* leaves on the production of cytokines TNF- α and IL-1 β using enzyme-linked immunosorbent assay (ELISA) in lipopolysaccharide-stimulated human U937 macrophages. Among the 14 different leaf extracts studied, the extracts processed by ultrasonic extraction in dichloromethane and ethanol soaking exhibited the highest activity in inhibiting TNF- α and IL-1 β production in human U937 macrophages [26]. Additionally, Mariko Matsui et al. (2012) studied the effects of *V. trifolia* leaf extract on lipopolysaccharide (LPS)-induced inflammatory gene expression, focusing on the

regulation of chemokine C-X-C motif 10 (CXCL-10) and C-C motif ligand 3 (CCL-3) and cyclooxygenase (COX)-2. Their results showed that *V. trifolia* extract at a concentration of 5000 µg/ml significantly inhibited the expression of multiple LPS-induced inflammatory genes in RAW 264.7 cells after 8 hours of incubation. TransAM assays indicated that *V. trifolia* extract also inhibited LPS-induced NF-κB translocation at 250 µg/mL [27].

Of the prevalent metabolites in VTE and extracts of other *Vitex* species, agnuside and casticin are the best characterized for their anti-inflammatory activities [28],[29],[30],[31]. While pharmacokinetic evidence indicates agnuside crosses the blood brain barrier [32], only indirect evidence is available for casticin [33]. Additional studies are required to document their anti-inflammatory activities in the CNS.

Our study provides evidence regarding the anti-inflammatory effects of VTE and the knowledge from extensive traditional uses for menopausal symptoms support its potential for prevention or treatment of inflammation-related postmenopausal CNS conditions. Given the evidence that hormone replacement therapies containing estrogen receptor modulators may cause dementia and related neurocognitive

conditions [34], alternative treatments are needed. Further studies are needed to evaluate the anti-inflammatory and potential estrogenic effects of compounds isolated from *V. trifolia* fruits as well as to investigate the underlying mechanisms of action.

5. Conclusion

The results from the acute oral toxicity test showed that the VTE has an LD₅₀ of 26.0 g/kg BW. In the carrageenan-induced paw edema rat model, VTE at both doses of 150 mg/kg and 300 mg/kg significantly reduced the paw edema volume at 4 hours and 6 hours post-inflammatory induction. In addition, VTE at both doses of 150 mg/kg and 300 mg/kg also significantly decreased the volume of inflammatory exudate, the number of leukocytes, and the protein content in the exudate in the carrageenan and formaldehyde-induced peritonitis model. Taken together, these results indicated that VTE has significant anti-inflammatory effects.

Acknowledgments: *The research was funded partly by the Ministry of Health in Vietnam, Decision No. 1600/QD-BYT dated 04th April 2020. We thank Dr. Nguyen Van Tai and the Department of Phytochemistry, National Institute of Medicinal Materials, Hanoi, Vietnam for conducting the *Vitex trifolia* L. extract.*

References

1. Kamal N., Mio Asni N. S., Rozlan I. N. A., Mohd Azmi M. A. H., Mazlan N. W., Mediani A., Baharum S. N., Latip J., Assaw S., Edrada-Ebel R. A. (2022), Traditional medicinal uses, phytochemistry, biological properties, and health applications of *Vitex sp. Plants*, 211(15), 1944.
2. Yan C. X., Wei Y. W., Li H., Xu K., Zhai R. X., Meng D. C., Fu X. J., Ren X. (2023), *Vitex rotundifolia* L. f. and *Vitex trifolia* L.: A review on their traditional medicine, phytochemistry, pharmacology. *Journal of Ethnopharmacology*, 308, 116273.
3. Mottaghipisheh J., Kamali M., Doustimotlagh A. H., Nowroozzadeh M. H., Rasekh F., Hashempur M. H., Iraj A. (2024), A comprehensive review of ethnomedicinal approaches, phytochemical analysis, and pharmacological potential of *Vitex trifolia* L. *Frontiers in Pharmacology*, 15, 1322083.
4. Metcalf C. A., Duffy K. A., Page C. E., Novick A. M. (2023), *Cognitive problems in Perimenopause: A review of recent evidence. Current Psychiatry Reports*, 25(10), 501-511.
5. Liang G., Kow A. S. F., Yusof R., Tham C. L., Ho Y. C., Lee M. T. (2024), Menopause-associated depression: Impact of oxidative stress and neuroinflammation on the central nervous system—A review. *Biomedicine*, 12(1), 184.
6. Zhang Y., Tan X., Tang C. (2024), Estrogen-immuno-neuromodulation disorders in menopausal depression. *Journal of Neuroinflammation*, 21(1), 159.
7. Turek J., Gašior Ł. (2023), Estrogen fluctuations during the menopausal transition are a risk factor for depressive disorders. *Pharmacological Reports*, 75(1), 32-43.
8. Pham T. N. H., Do T. P., Nguyen T. P., Can V. M., Nguyen M. K. (2014), Neuropharmacological effect of *Vitex trifolia* L. on ovariectomized mice. *Journal of Medicinal Materials*, 19(3), 145-150.
9. Do T. H. K., Pham T. N. H., Le T. X., Nguyen T. P., Dinh T. M., Nguyen V. H., Nguyen V. T., Bui T. T. (2023), Effects of n-butanol extract from *Vitex trifolia* fruits on cognitive function deficit in ovariectomized mice. *Journal of Medicinal Materials*, 28(4), 234-240.
10. Truyen L. V., Chan N. G. (1999), *Selected Medicinal Plants in Vietnam*. Vol. II, Hanoi, Vietnam, National Institute of Materia Medica - Science and Technology Publishing House.
11. Vo V. C. (2018), *The Dictionary of Vietnamese Medicinal Plants*. Vol. 2, Hanoi, Vietnam, Medical Publisher.
12. Zhang W., Wang J. L., Tang L. Y., Zhan Z. L., Peng H. S., Yang H. J. (2019), Herbal textual research on Chinese medicine "Manjingzi" (*Vitex Fructus*). *Zhongguo Zhong Yao Za Zhi*, 44(24), 5503-5507.
13. Meng X., Wang H., Kuang Z., Wu Y., Su X., Wang J., Li L., Liu C., Jia M. (2023), Traditional use, phytochemistry and pharmacology of *Vitex Fructus*. *Heliyon*, 9(9), e19144.
14. Hu Y., Zhang Q., Xin H., Qin L. P., Lu B. R., Rahman K., Zheng H. (2007), Association between chemical and genetic variation of *Vitex rotundifolia* populations from different locations in China: its implication for quality control of medicinal plants. *Biomedical Chromatography*, 21(9), 967-75.
- 15.

Cousins M. M., Briggs J., Whitwell T. (2017), Beach *Vitex* (*Vitex rotundifolia*): Medicinal properties, biology, invasive characteristics and management options. *Journal of Environmental Horticulture*, 35(4), 128-137. **16.** Yang X. Y., Gao P. Y., Chen X. X., Wang L. X., Jiang T., Wu T., Chen Y. Y., Yue C. Y., Wu H. W., Tang L. Y., Wang Z. J. (2023), Comparison of HPLC fingerprints and determination of main components of *Vitex fructus* from different species. *Zhongguo Zhong Yao Za Zhi*, 48(9), 2471-2479. **17.** Sun Y. Q., Zhao L. Y., Zhu B., Jia M., Zhang Q. Y., Qin L. P. (2021), Genetic diversity and genetic structures of original plants of *Vitex fructus*: an SSR markers-based analysis. *Zhongguo Zhong Yao Za Zhi*, 46(15), 3824-3831. **18.** Bramley G. L. C., Forest F., R. P. J. (2009), Troublesome tropical mints: Re-examining generic limits of *Vitex* and relations (Lamiaceae) in south east asia. *Taxon*, 58(2), 500-510. **19.** Do T. D. (2014), *Phương pháp xác định độc tính của thuốc*. NXB Y học. Hà Nội. **20.** Do T. D. (1997), Đánh giá mô hình gây phù thực nghiệm bằng cao lạnh và carrageenan để nghiên cứu tác dụng chống viêm của thuốc. *Tap chí Dược học*, 12, 18-20. **21.** Vogel H. G. (2002), Drug Discovery and Evaluation: Pharmacological Assays. *Springer Science & Business Media*. (ed). **22.** Vogel H. G. (2008), Drug Discovery and Evaluation: Pharmacological Assays. *Springer Science & Business Media*. (ed). **23.** Jain N. K., Patil C. S., Singh A., Kulkarni S. K. (2001), A simple technique to evaluate inflammatory pain along with anti-inflammatory studies in carrageenan-induced paw edema. *Indian Journal of Pharmacology*, 33(2), 114-115. **24.** Sugishita E., Amagaya S., Ogihara Y. (1981), Anti-inflammatory testing methods: comparative evaluation of mice and rats. *Journal of Pharmacobio-dynamics*, 4(8), 565-575. **25.** Annamalai P., Thangam E. B. (2022), *Vitex trifolia* L. modulates inflammatory mediators via down-regulation of the NF- κ B signaling pathway in carrageenan-induced acute inflammation in experimental rats. *Journal of Ethnopharmacology*, 298, 115583. **26.** Wee H. N., Neo S. Y., Singh D., Yew H. C., Qiu Z. Y., Tsai X. R. C., How S. Y., Yip K. Y. C., Tan C. H., Koh H. L. (2020), Effects of *Vitex trifolia* L. leaf extracts and phytoconstituents on cytokine production in human U937 macrophages. *BMC Complementary Medicine and Therapies*, 20, 1-15. **27.** Matsui M., Adib-Conquy M., Coste A., Kumar-Roiné S., Pipy B., Laurent D., Pauillac S. (2012), Aqueous extract of *Vitex trifolia* L. (Labiatae) inhibits LPS-dependent regulation of inflammatory mediators in RAW 264.7 macrophages through inhibition of nuclear factor kappa B translocation and expression. *Journal of Ethnopharmacology*, 143(1), 24-32. **28.** Zheng C. J., Li H. Q., Ren S. C., Xu C. L., Rahman K., Qin L. P., Sun Y. H. (2015), Phytochemical and pharmacological profile of *Vitex negundo*. *Phytotherapy Research*, 29(5), 633-47. **29.** Yao J. L., Fang S. M., Liu R., Oppong M. B., Liu E. W., Fan G. W., Zhang H. (2016), A review on the terpenes from genus *Vitex*. *Molecules*, 21(9). **30.** Chan E. W. C., Wong S. K., Chan H. T. (2018), Casticin from *Vitex* species: A short review on its anticancer and anti-inflammatory properties. *Journal of Integrative Medicine*, 16(3), 147-152. **31.** Le D. D., Han S., Yu J., Ahn J., Kim C. K., Lee M. (2023), Iridoid derivatives from *Vitex rotundifolia* L. f. with their anti-inflammatory activity. *Phytochemistry*, 210, 113649. **32.** Ramakrishna R., Bhatia M., Singh R., Puttreu S.K., Bhatta R. S. (2016), Plasma pharmacokinetics, bioavailability and tissue distribution of agnuside following peroral and intravenous administration in mice using liquid chromatography tandem mass spectrometry. *Journal of Pharmaceutical and Biomedical Analysis*, 125, 154-64. **33.** Kim J., Seo Y. H., Kim J., Goo N., Jeong Y., Bae H. J., Jung S. Y., Lee J., Ryu J. H. (2020), Casticin ameliorates scopolamine-induced cognitive dysfunction in mice. *Journal of Ethnopharmacology*, 259, 112843. **34.** Nerattini M., Jett S., Andy C., Carlton C., Zarate C., Boneu C., Battista M., Pahlajani S., Loeb-Zeitlin S., Havryulik Y., Williams S., Christos P., Fink M., Brinton R. D., Mosconi L. (2023), Systematic review and meta-analysis of the effects of menopause hormone therapy on risk of Alzheimer's disease and dementia. *Frontiers in Aging Neuroscience*, 15, 1260427.

Journal of Medicinal Materials, 2024, Vol. 29, No. 6 (pp. 377 - 384)

BINARY ETHOSOMES FOR ENHANCING SKIN DELIVERY OF RUTIN BY SOLVENT INJECTION

Nguyen Hong Van^{1*}, Phan Huu Phuoc¹, Nguyen Xuan Tung²

¹Life Sciences Department, University of Science and Technology of Hanoi, Hanoi, Vietnam

²VNU University of Medicine and Pharmacy, Vietnam National University, Hanoi, Vietnam

*Corresponding author: chodomthanyeu@gmail.com

(Received November 05th, 2024)

Summary

Binary Ethosomes for Enhancing Skin Delivery of Rutin by Solvent Injection

Rutin, a natural extract from buckwheat, tea, and apple, has powerful pharmacological properties, especially antioxidant effects. However, the bioactivity of rutin is limited since it has low solubility and poor permeability. Nanovesicles, especially ethosomes, have been a non-invasive drug carrier for skin delivery with high entrapment efficiency and stability. In this research, the simple solvent injection was used to fabricate classical ethosomes, and binary ethosomes. Various polyols, like propylene glycol, isopropyl alcohol, and glycerol at different ratios were investigated in rutin binary ethosome preparation. Then, rutin ethosomes were characterized by physical properties, loading efficiency, drug release, and short-term stability. The optimum binary ethosomes were made from the mixture of ethanol and glycerol at the ratio of 3:7. Rutin binary ethosomes had a lower size than classical ethosomes and better stability during 30 days. Rutin ethosomes posed sustained release through dialysis membrane and mouse skin and significantly improved the drug release in the Franz cell model. Therefore, binary ethosomes could be considered as potential nanovesicles to deliver rutin via the skin route.

Keywords: *Ethosomes, Classical ethosomes, Binary ethosomes, Skin delivery, Rutin.*

1. Introduction

Herbal medicines have been used to treat various diseases for thousands of years in history. In modern pharmaceuticals, bioactive compounds and their derivatives, extracted from natural sources, have been recognized as new alternative drugs and supplements, to improve human health, cure, and prevent pathologies [1]. Rutin is a significantly familiar Vietnamese herbal compound, from *Sophora japonica L.*, and is traditionally used in daily life in the form of tea, food, and even as an active pharmaceutical ingredient in marketed drugs [2]. In terms of chemistry, rutin is a flavonol glycoside between quercetin and disaccharide rutinose. Rutin has activities of kidney protection, neuroprotection, hepatitis protection, inflammation, antidiabetic, anticancer, reducing blood pressure, etc. The bioactivity of rutin refers to its capabilities of regulating and signaling pathways involving gene expression, oxidative stress, apoptosis...[3],[4],[5]. In dermatology, bioactivities such as antioxidant, free-radical scavenging, oxidative-stress prevention, and collagen synthesis modulators enable rutin usage for skin anti-aging, and skin protection [6]. Moreover, rutin is antibacterial [7], wound-healing [8], skin-whitening [9], and UV protectant, and strengthens the UV-blocking ability of sun protection factor (SPF) agents [10], which has been widely applied in skin products. However, rutin and almost all bioactive natural substances have a high molecular weight, poor solubility, and low penetrability, which limit the permeation into skin layers.

Therefore, nanotechnology has been used in pharmaceutical preparations to make a number of botanical bioactive substances more bioavailable, target bioactive sites, and control drug release rate [1]. Several pharmaceutical ingredients from natural bioactive compounds, with applied nanotechnology, were approved by US-FDA and EMA [11]. For skin delivery, ethosomes have been considered as one of the most outstanding nanocarriers [12]. The combination of bilayer nanostructure, composed of phospholipid and ethanol, enables facile penetration of ethosomes into the skin layer, as well as improves the stability and deformity compared to liposomes (Fig. 1.) [13]. Ethanol in ethosomal structure causes two effects to enhance the penetration through the

skin layer of active pharmaceutical ingredients (API) [14]. In the former effect, ethanol interacts with the hydrophobic head in the stratum corneum, which softens and loosens the stratum corneum layer. Consequently, APIs penetrate through the skin efficiently. In the latter effect, ethanol in vesicle structure improves the ability to fuse membranes, facilitating the process of API permeation into dermal and hypodermal cells. Ethosomes, with the involvement of other polyols, such as PG [12],[15], IPA [16], and glycerol [17], are called binary ethosome. Binary ethosomes have greater stability and drug permeability than classical ethosomes [15],[18]. Specifically, binary ethosomes increased 7 folds in permeability *ex-vivo*, and 1.5 fold in *in vivo* anti-inflammatory [15]. Additionally, blending propylene glycol in phloretin binary ethosomes raised the precutaneous permeability 1.06 folds more than classical ethosomes, and 2.4 folds than PG solution [19]. The major methods for ethosome preparation are thin film hydration [18] and solvent - injection [12]. Solvent - injection is a more advantageous method for ethosome fabrication due to the simple process and scale - up [20].

However, there have been a few studies on dermal nanovehicles loading rutin, including the ethosomal system. Candido and his colleagues [21] prepared a rutin ethosome with a size of 369 nm and a zeta potential (ZP) of -19.6 mV. In another study, the optimized rutin ethosome has a size of 112 nm and an entrapment efficiency (EE) of 67.5% [22]. Although previous studies suggested rutin ethosome had a better antioxidant than free rutin, the enhancement of rutin penetrability by ethosome still did not clarify. Moreover, the articles only presented the classical ethosome, while the latter ethosome generation may express more potential effectiveness. Therefore, research about rutin ethosomes should be carried out to improve the therapeutic treatment of this Vietnamese bioactive agent, specifically for skin delivery. Hence, this study aims to fabricate the more modern type of ethosome - binary ethosome by facile solvent injection method for improvement of the therapeutic effectiveness of rutin for dermal treatment.

2. Materials and methods

2.1. Materials

Rutin was an active pharmaceutical ingredient

(CAS 153-18-4). Ethanol was from Xilong Scientific Co., Ltd (China). Lecithin (>90% Phosphatidylcholine) was from Yuanye Biology, Shanghai (China). Propylene glycol (PG), isopropyl alcohol (IPA), and glycerol were from Xilong Scientific Co. Ltd (China).

2.2. Methods

2.2.1. Ethosome preparation:

Rutin ethosome samples were prepared following the solvent injection method with mild modifications [23],[24]. Firstly, rutin was dissolved in ethanol/polyols using a magnetic stirrer (IKA C-MAG HS 4). At 30°C, lecithin was added and dissolved completely to form a homogeneous

organic phase. Distilled water (aqueous phase) was added to the organic phase by a syringe pump (Perfusor Compact) at a constant rate of 300 $\mu\text{L}/\text{min}$. Then, the ethosomes were sonicated by a probe sonicator (Q-Sonica) at 50W, 45/15 seconds for pulse on/ pulse off time, in 5 minutes to obtain uniform ethosomes. Finally, the products were stored in closed glass vials for further studies (Fig. 1). Rutin was fixed at 2.5 mg/mL, various lecithin ratios of 3%, 1.5%, 0.5% (w/v), ethanol concentrations at 20%, 35%, 50% (v/v), and different polyols, including PG/IPA/Glycerol, were investigated to prepare ethosomes.

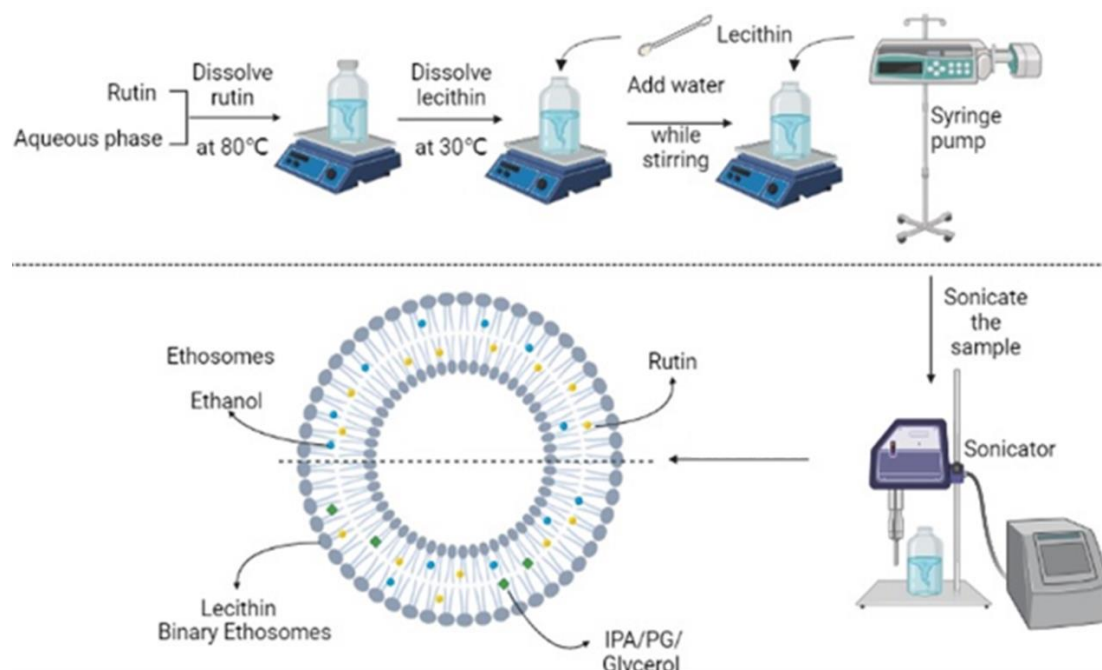


Fig. 1. Rutin ethosome fabrication

2.2.2. Size, polydispersity index, and zeta potential:

Size, polydispersity index (PDI), and zeta potential (ZP) of ethosome vesicles were measured by a nanoparticle analyzer (HORIBA nanoPartica SZ-100). Vesicle size was calculated based on the Stock - Einstein equation. ZP was calculated according to laser doppler electrophoresis (HORIBA Scientific 2023). Method setting included water as a medium, 4 opening cuvettes for size measurement, and carbon electrode zeta cuvettes for ZP measurement. Ethosome samples were diluted with water to ensure precise measurement when

measuring size, PDI, and ZP.

2.2.3. Morphology:

The visualization of ethosome samples was investigated by transmission electron microscopy (TEM) (JEOL Inc, Jem - 1400).

2.2.4. Rutin quantification:

The quantification rutin was evaluated by an HPLC method [21]. The stationary phase was a C18 reversed-phase column (150 x 4.6 mm, 5 μm), while the mobile phase was mixed from acetic acid 1% and acetonitrile (80:20) with the flow rate of 1 mL/min, 355 nm (Thermo Scientific™, UltiMate™ 3000 Standard (SD) HPLC Systems).

2.2.5. Drug entrapment efficiency (EE):

EE was a value showing the content of rutin which was encapsulated in ethosomal vesicle according to the equation below:

$$EE = \frac{R_e}{R_t} \cdot 100\% = \frac{R_t - R_f}{R_t} \cdot 100\%$$

Where R_e is encapsulated rutin, R_f is free rutin, R_t is the total content of rutin.

To determine free rutin content, the ultrafiltration method was applied with a 10000 Da cutoff at the speed of 10.000 rpm in 15 min. The rutin in the filtrate was quantified by HPLC.

2.2.6. Stability test:

Rutin ethosomes were stored in various conditions: at 4°C, at 25°C at a relative humidity of 60%, for 30 days to check the change in physical properties, like size, PDI, ZP, and EE.

2.2.7. Drug release study:

The penetration ability of rutin ethosome formulations was investigated by an experiment using Franz vertical diffusion cells. A dialysis membrane/or mouse skin was placed in the joint to separate the donor and receptor chambers. A volume of samples containing 5 mg rutin was added into a donor compartment. In the receptor compartment, a phosphate buffer pH 6.8 was filled to mark and stirred at a fixed rate. The temperature of the receptor compartments was kept at 37±0.5°C during the experiments. At time interval points, a fixed volume of medium was collected to determine rutin concentration by the HPLC method.

2.2.8. Data analysis:

T-test and one-way ANOVA test to evaluate statistical significance (setting at $p < 0.05$) were performed with Microsoft Excel. Data was reported as average ± standard deviation (SD). A value of $p < 0.05$ was considered statistically significant (*). Each experiment was carried out in triplicate.

3. Results and discussion

3.1. Effect of different concentrations of lecithin on rutin ethosome properties

The ratios of phospholipid bases strongly affected the size and PDI of ethosomes (Fig. 2A). At 3% (w/v) of lecithin, the size is 201.45 ± 0.15 nm, larger than that of 1.5%, 190.32 ± 3.56 nm, and 0.5%, 161.07 ± 0.89 nm. Conversely, the ethosome homogeneity at 0.5% lecithin was marginally better than that of 1.5% and 3% concentrations, as the PDI was 0.13 and around 0.25, respectively. The ZP is used to quantify the charge of the vesicles, of which the parameter reflects the stability of the formulation. The lower the lecithin ratios, the higher the absolute value of ethosome ZP [25]. At 3%, 1.5%, and 0.5% of the lecithin concentration, the charges were -13.76 ± 0.32, -20.09 ± 0.45, and -24.13 ± 1.21, respectively. The absolute value of ZP in the range of 20-30 mV could be considered acceptable for supporting the stability of these nanovesicles. Based on the physical properties, 0.5% of lecithin (w/v) was chosen for further experiments.

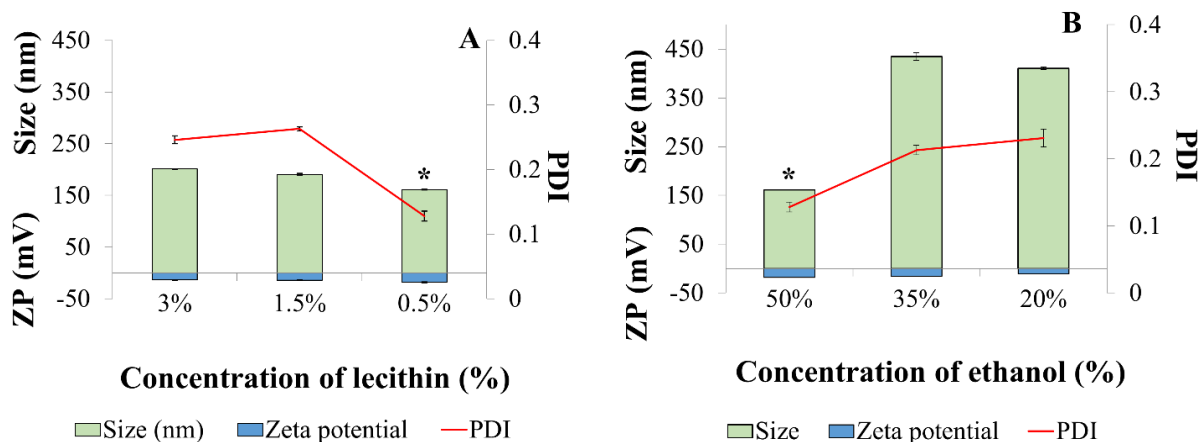


Fig. 2. Rutin ethosome physical properties at different lecithin ratios (w/v) and ethanol concentrations (v/v), 2A. Lecithin ratios, 2B. Ethanol ratios

3.2. Effect of different concentrations of ethanol on rutin ethosome properties

Formulations of ethosomes were evaluated with the different ratios of ethanol: 50%, 35%, and 20% (v/v) (Fig. 2B). With 20% ethanol, the nanoparticle size was 410.57 ± 5.08 nm, significantly larger than that of 50% ethanol, 161.0 ± 0.89 nm. The ethanol concentrations affected ethosome size, as the higher the ethanol concentration, the lower the ethosomal size [25]. At higher concentrations of ethanol (55% and 60%), the ethosomal vesicles disappeared, confirmed by the abnormal size value (under 20nm) and higher PDI (above 0.4), agreed with previous studies [13]. Hence, the 50% ethanol (v/v) was chosen for the rutin ethosome. When compared to pure rutin (about $21.23 \mu\text{m}$), and other rutin ethosomes by the same method, the resulting ethosomes in this study had a smaller size. In other research, the size of the ethosomal nanoparticle was 634.9nm (without sonication) [26], and rutin-loaded ethosomes, prepared by the thin-film hydration method, had the size of 247 ± 7 nm or 369.5 ± 4.2 nm [27].

3.3. Effect of other polyols in binary ethosomes

Different types of polyols were used to prepare rutin binary ethosomes with various blended ratios of ethanol: polyols at 3:7, 5:5, and 7:3 (Fig. 3) Other polyols could be considered as permeability enhancers and stabilizers [25].

3.3.1. Effect of propylene glycol in binary ethosomes:

The higher the PG ratios in rutin binary ethosomes, the smaller the size, in agreement with the previous study [25]. At ratios 7:3, 5:5, and 3:7 ratio of ethanol to propylene glycol, rutin ethosomal size reduced from above 350 nm to around 140 nm. In another study, optimum nicotine ethosomes containing ethanol: PG at the ratio of 5:5 were productive transdermal delivery systems [12]. In the case of PG, all rutin binary ethosomes had the PDI in the preferable range ($\text{PDI} < 0.3$). The binary ethosomes with PG exhibited ZP value in the acceptable range to prevent agglomeration. In addition, increasing PG quantities decreased the ethosomal ZP from -20.5 ± 0.47 mV to -23.8 ± 0.70 mV. Hence, ethanol: PG at the ratio of 7:3 had the smallest size, 137.7 ± 0.40 nm, and the best homogeneity.

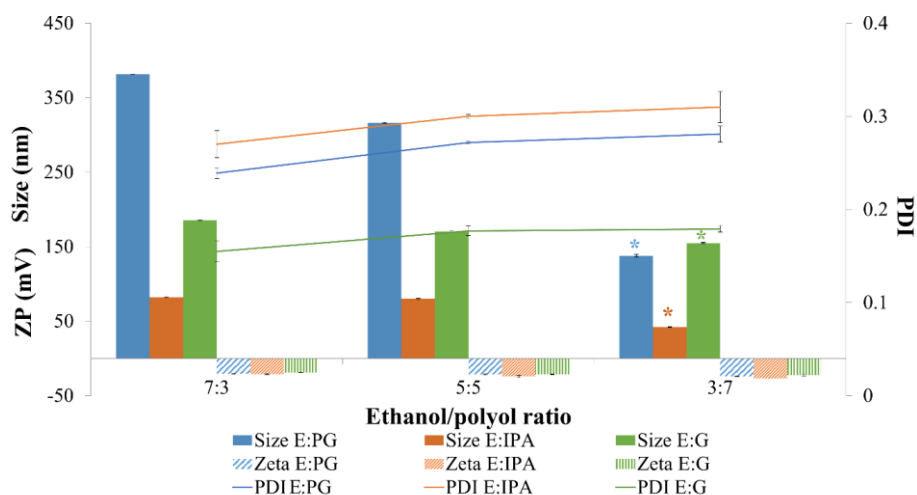


Fig. 3. Binary ethosomes at different ethanol/polyol ratios
E: ethanol, PG: propylene glycol, IPA: isopropanol alcohol, G: glycerol

3.3.2. Effect of isopropyl alcohol in binary ethosomes:

The second polyol investigated in rutin binary ethosomes formulation was isopropyl alcohol (Fig. 3.). With mixtures of ethanol and IPA, at any ratios, the size of the ethosome significantly reduced, compared to solely ethanol. Noticeably, at the blend

ratio of 7:3 of ethanol: IPA, the nanovesicle size dropped from above 160 nm to only 42.31 ± 0.85 nm. Conversely, the PDI increased considerably in the presence of IPA in ethosomes, from below 0.2 in classical ethosomes, up to around 0.3. Moreover, the presence of IPA increased the negative charge in the ZP of ethosomes.

3.3.3. Effect of glycerol in binary ethosomes:

The third polyol studied for rutin binary ethosomes was glycerol (Fig. 3.). The presence of glycerol in the binary ethosomes caused a slight decrease in nanovesicular size from 185.58 ± 0.55 nm (ethanol: glycerol = 7:3) to 155.09 ± 1.76 nm (ethanol: glycerol = 3:7), which demonstrated the effect of glycerol on particle size reduction. Furthermore, the PDI of all three formulations revealed a uniform size, with a PDI of less than 0.2. The increase in ZP with glycerol strengthened the stability of the rutin binary ethosome.

Among the three investigated polyols, IPA induced the greatest reduction in the size of binary ethosomes, as the size went down 4

folds related to classical ethosomes. However, in consideration of uniformity, the involvement of glycerol resulted in better PDI, below 0.2. Almost all rutin ethosomes had a high EE, more than 90%. Therefore, the alcohols for rutin binary ethosomes should be the mixture of ethanol and glycerol at the ratio of 3:7, with a size of 155.16 ± 1.76 , PDI of 0.18 ± 0.01 , ZP of -22.61 ± 2.46 mV, and EE of $92.41 \pm 0.08\%$ with the spherical shape shown in TEM images (Fig. 4.). In comparison with meloxicam ethosomes, 169 nm, 0.2 PDI, and 83.1 EE%, rutin binary ethosome could be considered successfully prepared and had better physical properties and drug loading [15].

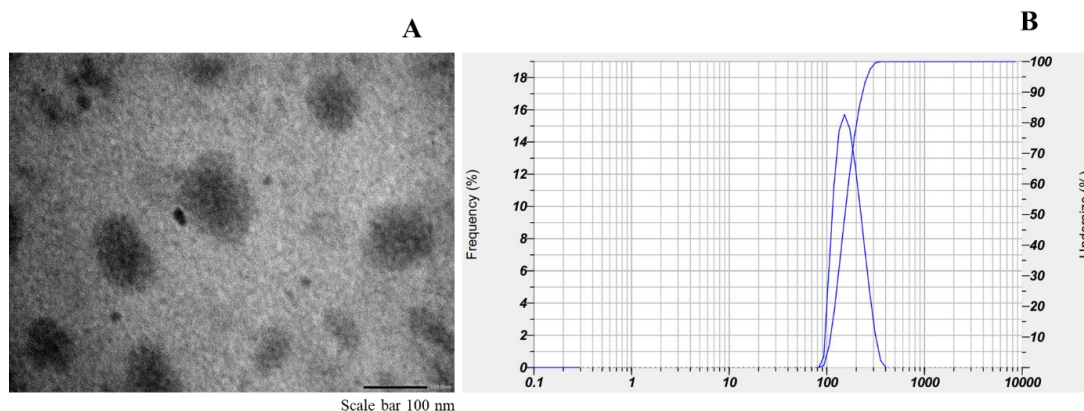


Fig. 4. TEM image and size distribution histogram of rutin binary ethosomes with glycerol
A. TEM image, B. size distribution histogram

3.4. Stability test

Initial investigation on the stability of rutin ethosomes was carried out in 30 days at 4°C and 25°C. The changes in size, PDI, ZP, and EE of classical ethosomes and binary ethosomes were presented in Table 1. There were significant increases in the size and PDI of all ethosomes in both tested temperatures. The size of the glycerol binary ethosomes rose from above 150 nm to approximately 200 nm after 30 days. Additionally, the PDI gained from 0.18 ± 0.01 to 0.23 ± 0.01 after 30 days at 25°C. Also, the absolute value of ZP slightly decreased from nearly 23 mV to about 20 mV after 30 days. In particular, the changes in physical characteristics and EE of various types of ethosomes at 4°C were slower than at 25°C. For example, after 30 days, the size of classical ethosomes at 4°C was

considerably smaller than that at 25°C, 221.03 ± 0.08 nm, and 320.04 ± 1.87 nm, respectively. Moreover, the EE of binary ethosomes with glycerol slightly fell from 92.41 ± 0.08 to 89.17 ± 0.15 after 30 days at 4°C. These observations suggested that storage in a colder environment provides better stabilization for rutin ethosomes.

The stability of rutin ethosomes could be improved by using combinations of ethanol and PG, IPA, and glycerol. In particular, after 30 days at 25°C, the size of classical ethosomes increased 2 folds from 161.02 ± 0.89 nm to 320.04 ± 1.87 , while for binary ethosomes with glycerol, the size only gained 1.2 times, from 155.09 ± 1.76 nm to 202.82 ± 1.27 nm. These results suggested the combination of polyols stabilized the ethosome structures more than using solely ethanol.

Table 1. Size, PDI, ZP, and EE of binary ethosomes after 15 days and 30 days

Freshly preparation	Size (nm)	PDI	ZP (mV)	EE (%)
Classical ethosomes	161.02 ± 0.89	0.13 ± 0.02	-24.16 ± 1.21	90.89 ± 0.05
Binary ethosomes with glycerol	155.09 ± 1.76	0.18 ± 0.01	22.61 ± 2.46	92.41 ± 0.08
4°C -15 days				
Classical ethosomes	201.02 ± 0.08	0.22 ± 0.03	-16.58 ± 2.96	87.91 ± 0.10
Binary ethosomes with glycerol	190.82 ± 1.91	0.21 ± 0.01	-20.86 ± 1.96	90.40 ± 0.10
4°C -30 days				
Classical ethosomes	221.03 ± 0.08	0.33 ± 0.06	-13.72 ± 1.98	79.96 ± 0.02
Binary ethosomes with glycerol	200.35 ± 1.26	0.22 ± 0.01	-20.64 ± 0.01	89.17 ± 0.15
25°C -15 days				
Classical ethosomes	290.05 ± 0.08	0.29 ± 0.04	-15.51 ± 1.91	85.56 ± 0.02
Binary ethosomes with glycerol	200.92 ± 0.81	0.22 ± 0.36	-20.13 ± 0.64	89.96 ± 0.05
25°C -30 days				
Classical ethosomes	320.04 ± 1.87	0.376 ± 0.08	-12.63 ± 1.48	79.06 ± 0.01
Binary ethosomes with glycerol	202.82 ± 1.27	0.23 ± 0.01	-19.21 ± 0.07	86.93 ± 0.03

3.5. In-vitro rutin release

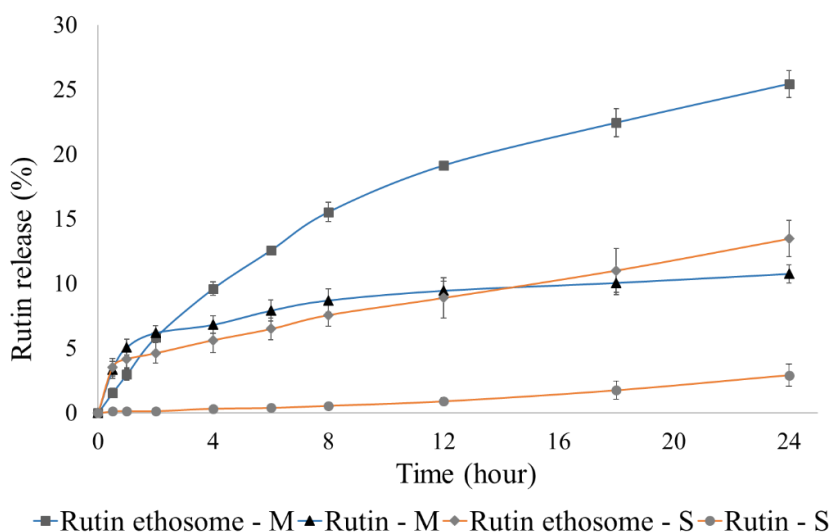


Fig. 5. Rutin release profile from binary ethosomes with glycerol
S- mouse skin, M- dialysis membrane

The rutin release was evaluated through the Franz-cell model, through mouse skin and dialysis membrane, from binary ethosomes with glycerol (Fig. 5.). Generally, in both mouse skin and dialysis membrane, ethosomes also expressed sustained releases. Additionally, ethosomes improved the permeability of rutin not only through the dialysis membrane but also through mouse skin. Specifically, after 24 hours, rutin released more than 2.5 folds through mouse skin and nearly four folds through the dialysis membrane than rutin itself. Therefore, binary ethosomes were effective nanocarriers to enhance drug delivery through the skin, as confirmed by a previous study [28].

4. Conclusion

Rutin ethosomes and binary ethosomes were successfully fabricated. The optimum formulation was the mixture of ethanol and glycerol at the ratio of 3:7, the total volume of polyols at 50% (v/v), lecithin at 0.5% (w/v) and rutin at a final concentration of 2.5 mg/mL. These binary ethosomes had a size above 150 nm and were homogenous (PDI<0.2). Besides, the ZP absolute value was greater than 30 mV and the EE was at around 92%. Additionally, the physical properties and drug loading hardly changed during 30 days at 4°C. Moreover, these rutin binary ethosomes exhibited sustained release and improved the

permeability of the drug through the dialysis membrane as well as mouse skin during 24 hours. Hence, rutin binary ethosomes may be considered as potential drug delivery systems for skin anti-aging, skin healing, and furthermore.

Declaration of Competing Interest: *The authors report no conflicts of interest.*

Acknowledgment: *This research received funding from University of Science and Technology of Ha Noi (USTH) under Grant Agreement No [USTH.LS.01/24].*

References

1. Watkins R., Wu L., Zhang C., Davis R. M., Xu B., (2015), Natural product-based nanomedicine: recent advances and issues, *International Journal of Nanomedicine*, 10, 6055-74.
2. Habtemariam S., Varghese G. K., (2015), Extractability of rutin in herbal tea preparations of *Moringa stenopetala* leaves, *Beverages*, 1(3), 169-182.
3. Enogieru A. B., Haylett W., Hiss D. C., Bardien S., Ekpo O. E., (2018), Rutin as a potent antioxidant: implications for neurodegenerative disorders, *Oxidative Medicine and Cellular Longevity*, 2018(1), 6241017.
4. Negahdari R., Bohlouli S., Sharifi S., Dizaj S. M., Saadat Y. R., Khezri K., Jafari S., Ahmadian E., Jahandizi N. G., Raeesi S., (2020), Therapeutic benefits of rutin and its nanoformulations, *Phytotherapy Research*, 35(4), 1719-1738.
5. Satari A., Ghasemi S., Habtemariam S., Asgharian S., Lorigooini Z., (2021), Rutin: a flavonoid as an effective sensitizer for anticancer therapy; insights into multifaceted mechanisms and applicability for combination therapy, *Evidence-Based Complementary and Alternative Medicine*, 2021(1), 9913179.
6. Choi S. J., Lee S. N., Kim K., Joo D. H., Shin S., Lee J., Lee H. K., Kim J., Kwon S. B., Kim M. J., Ahn K. J., An I. S., An S., Cha H. J., (2016), Biological effects of rutin on skin aging, *International Journal of Molecular Medicine*, 357-363.
7. Ivanov M., Novović K., Malešević M., Dinić M., Stojković D., Jovčić B., Soković M., (2022), Polyphenols as inhibitors of antibiotic resistant bacteria—mechanisms underlying rutin interference with bacterial virulence, *Pharmaceutics*, 15(3), 385.
8. Chen L. Y., Huang C. N., Liao C. K., Chang H. M., Kuan Y. H., Tseng T. J., Yen K. J., Yang K. L., Lin H. C., (2020), Effects of rutin on wound healing in hyperglycemic rats, *Antioxidants*, 9(11), 1122.
9. Jo Y. J., Yoo D. H., Lee I. C., Lee J., Jeong H. S., (2022), Antioxidant and skin whitening activities of sub- and super-critical water treated rutin, *Molecules*, 27(17), 5441.
10. Tomazelli L. C., de Assis Ramos M. M., Sauce R., Cândido T. M., Sarruf F. D., de Oliveira Pinto C. A. S., de Oliveira C. A., Rosado C., Velasco M. V. R., Baby A. R., (2018), SPF enhancement provided by rutin in a multifunctional sunscreen, *International Journal of Pharmaceutics*, 552(1-2), 401-406.
11. Rahman H., Othman H., Hammadi N., Amin K., Samad A. N., Alitheen N., (2020), Novel drug delivery systems for loading of natural plant extracts and their biomedical applications, *International Journal of Nanomedicine*, 15, 2439-2483.
12. Wang H., Shao Q., Zhang Y., Ding J., Yang M., Yang L., Wang W., Cui P., Dai Z., Ma L., (2024), Preparation and evaluation of liposomes containing ethanol and propylene glycol as carriers for nicotine, *Current Drug Delivery*, 21(2), 249-260.
13. Abdulbaqi I. M., Darwis Y., Khan N. A. K., Abou Assi R., Khan A. A., (2016), Ethosomal nanocarriers: the impact of constituents and formulation techniques on ethosomal properties, *in vivo* studies, and clinical trials, *International Journal of Nanomedicine*, 11, 2279.
14. Sherin F., Saju F., Jagadeesh A., Syamasree S., Paul N., Venugopal A., (2019), Ethosome: A novel approach to enhance drug permeation, *International Journal of Pharmaceutical Sciences Review and Research*, 55(1), 18-22.
15. Al-Ameri A. A. F., Al-Gawhari F. J., (2024), Formulation development of meloxicam binary ethosomal hydrogel for topical delivery: *in vitro* and *in vivo* assessment, *Pharmaceutics*, 16(7), 898.
16. Sayed O. M., Abo El-Ela F. I., Kharshoum R. M., Salem H. F., (2020), Treatment of basal cell carcinoma via binary ethosomes of vismodegib: *in vitro* and *in vivo* studies, *Aaps Pharmscitech*, 21, 1-11.
17. Sharma D., Rani A., Singh V. D., Shah P., Sharma S., Kumar S., (2023), Glycosomes: novel nano-vesicles for efficient delivery of therapeutics, *Recent Advances in Drug Delivery and Formulation*, 17(3), 173-182.
18. Hamzah M. L., Kassab H. J., (2024), Formulation and characterization of intranasal drug delivery of frovatriptan-loaded binary ethosomes gel for brain targeting, *Nanotechnology, Science and Applications*, 1-19.
19. Zhang M., Zhuang X., Li S., Wang Y., Zhang X., Li J., Wu D., (2023), Designed fabrication of phloretin-loaded propylene glycol binary ethosomes: stability, skin permeability and antioxidant activity, *Molecules*, 29(1), 66.
20. Wang J., He W., Cheng L., Zhang H., Wang Y., Liu C., Dong S., Zha W., Kong X., Yao C., (2022), A modified thin film method for large scale production of dimeric artesunate phospholipid liposomes and comparison with conventional approaches, *International Journal of Pharmaceutics*, 619, 121714.
21. Cândido T. M., Camila A. D. O., Maíra B. A., Maria V. R. V., Catarina R., André R. B., (2018), safety and antioxidant efficacy profiles of rutin-loaded ethosomes for topical application, *American Association of Pharmaceutical Scientists*, 19, 1773-80.
22. Cristiano M. C., Barone A., Mancuso A., Torella D., Paolino D., (2021), Rutin-loaded nanovesicles for improved stability and enhanced topical efficacy of natural compound, *Journal of Functional Biomaterials*, 12(4), 74.
23. Somwanshi S. B., (2019), Development and evaluation of novel ethosomal vesicular drug delivery system of *Sesamum indicum* L. seed extract, *Asian Journal of Pharmaceutics*, 12(4), 1290.
24. Andleeb M., Shoaib Khan H.M., Daniyal M., (2021), Development, characterization and stability evaluation of topical gel loaded with ethosomes containing *Achillea millefolium* L. extract, *Frontiers in Pharmacology*, 12, 336.
25. Aljohani A. A., Alanazi M. A., Munahhi L. A., Hamroon J. D., Mortagi Y., Qushawy M., Soliman G. M., (2023), Binary ethosomes for the enhanced topical delivery and antifungal efficacy of ketoconazole, *OpenNano*, 11, 100145.
26. Dhiman A., Singh D., Fatima K., Zia G., (2019), Development of rutin ethosomes for enhanced skin permeation, *International Journal of Traditional Medicine and Applications*, 1, 4-10.
27. Cândido T. M., De Oliveira C. A., Ariede M. B., Velasco M. V. R., Rosado C., Baby A. R., (2018), Safety and antioxidant efficacy profiles of rutin-loaded ethosomes for topical application, *Aaps Pharmscitech*, 19(4), 1773-1780.
28. Jiang D., Jiang Y., Wang K., Wang Z., Pei Y., Wu J., He C., Mo X., Wang H., (2022), Binary ethosomes-based transdermal patches assisted by metal microneedles significantly improve the bioavailability of carvedilol, *Journal of Drug Delivery Science and Technology*, 74, 103498.